THE IMPACT OF MTOR, TFEB AND BID ON NON-ALCOHOLIC FATTY LIVER DISEASE AND METABOLIC SYNDROME

Hao Zhang

Submitted to the faculty of the University Graduate School

in partial fulfillment of the requirements

for the degree

Doctor of Philosophy

in the Department of Pathology and Laboratory Medicine

Indiana University

August, 2015

Accepted by the Graduate Faculty, Indiana University, in partial fulfillment of the requirements for the degree of Doctor of Philosophy.

Xiao-Ming Yin, M.D., PhD, Chair

Doctoral Committee

Naga P. Chalasani, M.D.

May 18, 2015

Raymond L. Konger, M.D.

Jill R. Murrell, PhD

Dedication

To my parents, Dalu Zhang and Jie Gao, who always stay with me and give me tremendous love. All I have and will accomplish are only possible due to their support and sacrifice.

Acknowledgments

First, I would like to extend my most sincere and deepest gratitude to my mentor, Dr. Xiao-Ming Yin. It has been very fortunate of me and my honor to be able to work under his supervision. Dr. Yin is an extremely busy clinician scientist and undertaking administration responsibilities. However, he still has devoted huge amount of time in training me to be a scientist. He has instructed me from every single experiment design to each of word and grammar correction in manuscript writing. As a mentor, he not only has guided me through the research projects, but also provided great support for my future career development. Without Dr. Yin's care and support in the last five years, it is impossible for me to fulfill my dream of being a physician scientist. Again, it is with deep gratitude that I say I could not have asked for a better mentor. I will always remember his help and kindness in this most important five years of my life.

I would also like to express my sincere gratitude to other research committee members: Dr. Chalasani, Dr. Konger and Dr. Murrell. Thank you for your guidance and suggestions in my thesis projects. My committee members also have kindly helped me in my career development. They were always standing with me whenever I need any help.

I also want to take this opportunity to express my heartfelt appreciation to members in Dr. Yin lab. Dr. Khambu, who has stayed alongside with me for

almost four years. Dr. Khambu not only has helped me tremendously in improving my experimental techniques but also have celebrated with me on good days and offered insightful advice in my bad days. It was my fortunate to work with him. I would also like to thank Dr. Jane Chen, who guided me through experiment when I first entered the lab. She have also helped me with all my animal experiments. Without Dr. Chen, I would not have finished these two thesis projects smoothly. I thank Dr. Yong Li for his virus and molecular biology support for my projects; Dr. Changshun Yu for his computer and software support; previous lab members Dr. Min Li and Dr. Xi Chen for their guidance and help in my experiments.

Finally, I would like to thank my parents. They are the people who made me where I am now. They are the people who always stay with me whenever I am in frustration. I hope my accomplishment could make them proud.

Hao Zhang

THE IMPACT OF MTOR, TFEB AND BID ON NON-ALCOHOLIC FATTY LIVER DISEASE AND METABOLIC SYNDROME

Non-alcoholic fatty liver disease and metabolic syndrome induced by high nutrient status have increasingly become a global health concern as it cause multiple complications. The mTOR complex is central in regulating anabolic reactions within cells under growth factors or under high nutrients stimulation. Constitutive and persistent activation of mTOR can impair cellular functions. In the first part of this study, we demonstrate a damping oscillation of mTOR activity during a long-term treatment of high fat diet. TFEB translocation and lysosomal enzyme activity also oscillate, but in an opposite direction. TFEB controls the lysosomal activity, autophagic degradation and lipid metabolism. Overexpression of wild type and mutant TFEB could inhibit NAFLD development in mice. In addition, TFEB location in nucleus inversely correlates with NAFLD severity in patients. mTOR activation under hypernutrition status suppresses TFEB translocation, inhibits lysosomal functions and autophagic degradation of lipid droplets. Inhibition of mTOR activity by rapamycin reverse the above phenotypes. Because mTOR activation also requires normal lysosomal function, the inhibition of TFEB by mTOR leads to decreased lysosomal function and mTOR downregulation. This negative feedback may explain the oscillation pattern of mTOR activation in long term high fat diet regimen and is a novel mechanism for inhibition of mTOR. In the second part of study, we report that Bid

protein, previously known for its pro-apoptosis function in promoting mitochondrial permeability, plays an unexpected role in regulating fatty acid beta oxidation. Deletion of Bid in mice reprograms the body's response to hyper-nutrition caused by high fat diet, leading to the resistance to the development of obesity, liver steatosis and metabolic syndrome. These mice present a higher oxygen consumption, a lower respiratory quotient, and an increased beta-oxidation rate. Mechanistically, the high fat diet regimen triggers translocation of the full length Bid molecule to mitochondrial membrane. Genetic deletion of Bid also affects the stability of its binding protein, MTCH2 in the mitochondrial membrane. In summary, we describe in this study a mTOR-TFEB-lysosome feedback loop, which can regulate NAFLD development, and a novel Bid-mediated regulatory mechanism in beta-oxidation, which limits energy expenditure and promotes obesity development.

Xiao-Ming Yin, M.D., PhD, Chair

Table of Contents

Part I. The Function of mTOR and TFEB in NAFLD and Obesity

1.1 Introduction

1.1.1 mTOR, the Pathway and The Regulation.

1.1.1.1 Introduction

The mammalian target of rapamycin (mTOR) has a central role in cell metabolism, proliferation and survival. As an energy sensor, it can sense intracellular and extracellular signals. Discoveries that have been made over the last decade have shown that the mTOR pathway is activated during various pathophysiological processes (e.g. tumor formation and angiogenesis, insulin resistance, adipogenesis and T-lymphocyte activation etc.) and is deregulated in human diseases such as cancer and type 2 diabetes [1]. Most importantly, mTOR is a central intracellular molecule in controlling the transition between catabolic and anabolic states, allowing mammals to survive and to grow in different environments.

mTOR interacts with many proteins to form two basic multiprotein complexes: mTOR complex 1 (mTORC1) and mTOR complex 2 (mTORC2). In addition to their different protein compositions, the mTOR complexes have important differences in their sensitivities to rapamycin, in the upstream signals they

integrate, in the substrates they regulate, and in the biological processes they control [2]. mTORC2 is not as well studied for its regulation and for its function in energy regulation [3]. We will discuss primarily mTORC1 in this thesis.

1.1.1.2 mTOR Complex and Upstream Regulators

mTORC1 is sensitive to rapamycin and integrates inputs from at least five major signals—growth factors, genotoxic stress, energy status, oxygen, and amino acids—to regulate many processes involved in the promotion of cell growth and proliferation. The complex of mTORC1 consists of a regulatory component known as regulatory-associated protein of mTOR (RAPTOR), The regulatory component of mTORC2 is called rapamycin-insensitive companion of mTOR (RICTOR) [4, 5]. These companions function as scaffolds for assembling the complexes and for binding substrates and regulators. mTORC1 and mTORC2 share a common component, mammalian lethal with SEC13 protein 8 (mLST8; also known as GβL), and the recently identified DEP domain-containing mTOR-interacting protein (DEPTOR), which play a positive function and negative function, respectively [6, 7]. However, mTORC1 also includes a negative regulator, Pro-rich Akt substrate (PRAS40) [8]. The domain organization of mTOR resembles that of other PI3K-related protein kinases (PIKK) family members. Biochemical and structural evidence has also suggests that mTORC1 may exist as dimers [9, 10].

mTORC1 has a number of very diversified upstream regulators. The mTORC1 pathway integrates inputs from at least five major intracellular and extracellular signals--growth factors, stress, energy status, oxygen, and amino acids. The heterodimer complex consisting of tuberous sclerosis 1 (TSC1; also known as hamartin) and TSC2 (also known as tuberin) is the key upstream regulator of mTORC1 and functions as a GTPase-activating protein (GAP) for the Ras homolog enriched in brain (Rheb) GTPase. Rhab activates mTORC1 but TSC1/2 inhibits Rhab as its GAP. The GTP-bound form of Rheb directly interacts with mTORC1 and strongly stimulates its kinase activity. As a Rheb GAP, TSC1/2 negatively regulates mTORC1 by converting Rheb into its inactive GDP-bound state [11, 12]. TSC1/2 transmits many of the upstream signals to mTORC1, including growth factors, such as insulin and insulin-like growth factor 1 (IGF1), which can further stimulate PI3K and Ras pathways. The effector kinases of these pathways—protein kinase B (Akt/PKB), extracellular-signal-regulated kinase 1/2 (ERK1/2), and ribosomal S6 kinase (RSK1) can directly phosphorylate the TSC1/TSC2 complex to inactivate it and thus activate mTORC1 [12-14].

TSC2 can also be directly phosphorylated by Akt, which destabilizes and disrupts its interaction with TSC1. This process is involved in stimulating cell growth. Akt also signals to mTORC1 in a TSC1/2-independent fashion by phosphorylating and causing the dissociation from raptor of PRAS40, an mTORC1 inhibitor [15, 16]. Pro-inflammatory cytokines, like tumor necrosis factor-α (TNFα) can also activate mTORC1 [17]. IKKbeta, a major downstream kinase in the TNFalpha

signaling pathway, physically interacts with and phosphorylates TSC1 at Ser487 and Ser511, resulting in suppression of TSC1. The IKKbeta-mediated TSC1 suppression activates the mTOR pathway, enhances angiogenesis, and results in tumor development. Lastly, the canonical Wnt pathway, a major regulator of cell growth, proliferation, polarity, differentiation, and development, also activates mTORC1 through TSC1/2. Wnt activates mTOR via inhibiting GSK3 without involving beta-catenin-dependent transcription. GSK3 inhibits the mTOR pathway by phosphorylating TSC2 [18].

Stress signal can also activate/suppress mTORC1 through TSC1/2. Among the stress inducers, low energy and oxygen levels and DNA damage being the best characterized. Adenosine monophosphate-activated protein kinase (AMPK), in response to hypoxia or a low energy state, phosphorylates TSC2. Like Akt, AMPK also communicates directly with mTORC1; it phosphorylates RAPTOR, leading to 14-3-3 protein to bind and inhibit mTORC1 [19]. DNA damage, as an internal stress signal, signals to mTORC1 through multiple mechanisms, all of which require p53-dependent transcription. DNA damage induces the expression of Tsc2 and PTEN, causing downregulation of the entire PI3K-mTORC1 axis [20] and activating AMPK through a mechanism that depends on the induction of Sestrin1/2 [21].

Different amino acids, particularly leucine and arginine, activate mTORC1 and must be present for any upstream signals, including growth factors, to activate

mTORC1 [22]. Although it has been known for some times that amino acids act independently of TSC1/2, the molecular mechanism through which mTORC1 senses intracellular amino acids remains unknown until in 2008 when the Sabatini and Guan's group has found that the Rag proteins--a family of four related small guanosine triphosphatases (GTPases)--interacted with mTORC1 in an amino acid-sensitive manner and were necessary for the activation of the mTORC1 pathway by amino acids. A RagA or RagB binding to GTP can reduce mTORC1 pathway resistant to amino acid deprivation where expression of a GDP bound RagA or RagB mutant can prevent stimulation of mTORC1 by amino acids. The Rag proteins do not directly stimulate the kinase activity of mTORC1, but, like amino acids, promote the intracellular localization of mTOR to lysosome membranes, which harbor its activator Rheb [23]. Mammals have four Rag proteins, RagA to RagD, which form obligate heterodimers consisting of RagA or RagB with RagC or RagD. The two members of the heterodimer have opposite nucleotide states, so that when RagA/B is bound to GTP, RagC/D is bound to GDP and vice versa. Amino acids can promote the loading of RagA/B with GTP, which enables the lysosome-associated heterodimer to interact with the RAPTOR component of mTORC1 [23], thus recruiting mTORC1 to the lysosomal membranes, where the Rag proteins reside. How do amino acids activate Rag proteins? A set of proteins encoded by complex encoded by the MAPKSP1, ROBLD3, and c11orf59 genes, which was collectively termed as Ragulator, interact with the Rag GTPases upon the effect of amino acid, recruit them to lysosomes, and are essential for mTORC1 activation. This interaction results in

the translocation of mTORC1 from a poorly characterized cytoplasmic location to the lysosomal surface [10, 24]. More recent findings have shown that different amino acids use different mechanisms to activate mTORC1 [25], mTORC1 is differentially regulated by glutamine and leucine. RagA and RagB are essential for mTORC1 activation by Leucine, but not by Glutamine.

The localization of the Ragulator and Rag GTPases to the lysosomal surface, but not on other endomembranes where Rheb also resides, suggests the sensing of amino acids happens by lysosome. In the year 2011, an inside-out model of amino acid sensing was established [26]. The vacuolar H(+)-adenosine triphosphatase ATPase (v-ATPase) located in the lysosome membrane is necessary for amino acids to activate mTORC1. The v-ATPase engages in extensive amino acid-sensitive interactions with the Ragulator. In a cell-free system, ATP hydrolysis by the v-ATPase is necessary for amino acids to regulate the v-ATPase-Ragulator interaction and to promote mTORC1 translocation. These findings suggest that amino acid signaling begins within the lysosomal lumen and initiate the downstream events. The v-ATPase directly interacts with the Ragulator, providing a physical link between the v-ATPase and the Rag GTPase on the surface of lysosomes. The ATPase activity of the v-ATPase and the associated rotation of its V0 section appear to be essential to deliver the amino acids signal from the lysosomal lumen to the Ragulator and Rag GTPases [26].

mTOR activation by amino acid is also regulated by a feed-back loop in lysosomal function. Researchers have found that mTORC1 regulates the expression of, among other lysosomal genes, the V-ATPases. mTORC1 regulates V-ATPase expression both in cells and in mice. V-ATPase regulation by mTORC1 involves a transcription factor translocated in renal cancer, TFEB. TFEB is required for the expression of a large subset of mTORC1 responsive genes. mTORC1 coordinately regulates TFEB phosphorylation and nuclear localization in a manner dependent on both TFEB and V-ATPases. [27]. Finally, phosphatidic acid (PA) has also been identified as an activator of mTORC1 [28].

1.1.1.3 Cellular Process Downstream of mTOR Signaling

With the unique composition of the mTORC1, the protein complex controls cellular protein synthesis by regulating its substrates. The two major mTORC1 substrates are P70S6 kinase 1 (p70S6K1) and eIF4E-binding protein 1 (4E-BP1). They are associated with mRNAs and regulate mRNA translation initiation and progression, thus controlling the rate of protein synthesis [29]. 4E-BP1 are translational repressors which upon phosphorylation by mTORC1, dissociate from eIF4E. This leads to the binding of eIF4G to eIF4E at the 5′-end of mRNAs and promotes cap-dependent translation initiation.[30]. When phosphorylated by mTORC1, P70S6K1 first phosphorylates S6, which than further promotes mRNA translation by phosphorylating or binding multiple proteins, including eukaryotic elongation factor 2 kinase (eEF2K) [31], and S6K1 Aly/REF-like target [30], which

collectively affect translation initiation and elongation. Recent studies found that mRNAs under control of mTOR encode proteins belonging to the translation machinery, such as ribosomal proteins or elongation factors [10, 32].

mTORC1 mainly regulates protein synthesis by directly phosphorylates the translational regulators eukaryotic translation initiation factor 4E (eIF4E) binding protein 1 (4E-BP1) and p70S6 kinase 1 (p70S6K1). Regulation of the mRNA cap-binding protein eIF4E is mediated directly by mTORC1, which phosphorylates the eIF4E inhibitors — the 4E-BPs [33]. In quiescent cells, hypophosphorylated 4E-BP1 binds tightly to eIF4E. As 4E-BP1 competes with eIF4G for an overlapping binding site on eIF4E, 4E-BP1 prevents eIF4G from interacting with eIF4E. On mTORC1 activation, hyperphosphorylated 4E-BP1 dissociates from eIF4E, allowing for the recruitment of eIF4G and eIF4A to the 5' end of an mRNA. Finally, eIF3, the small ribosomal subunit and the ternary complex (comprising eIF2, Met-tRNA and GTP) are recruited to the cap, resulting in the assembly of the 48S translation pre-initiation complex, ribosome scanning and translation initiation [34, 35].

The activation of S6K1 leads, through a variety of effectors, to an increase in mRNA biogenesis, as well as translational initiation and elongation. S6K1 was originally thought to control the translation of an abundant subclass of mRNAs characterized by an oligopyrimidine tract at the 5′ end (5′ TOP mRNAs), which encode most of the protein components of the translational machinery. Two

essential phosphorylation sites have been identified, including Thr229, which is located in the catalytic activation loop, and Thr389, which is located at a hydrophobic motif that is carboxy-terminal to the kinase domain [36]. S6K activation is initiated by mTORC1-mediated phosphorylation of Thr389, resulting in the formation of a docking site for phosphoinositide-dependent kinase 1 (PDK1), which then phosphorylates Thr229 to activate S6K [36]. S6Ks are also thought to coordinate the regulation of ribosome biogenesis, which in turn drives efficient translation [35, 37].

mTORC1 also upregulates the protein synthesis machinery in other ways. For example, it regulates Pol I transcription by modulating the activity of motif-containing protein-24(TIF-IA), a regulatory factor that senses nutrient and growth-factor availability [38]. mTORC1 also participates in regulating TSC2- VEGF pathway. TSC2 loss results in the accumulation of HIF-1alpha and increased expression of HIF-responsive genes including VEGF [39]. Other study has confirmed mTORC1 as the upstream regulator of HIF-1. Amplified signaling through mTOR can enhance HIF-1-dependent gene expression in certain cell types and cancer model [40].

1.1.2 mTOR in Lipid synthesis, Liver Function and Metabolism Syndrome/NAFLD

1.1.2.1 mTOR and Lipid Homeostasis

mTOR protein kinase has emerged as a crucial link between growth signals and the regulation of lipid metabolism. The regulation of de novo sterol and fatty acid synthesis by signaling pathways, especially insulin signaling could be one of the activator of mTOR. Unlike most terminally differentiated cells, hepatocytes and adipocytes can synthesize lipids de novo through pathways in which cytosolic acetyl-CoA, derived from glucose or amino acid catabolism, is used to form the hydrophobic carbon backbone of lipids [41, 42]. Both the sterol and fatty acid synthesis branches comprise of many steps requiring many specific enzymes. Importantly, the SREBPs are transcription factors that stimulate the expression of genes encoding nearly all of these lipogenic enzymes [42]. SREBP1a and 1c are products of alternative splicing of the SREBF1 gene and have been primarily implicated in the control of genes involved in fatty acid synthesis, although SREBP1a is thought to activate most SRE-containing genes [42]. SREBP2 is encoded by SREBF2 and is believed to have a more important role in the transcription of steroidogenic genes, including those involved in cholesterol synthesis in the liver [43]. Studies have identified the SREBPs as major transcriptional effectors of mTORC1 signaling. mTORC1 signalling promotes SREBP activation and lipogenesis in response to both physiological and genetic

stimuli. Insulin or feeding has been shown to increase the expression of the major liver isoform of SREBP1c and its targets, and to promote de novo lipid synthesis in a manner that is sensitive to rapamycin [44]. mTORC1 may also regulate the SREBP transcriptional network via the negative regulation of lipin1 [45]. Lipin1 is an mTORC1 substrate with multiple phosphorylation sites, including both rapamycin-sensitive sites and sites phosphorylated by mTORC1 that are relatively insensitive to rapamycin. Phosphorylation of lipin1 by mTORC1 regulates its subcellular localization, with phosphorylated lipin1 residing in the cytoplasm and dephosphorylated lipin1 accumulating in the nucleus. Inhibition of mTORC1 in the liver significantly impairs SREBP function and makes mice resistant, in a lipin 1-dependent fashion, to the hepatic steatosis and hypercholesterolemia induced by a high-fat and -cholesterol diet. [45].

Different studies also suggest that mTORC1 may control lipid homeostasis by regulating the expression and the activation state of PPAR-γ. Many independent groups [46] have reported that mTOR inhibition with rapamycin reduces mRNA and protein levels of PPAR-γ and C/EBP-α and the expression of numerous lipogenic genes in vitro. PPAR-gamma activity is dependent on amino acid sufficiency, revealing a molecular link between nutrient status, adipogenesis and possibly, mTOR status. The mTOR pathway and the phosphatidylinositol 3-kinase/Akt pathway act in parallel to regulate PPAR-gamma activation during adipogenesis by mediating nutrient availability and insulin signals [47]. Additionally, constitutive activation of mTORC1 through TSC2 deletion increases

PPAR-γ and C/EBP-α expression and promotes adipogenesis [48]. Some evidences indicate that 4E-BP1 and 2, which are negative regulators of translation that are inhibited by mTORC1, are important for the regulation of PPAR-γ and C/EBPs by mTORC1 [49, 50]. Although the activation of S6K1, and probably other mTORC1 substrates, is induced by the deletion of 4E-BP1/2, these results suggest that mTORC1 controls adipogenesis/lipogenesis by inducing the translation of mRNA coding for key components of the adipogenic program.

Direct knock-out of mTOR downstream genes also has effects on glucose/lipid metabolism. Mice deficient for S6K1, an effector of the mTOR that acts to integrate nutrient and insulin signals, were shown to be hypoinsulinaemic, glucose intolerant and have reduced beta-cell mass. However, S6K1-deficient mice maintain normal glucose levels during fasting, suggesting hypersensitivity to insulin. S6K1-deficient mice are protected against obesity owing to enhanced beta-oxidation. However on a high fat diet, levels of glucose and free fatty acids still rise in S6K1-deficient mice, resulting in insulin receptor desensitization. S6K1-deficient mice remain sensitive to insulin owing to the apparent loss of a negative feedback loop from S6K1 to IRS1 [51].

1.1.2.2 Role of mTOR in Liver Metabolic Functions.

The liver is the most important metabolic organ which carries most of the metabolic functions. mTOR is a well-known regulator of metabolism and is highly expressed in hepatocyte, indicating its important role in metabolism regulation in the liver.

First, mTORC1 signaling in the liver affects systemic glucose and insulin homeostasis. In the liver of liver-specific TSC1 knockout mice, chronic activation of mTORC1 signaling has very strong inhibition effect on IRS-1, resulting in decreased Akt signaling. This impairs hepatic glycolytic flux and hence glucose clearance from the blood, leading to glucose intolerance [52, 53]. Contrary to the TSC knockout mouse, liver-specific raptor knockout mice have increased systemic glucose tolerance that can be explained by enhanced Akt signaling and insulin-induced glucose uptake in the liver [45, 54]. Hence, hepatic mTORC1 signaling results in systemic regulation of glucose and insulin signaling, most probably due to changes in AKT pathway. In a normal liver, insulin suppresses gluconeogenesis and promotes lipogenesis. In type 2 diabetes, the liver exhibits selective insulin resistance by failing to inhibit hepatic glucose production while maintaining triglyceride synthesis. Evidence suggests that the insulin pathway bifurcates downstream of Akt to regulate these two processes. Second, Obesity-induced insulin resistance depends, in part, on chronic activation of mammalian

target of rapamycin complex 1 (mTORC1), as another evidence of mTOR in liver glucose homeostasis [2, 55].

Interestingly, TSC knockout mice that have constitutive mTORC1 activation in the liver have dramatic effect on its normal function. These mice developed normally but displayed mild hepatomegaly and insulin resistance without obesity. Unexpectedly, the TSC-null livers showed minimal signs of steatosis even under high-fat diet condition. This 'resistant' phenotype was reversed by rapamycin. These observations suggest that mTORC1 activation only by genetic modulation is not sufficient for steatosis and may need outside stimulations such as high fat diet feeding [55].

A recent study by Cornu et al. [56] demonstrated another interesting connection between hepatic mTORC1 signaling and whole body physiology in liver specific TSC1 KO mice. They displayed reduced locomotor activity, body temperature, and hepatic triglyceride content in a rapamycin-sensitive manner. Ectopic activation of mTORC1 also caused depletion of hepatic and plasma glutamine, leading to peroxisome proliferator-activated receptor γ coactivator-1α (PGC-1α)-dependent fibroblast growth factor 21 (FGF21) expressions in the liver. Injection of glutamine or knockdown of PGC-1α or FGF21 in the liver suppressed the behavioral and metabolic defects due to mTORC1 activation. Thus, mTORC1 in the liver controls whole-body physiology possibly through PGC-1α and FGF21. By an unknown mechanism, this metabolic stress stimulates PGC-1α-dependent

FGF-21 production in the liver. FGF-21 in turn acts on the central nervous system to decrease locomotor activity and body temperature.

mTORC1 also promotes glutamine anaplerosis (i.e. formation of an intermediate metabolic alpha-ketoglutarate from glutamate) by activating glutamate dehydrogenase (GDH). This regulation requires transcriptional repression of SIRT4. Mechanistically, mTORC1 represses SIRT4 by promoting the proteasome-mediated destabilization of cAMP-responsive element binding 2 (CREB2). Glucose-limited TSC-deficient cells are addicted to glutamine as an alternative carbon source, further accentuating the role of mTORC1 in regulating glutamine metabolism [57, 58]. Other study found the central regulator of energy intake molecule ghrelin also has its function carried by mTOR [59]. By interacting with peroxisome proliferator-activated receptor-γ (PPARγ), mTOR mediates the ghrelin-induced up-regulation of lipogenesis in hepatocytes. The stimulatory effect of ghrelin on hepatic lipogenesis was significantly attenuated by PPARγ antagonism in cultured hepatocytes and in PPARγ gene-deficient mice.

Another interesting study has linked mTOR with ketogensis in the liver. Sabatini's group found that liver-specific loss of TSC1 leads to a fasting-resistant increase in liver size and to a pronounced defect in ketone body production and ketogenic gene expression on fasting. The loss of raptor has the opposite effects. In addition, the inhibition of mTORC1 is required for the fasting-induced activation of PPARα, the master transcriptional activator of ketogenic genes, and that

suppression of NCoR1 (nuclear receptor co-repressor 1), a co-repressor of PPARα, reactivates ketogenesis in cells and livers with hyperactive mTORC1 signaling. Moreover, the suppressive effects of mTORC1 activation and ageing on PPARα activity and ketone production are not additive, and that mTORC1 inhibition is sufficient to prevent the ageing-induced defect in ketogenesis. Thus, those findings reveal that mTORC1 is a key regulator of PPARα function and hepatic ketogenesis [52].

Similar to hepatic mTORC1, mTORC2 signaling in the liver also affects systemic glucose and insulin homeostasis. Liver-specific rictor knockout (LiRiKO) mice have increased circulating insulin levels and impaired glucose tolerance and insulin sensitivity. Fed LiRiKO mice displayed loss of Akt Ser473 phosphorylation and reduced glucokinase and SREBP1c activity in the liver, leading to constitutive gluconeogenesis, and impaired glycolysis and lipogenesis, suggesting that the mTORC2-deficient liver is unable to sense satiety. Hepatic mTORC2 affects systemic glucose and insulin homeostasis mainly by affecting hepatic glucose uptake via Akt signaling [60, 61]. Rapamycin-induced insulin resistance is mediated by mTORC2 loss and uncoupled from longevity, the first study indicating rapamycin in liver can affect longevity by suppreing the mTOR [62].

1.1.3. TFEB-lysosome Regulation Pathway

1.1.3.1 Introduction

TFEB (transcription factor EB) is a transcription factor within the family of basic/helix–loop–helix/leucine zipper (bHLH-LZ) transcription factors. This family also includes Microphthalmia-associated transcription factor (MITF), TFE3, and TFEC [63-65]. All members of the MITF/TFE family share a similar structure that includes three critically important regions. The basic motif binds to specific areas of DNA while the helix–loop–helix and the leucine-zipper motifs are critical for protein interactions. Homodimerization and heterodimerization within members of the MITF/TFE family is critical for binding to DNA and transcriptional activation of target genes [66]. In addition, it is well established that the MiTF/TFE family specifically binds to E-box (CANNTG) and/or M-box (AGTCATGTGCT) response elements present in the promoter region of their downstream target genes [67].

TFE3 and TFEB show a very ubiquitous pattern of expression and have been detected in multiple cell types [68]. TFEB and TFEC contain multiple alternative first exons with restricted and differential tissue distributions, whereas the TFE3 gene seems to be regulated by a single promoter[69].

1.1.3.2 Regulation of TFEB

The major function of TFEB is to regulate lysosome biogenesis and function. Lysosome has been proved to be central in nutrient sensation and autophagy degradation. Therefore, a key point in understanding TFEB regulation is the change of cellular nutrient status. In fully fed cells, TFEB remains in the cytosol and cannot access the promoter region of its target genes. In contrast, upon short times of starvation, TFEB rapidly translocates to the nucleus and induces expression of autophagy and lysosomal genes [70, 71]. Therefore, TFEB can sense and respond to fluctuations of nutrient levels in the cell. [71, 72]. In fully fed cells, mTORC1 phosphorylates TFEB at several serine/threonine residues, including serine 211 (S211) [73]. Phosphorylated S211 functions as a binding site for the cytosolic chaperone 14-3-3, which keeps TFEB sequestered in the cytosol probably through masking the TFEB nuclear import signal. [73]. Settembre et al. [72] used an mTORC1 in-vitro kinase assay and a phosphor-specific antibody to demonstrate that besides S211, S142, previously found to be phosphorylated by ERK2, is also phosphorylated by mTOR and that this phosphorylation site has a crucial role in controlling TFEB subcellular localization and activity.

Interestingly, the Rag GTPase complex, which senses lysosomal amino acids and activates mTORC1, is both necessary and sufficient to regulate starvation- and stress-induced nuclear translocation of TFEB. This Rag-mediated

redistribution of TFEB to the lysosomal surface facilitates the phosphorylation of TFEB by mTORC1 and constitutes an efficient mechanism to link nutrient availability to TFEB inactivation. Inhibition of the interaction between TFEB and Rags results in accumulation of TFEB in the nucleus and constitutive activation of autophagy under nutrient-rich conditions, thus indicating that recruitment of TFEB to lysosomes is critical for proper control of this transcription factor [72]. When nutrient levels are low, mTORC1 is inactivated, the TFEB/14-3-3 complex dissociates, and TFEB is free to translocate to the nucleus and activate processes (such as autophagy and lipid degradation) that will assist in cellular survival during starvation conditions [29]. Since lysosomes play a critical role in the activation of mTORC1, TFEB and mTORC1 would work together as major regulators of cellular homeostasis by coordinating nutrient sensing with transcriptional regulation of lysosomal biogenesis, autophagy, and lipid catabolism.

In addition to mTORC1, other cellular kinases may contribute in regulation of TFEB activation. For example, phosphorylation of Ser142 by ERK2 helps promote cytosolic retention of TFEB [70], whereas TFEB becomes more resistant to degradation upon phosphorylation by PKCβ [74]. Furthermore, cells in which mTORC1 is hyperactivated, such as TSC2-null murine embryonic fibroblasts, TFEB is phosphorylated in several serine residues located between amino acids 462–469, and this modification promotes its nuclear translocation [27]. Self-regulatory mechanism also attributed to TFEB. Under starvation conditions,

TFEB translocates to the nucleus and binds to several CLEAR motifs present on its own promoter, thus enhancing its own expression [75]. The CLEAR network regulation of TFEB is discussed in the next section. It is thought that this auto-regulatory feedback loop is particularly relevant to achieve a sustained response under prolonged starvation conditions.

Activation of TFEB also happens when the lysosome function is affected. Incubation with chloroquine, a lysosomotropic agent that prevents lysosomal acidification, induces rapid redistribution of TFEB to the nucleus [72, 73]. TFEB also shows a predominantly nuclear distribution in several different cellular models of Lysosomal Storage Disorders (LSDs) [76]. LSDs are metabolic disorders characterized by the progressive accumulation of undigested material in lysosomes that subsequently disrupts cellular physiology. These observations suggest that TFEB is involved in a broader pathway of cellular response to lysosomal stress.

1.2.3.3 Downstream Effects upon TFEB Activation

The downstream effects of transcription factor TFEB are mainly targeting at autophagy and lysosome related genes, and lipid metabolism.

Autophagy is a critical cellular process that allows cells to degrade their own components and recycle important molecules in situations of nutrient deprivation.

Many autophagy-related genes (ATG) encode protein complexes that act sequentially to regulate engulfment of portions of the cytosol into autophagosomes and subsequent delivery to lysosomes for degradation. It is important for cells to possess the capability of increasing transcription of autophagy genes when nutrients are deficient as autophagy is a key process in acquiring energy in starvation. TFEB functions as a key transcriptional regulator of autophagy [70]. It directly binds to the TFEB-target sites present in the promoter regions of numerous autophagy genes and promotes their expression. These include UVRAG, WIPI, MAP1LC3B, SQSTM1, VPS11, VPS18, and ATG9B. In addition, its overexpression in various cell lines increases the number of autophagosomes, whereas depletion of endogenous TFEB by RNAi reduces autophagosome numbers [70]. TFEB is not the only transcription factor have effect on autophagy gene regulation. FoxO3, HIF-1, and p53 have also been shown to activate the expression of autophagy genes in response to various stresses [77, 78], However, while FoxO3, HIF-1, and p53 promote expression of genes implicated in the initial steps of autophagosome formation, TFEB appears to have a much broader role since it upregulates a more comprehensive network of autophagy genes. This network not only includes key regulators of autophagosome biogenesis but also proteins required for fusion between autophagosomes and efficient degradation of the autophagic content. In other words, TFEB is a major master autophagy regulator that control both the activation and degradation. In addition, by simultaneously regulating autophagy

induction and lysosomal formation, TFEB plays a unique role in the coordination of the two main degradative pathways in the cell.

As such TFEB can regulate lipid catabolism [75], via the autophagic-lysosomal pathway. It was shown that TFEB is induced by starvation through an autoregulatory feedback loop and exerts a global transcriptional control on lipid catabolism via Ppargc1α and Ppar1α. Thus, during starvation, a transcriptional mechanism links the autophagic pathway to cellular energy metabolism. TFEB's role in lipid metabolism is multi-faceted. Over-expression of TFEB in mouse liver leads to increased expression of genes implicated in different types of lipid breakdown, including fatty acid oxidation, lipophagy, and ketogenesis. TFEB over-expression is sufficient to reverse obesity and metabolic syndrome in mice. However, this rescue is not observed in autophagy-deficient animals (Atg7 −/−), thus suggesting that functional autophagy is essential for the role of TFEB in lipid metabolism. Finally, liver-specific TFEB knockout results in defective degradation of lipids during starvation, further showed the important role played by TFEB in responding to the varying energetic demands of the cell.

TFEB is critical in the regulation of a gene network named CLEAR (Coordinated Lysosomal Expression and Regulation) [79]. The CLEAR gene network and its master gene transcription factor TFEB can regulate lysosomal biogenesis and function. A combination of genomic approaches, including ChIP-seq (sequencing of chromatin immunoprecipitate) analysis, profiling of TFEB-mediated

transcriptional induction, genome-wide mapping of TFEB target sites and recursive expression meta-analysis of TFEB targets, has identified 471 TFEB direct targets that represent essential components of the CLEAR network. This analysis revealed a comprehensive system regulating the expression, import and activity of lysosomal enzymes that control the degradation of proteins, glycosaminoglycans, sphingolipids and glycogen. The CLEAR network also involved in the regulation of additional lysosome-associated processes, including autophagy, exo- and endocytosis, phagocytosis and immune response. Furthermore, non-lysosomal enzymes involved in the degradation of essential proteins such as hemoglobin and chitin are also part of the CLEAR network.

1.1.4. Autophagy, Its Regulation Pathways, and Functions in Liver

1.1.4.1 Introduction

Autophagy is an evolutionarily conserved cellular process essential for development, differentiation, homeostasis and survival. Although the concept of autophagy was established quite early [80], it is only recently that this phenomenon becomes an intensely studied subject for its implications in fundamental cell biology and its roles in the pathogenesis of such disease status as tissue injury, microbial infection, cancer, neurodegeneration, and aging [81].

Autophagy (from the Greek, “auto” oneself, “phagy” to eat) refers to cellular degradation that involves the delivery of cytoplasmic cargo (macromolecules or organelles) to the lysosome. There are three types of autophagy, macroautophagy, microautophagy and chaperone-mediated autophagy[82]. Macroautophagy is a process in which cytosolic materials are sequestered by autophagosomes, which transport them to the lysosome for degradation. Macroautophagy can be activated by many signals and is perhaps the most active form of autophagy in terms of the turnover of the cytosolic materials. The process of microautophagy includes direct engulfment of cytoplasmic cargo at a boundary membrane of the lysosome, which mediate both invagination and vesicle scission into the lumen of lysosomes [83]. Microautophagy is mainly defined in the yeast, but also seen in the mammalian cells [84]. Microautophagy

of soluble substrates can be induced by nitrogen starvation or by rapamycin. Microautophagy process is regarded as a protection mechanism in both mammalian and non-mammalian cells [85]. Similar to macroautophagy, mmicroautophagy is can be either non-selective or selective. Selective microautophagy includes micropexophagy, piecemeal microautophagy of the nucleus, and micromitophagy.[86-88] Chaperone mediated autophagy (CMA) involves direct shuttling of specific proteins across the lysosomal membrane for degradation in the lumen [89]. All the proteins internalized in lysosomes through CMA contain in their amino acid sequence a pentapeptide motif that is necessary and sufficient for their targeting to lysosomes. These sequences can be recognized by chaperone proteins. CMA thus does not involve the formation of non-lysosomal vesicles.

This section will focus on the signaling and role of macroautophagy in liver pathobiology and disease. Macroautophagy, referred to as autophagy here, has been widely studied in the context of liver pathophysiology. In fact, degradation of mitochondria and other intracellular structures was observed in 1960s by Christian de Duve and the colleagues in rat livers perfused with glucagon [90]. Autophagy in hepatocytes can be quite active at the basal stage as well as under stressed conditions, thus contributing to normal hepatocyte functions and pathogenic changes in the liver.

1.1.4.2 The Molecular Mechanism of Autophagosome Biogenesis

The cargo-carrying vesicular structure formed during autophagy is known as the autophagosome. The origin of the autophagosomal membrane has been controversial. Various models have been proposed [91]. These include that the membrane is synthesized de novo and that it is derived from pre-existing cellular membranes such as the endoplasmic reticulum (ER) [92, 93], the Golgi complex [94], the mitochondria [95] and the plasma membrane [96]. Recent studies suggest that the ER is the most plausible candidate for the initial membrane source and/or the platform for autophagosome formation following amino acid starvation [97]. Electron tomography studies found the connection of initial autophagosomal membranes to the ER membranes [98, 99]. An ER membrane structural known as the omegosome identified by the molecule DFCP1 seems to be a site where transition into autophagosomal membrane occurs [100]. In addition, ER-derived COPII-coated vesicles, which bud from a specialized domain of the ER called the ER exit site (ERES), are found to contribute to autophagosome formation [101]. COP II vesicles are generally transporter vesicles, migrating from ER to the Golgi. Consistently, Liang et al used a systematic membrane fractionation approach and identified the ER-Golgi intermediate compartment (ERGIC) as the most efficient membrane substrate for LC3 lipidation by recruiting the key early autophagic factor ATG14 [94]. It has to be noted that membranes other than that of ER could contribute to autophagosome formation and/or maturation at the early or later phase of the

process. This may be particularly meaningful in selective autophagy in which specific subcellular organelles are selectively targeted.

In the past decade, researchers have elucidated key molecular pathways that regulate the autophagy. These cascades consist mainly of Atg (Autophagy) proteins [102]. In mammalian cells, the initiation of autophagosomes requires ULK1 complex [103] and the autophagy-specific Beclin 1 complex, whereas autophagosomal membrane expansion requires two ubiquitin-like conjugation systems, Atg12 conjugation to Atg5 and LC3 conjugation to phosphatidylethanolamine (PE). The ULK complex is composed of ULK1 or ULK2 (the mammalian ortholog of yeast Atg1), FIP200, mAtg13 and Atg101 [104]. The autophagy-specific Beclin 1 complex is composed of Beclin 1 (the mammalian ortholog of yeast Atg6), Atg14, and class III phosphatidylinositol-3-kinase (PI3KC3) subunits Vps34, and Vps15. In response to decreased or increased nutrient and energy supplies, AMP activated protein kinase (AMPK) promotes autophagy, while the mTOR suppresses autophagy, respectively. AMPK can directly activate ULK1 by phosphorylation of the residues Ser^{317} and Ser^{777} while mTOR can inhibit ULK1 by phosphorylation of the residue Ser^{757}, which disrupts the interaction between ULK1 and AMPK [105]. This coordinated phosphorylation is important in autophagy induction. Following amino-acid starvation or mTOR inhibition, the activated ULK1 phosphorylates Beclin-1 on Ser^{14}, which is required for full autophagic induction by enhancing the activity of the ATG14-containing VPS34 complexes [106]. These events occur at the

candidate autophagosomal membranes following the recruitment of the molecular complexes, resulting in an increase of phosphatidylinositol 3-phosphate (PI3P) on these membranes.

Yeast Atg18/Svp1 and its related protein Atg21 both have the Phe-Arg-Arg-Gly (FRRG) motif, through which they can bind PI3P and phosphatidylinositol 3,5-bisphosphate ($PI(3,5)P_2$) [107, 108]. Atg18 localizes to the autophagosome initiation site in the yeast cells or the endosomes, and regulates the autophagy and vacuolar morphology through binding with PI3P and $PI(3,5)P_2$, respectively[109]. Atg2, an Atg18-interacting protein of ~200 kDa, is also important for the localization of Atg18 to the autophagy site in the yeast [110]. There are four mammalian Atg18 homologs, WIPI1, WIPI2, WIPI3 and WIPI4. However, it seems that only WIPI2 is recruited to the autophagosomal membranes via binding to PI3P [111](Sharon Tooze). WIPI2b can then recruit Atg16 complex onto the membranes via its interactions with Atg16 [112].

The latter is in a complex with the conjugated Atg12-Atg5. Conjugation of Atg12, a ubiquitin-like molecule, to Atg5 requires Atg7, a molecular similar to the ubiquitin-activating enzyme (E1), and Atg12, an E2-like molecule. The Atg12-Atg5 complex then binds to Atg16 to form a multimer-complex in which two units of Atg12-Atg5-Atg16 are presents [113]. Another ubiquitin-like pathway involves the conjugation of LC3 and several other yeast Atg8 homologs, also ubiquitin-like molecules, to phosphatidylethanolamine (PE) on autophagosomal membranes,

through the effect of Atg7, and another E2-like molecule, Atg3 [113]. Notably, the Atg5-Atg12-Atg16 complex is required for the efficient conjugation of LC3 to PE, thus acting like an E3 ligase functionally [114]. This requirement may also ensure that LC3 conjugate to the candidate autophagosomal membrane where Atg5-Atg12-Atg16 is located due to the interaction with AIPI2b [115]. The conjugation of LC3 is required for the autophagosomal membrane to expand and to complete the formation of the vesicular structure. The Atg5-Atg12-Atg16 complex disengages the membranes after LC3 is conjugated. These molecules are thus associated only with the early autophagosomal membrane and are considered as its markers. LC3 and other Atg8 homologs remains on the autophagosomes and are considered as the general marker of autophagosomes from the early to the later stage [116].

While there is only one Atg8 in the yeast, there are at least six Atg8 homologs in mammalian cells, which include three LC3 subfamily members (LC3A, LC3B, and LC3C), and three GABARAP subfamily members (GABARAP, GABARAP-L1/Atg8L, and GABRAP-L2/GATE16). Before activation by Atg7, Atg8 molecules have to be first processed by a cysteine protease, Atg4, at a conserved glycine site. This exposed glycine is required for these molecules to be conjugated to PE [116, 117]. There are four mammalian homologues of Atg4 including Atg4A, 4B, 4C, and 4D. Their cleavage activity is different with Atg4A mainly targeting to the GABARAP subfamily proteins while Atg4B can effectively cleave all but more so toward the LC3 subfamily members [118].

Atg9 is another important molecule for autophagosome expansion. Since it cycles between the initiation site and different cytoplasmic membranes [119], it has reasonably been assumed to be associated with membrane that contributes to autophagosomes. Recent studies in yeast suggested that tubulovesicular structures containing Atg9 are delivered to the initial membrane [120]. Mammalian Atg9 (mAtg9) was more recently implicated in autophagy. Under normal growth conditions, this transmembrane protein, which is synthesized in the ER, localizes to the Golgi complex, the trans-Golgi network, and the late endosomes. Following amino-acid starvation, this protein translocates to LC3-labeled autophagosomes in an ULK1- and PI3K-dependent manner [121]. Cycling of mAtg9 is negatively regulated by p38α MAPK, which competes with mAtg9 for binding to p38IP [122].

After autophagosome are formed, they migrate to where lysosomes are located and engaged in the fusion with the later form the autophagolysosome, in which the content of the autophagosome is degraded. The cytoskeleton seems to be involved in the movement of autophagosomes, which tend to be distributed closer to cell surface, toward the perinuclear region, where the lysosomes are enriched. Agents such as nocadazole, which are microtubule poisons, can block fusion of the autophagosome with the lysosome, perhaps by preventing the movement of autophagosomes. Numerous molecules can participate in the fusion process, including the Rab family GTPase Rab7, Sec18, the SNARE proteins Vam3, and the class C Vps/HOPS complex proteins. Recent findings

have identified syntaxin 17 (Stx17) as the autophagosomal SNARE required for fusion with the endosome/lysosome [123]. Stx17 localizes to the outer membrane of completed autophagosomes, interacts with SNAP-29 and the endosomal/lysosomal SNARE family molecule, VAMP8. Stx17 has a unique C-terminal hairpin structure mediated by two tandem transmembrane domains containing glycine zipper-like motifs, which is essential for its association with the autophagosomal membrane.

Once fused, the inner membrane of the autophagosome and the cytoplasm-derived materials contained in the autophagosome are degraded by lysosomal/vacuolar hydrolases i.e. Cathepsin B, Cathepsin D. Monomeric units of the digested macromolecules, such as amino acids, are exported to the cytosol for reuse.

1.1.4.3 Regulation of Autophagy by Metabolic and Stress Pathways

The process of autophagy is well regulated. Multiple stimuli can promote or inhibit autophagy via different mechanisms. Nutrient deprivation is one of the best known autophagy stimulators. Other autophagy inducers include ER stress, oxidative stress, DNA damage [124]. The presence of extracellular nutrients (i.e, amino acids, fatty acid, and glucose) and growth factors (e.g., insulin and insulin-like growth factor) can inhibit autophagy. The Class I phosphatidylinositol 3-kinase (PI3K) and the mammalian target of rapamycin (mTOR) are major

inhibitors of autophagy along the signaling pathways mediated by nutrients and growth factors [125]. AMPK, being a inhibitor of mTOR, can also promote autophagy. It seems that AMPK is particularly responsive to glucose level, and is thus responsible for autophagy triggered by glucose-deprivation [126]. As discussed above, AMPK and mTOR can directly modulate ULK1 and Beclin 1 complex to regulate autophagy induction.

ER stress is another well-known autophagy inducer. The ER is the key compartment in the cell to facilitate folding of newly synthesized proteins and initiate the pathway of vesicular movement of membrane and proteins to various organelles and the cell surface. A number of factors can serve as ER stress stimuli, including expression of aggregate-prone proteins, glucose deprivation (resulting in reduced glycosylation and decreased energy for chaperone activity), hypoxia and oxidative stress (causing decreased disulfide bond formation), Ca^{2+} efflux from the ER and inhibition of proteasomes, all leading to the accumulation of unfolded proteins in the ER [127]. When the folding capacity of ER is exceeded, the unfolded protein response (UPR) signaling is triggered. Mammalian UPR involves three distinct downstream pathways mediated by IRE1 (similar to yeast Ire1), ATF6 (activating transcription factor 6), and PERK (RNA-dependent protein kinase-like ER kinase), respectively. UPR causes a general reduction of protein synthesis but activation of the transcription of a selective group of proteins to increase ER folding capacity and degradation of unfolded or mis-folded proteins. The latter is mainly mediated by the proteasome, known as

the ER-associated degradation (ERAD), but also by autophagy, known as ER-associated autophagy (ERAA), particularly in the condition when the proteasome is suppressed [128-130]. It seems that mTOR is eventually suppressed, thus causing autophagy activation [131].

1.1.4.4 Autophagy in Liver Diseases-General Introduction

Among the body organs, liver seems to possess the highest protein turn-over rate, which mainly depends on autophagy. During starvation, mouse liver's protein degradation rate increases from 1.5% of total liver protein per hour to 4.5% per hour. If mice are starved for 48h, 40% of total protein in liver will be degraded [132, 133]. The high autophagy degradation rate is ensured by the abundant presence of lysosomes in the liver.

As discussed above, Atg7 and Atg5 are very important autophagy core proteins due to their roles in the conjugation reactions. Mice lacking Atg7 or Atg5 have severe hepatomegaly, and livers can weigh as much as 30% of the body weight [134, 135]. Hepatocytes contain mitochondria and peroxisomes with marked structural alterations, as well as abundant amounts of polyubiquitinated proteins. One of the significantly accumulated proteins is SQSTM1/p62. This protein is able to polymerize via an N-terminal PB1 domain and can interact with ubiquitinated proteins via the C-terminal UBA domain. SQSTM1/p62 can bind directly to LC3 and GABARAP family proteins via a specific sequence motif [136].

The protein is itself degraded by autophagy and may serve to link ubiquitinated proteins to the autophagic machinery to enable their degradation in the lysosome. The accumulation of the misfolded polyubiquitinated proteins in the Atg7-deficient mice could be eliminated by a co-deletion of SQSTM1/p62, supporting its role in the liver pathogenesis caused by Atg7-deletion [137]. Furthermore, accumulated p62 could interact with Keap1, releasing Nrf2 to dramatically increase Nrf2-dependent biological activity [138]. Although it is not quite understood, the liver injury caused by Atg5 or Atg7 deletion could be also reversed with the deletion of Nrf2 [138], suggesting that Nrf2 can mediate the liver injury phenotype in the absence of autophagy function.

Traditionally autophagy is viewed as a non-selective process under nutrient deprivation condition. The non-selective bulk degradation of cytoplasm and organelles by autophagy can provide the basic building materials to support anabolic metabolism during starvation. However, selective removal of specific organelles by autophagy has now been well recognized [139]. All major organelles could be specifically targeted by autophagy, including mitochondria (mitophagy), ribosomes (ribophagy), endoplasmic reticulum (ER-phagy), peroxisomes (pexophagy), and lipid droplets (lipophagy). The selective functions of autophagy indicate that it is important for maintaining cellular homeostasis by removing superfluous or injured organelles.

Selective autophagy can be important in liver disease. Autophagy induced by ethanol seems to be selective for damaged mitochondria and accumulated lipid droplets, but not long-lived proteins [140]. Hepatitis C Virus (HCV) induces intracellular events that trigger mitochondrial dysfunction and can induce mitophagy, this process is evidenced by the colocalization of LC3 puncta with Parkin-associated mitochondria and lysosomes [141]. Similarly, HBV can also induce mitophagy and attenuates apoptosis [141]. Other researchers found mitophagy sometimes is harmful to liver instead of protection. Cadmium-induced hepatotoxicity is one of the examples: Cadmium induces mitochondrial loss via the over-activation of mitophagy following dynamin-dependent mitochondrial fragmentation, which seems to be the main mechanism of its liver toxicity [142].

One major function of liver is drug metabolism. A well-studied example is the induction of the cytochrome P-450 system by phenobarbital (PB)[143]. Notably, this is usually accompanied by extensive proliferation of smooth ER, where the catabolic reactions occur. Interestingly, smooth ER membranes could be selectively sequestrated by autophagic vacuoles. This is perhaps the first demonstrated example of selective autophagy. The removal of extra ER membranes through autophagy, known as ER-phagy, was later on confirmed by detailed morphological studies as well as biochemical studies. In the latter, 2 typical ER membrane proteins, PB-inducible cytochrome P-450 and NADPH-cytochrome P-450 reductase, were found to be selectively degraded by autophagy in rat liver following phenobarbital withdrawal [144]. Thus, autophagy

is important for the recovery of normal ER structure and function after drug treatment in order to avoid potential cellular dysfunction.

1.1.4.5 Autophagy and Alcoholic/non-alcoholic Fatty Liver Disease

Alcoholic fatty liver disease (ALD) and non-alcoholic fatty liver disease (NAFLD) share similar pathological changes that involve steatosis, inflammation, fibrosis and cirrhosis. Autophagy has been found to be affected by the fatty liver disease and has been found to play important roles in the development of the disease. Autophagy function can vary in alcoholic livers depending on the stage. Acute alcohol treatment activated hepatic autophagy in vivo and in cultured primary hepatocytes, which required ethanol metabolism, generation of reactive oxygen species, and inhibition of mammalian target of rapamycin signaling [140, 145]. Suppression of autophagy with pharmacologic agents or small interfering RNAs significantly increased hepatocyte apoptosis and liver injury; autophagy therefore protected hepatocytes from the toxic effects of ethanol.

Chronic alcoholic treatment using the Lieber-DeCarli model also showed an elevation of autophagy when ethanol was given at a lower level (accounting for 29% of the caloric need), but signs of suppression when ethanol was given at a higher level (accounting for 36% of the caloric need) [146]. However, in both cases, suppression of autophagy exacerbated liver injury while enhancement of autophagy improved the condition. Chronic alcoholic treatment can lead to

decreases in both the number and the function of the lysosome, therefore reducing autophagic degradation [147]. Early studies showed the rate of hepatic protein degradation in EtOH-fed animals could decline significantly [148], which may be due to declines in both proteasome and autophagy function, contributing to the development of hepatomegaly and the development of Mallory-Denk body (MDB), a characteristic of alcoholic liver disease. MDB is positive for ubiquitin and p62/SQSTM1, a condition found in protein aggregates, which is often seen in autophagy deficiency. Indeed, by augmenting autophagy using rapamycin, an mTOR inhibitor, clearance of MDB can be achieved in a mouse model of MDB pathology [149].

NAFLD is more prevalent in the content of the metabolic syndrome together with obesity and diabetes [150], and accounts for 75% of all chronic liver disease. There is no effective therapeutic approach for NAFLD [151, 152]. Multiple etiologies and regulatory disturbances can be involved in the pathogenesis of NAFLD. Autophagy can affect, and in turn can be affected by, NAFLD. Mice with a hepatocyte-specific deletion of Atg7 developed markedly hepatic steatosis, which was exacerbated by high fat diet-feeding [153]. Conversely, in both genetic and dietary models of obesity, autophagy was suppressed in the liver at least in part due to a reduction in the expression level of key autophagy molecules, such as Atg7 [154]. Autophagy deficiency was accompanied with defective insulin signaling and elevated ER stress. Restoration of Atg7 expression in liver resulted in reduced hepatic steatosis, dampened ER stress,

enhanced hepatic insulin action, and systemic glucose tolerance in obese mice. The beneficial effects of Atg7 restoration in obese mice could be completely prevented by blocking a downstream mediator, Atg5, supporting its dependence on autophagy in regulating insulin action. These data indicate that autophagy is an important regulator, not only for the hepatic phenotype of the obesity, but also for the other metabolic disturbances, such as insulin resistance [154], which are often associated together [155].

In the development of NAFLD, autophagy can be regulated through different pathways and regulators, including the classic insulin-mTOR pathway [156]. More recent works have identified new regulators, such as p73, a member of the p53 tumor suppressor family. Mice functionally deficient in all the p73 isoforms exhibit decreased Atg5 expression and lower levels of autophagy in livers, and increased steatosis [157]. P73 can transcriptionally regulate the expression of Atg5. In a different scenario, stimulation of fatty acid β-oxidation by thyroid hormone (TH) is coupled with induction of hepatic autophagy, facilitating the delivery of fatty acids to mitochondria [158]. Blockade of autophagy markedly decreased TH-mediated fatty acid β-oxidation in both cell cultures and in animals. Consistent with this model, autophagy was altered in livers of mice expressing a mutant TH receptor that causes resistance to the actions of TH as well as in mice with mutant nuclear receptor corepressor (NCoR). These results demonstrate that THs can regulate lipid homeostasis via autophagy and help to explain how THs increase oxidative metabolism in liver.

Conversely, the fatty liver condition has significant effects on hepatic autophagy function. Steatosis can impair autophagic degradation. p62/SQSTM1, an autophagy adaptor molecule, was accumulated in the liver of Ob/Ob mice, suggesting a deficiency in autophagic degradation [159]. Indeed, the hepatic levels of cathepsin B and L in Ob/Ob mice and NAFLD patients were reduced, accompanied with a reduced lysosome proteolytic activity. In NAFLD patients, p62 aggregation was correlated with serum alanine aminotransferase value and inflammatory activity by NAFLD score [160]. In addition, the fusion between the autophagosome and the lysosome can be compromised by the excessive amount of lipids [161]. Hepatic lysosomal and autophagic compartments isolated from mice under different hepatic steatosis conditions had different levels of fusion. Increases in lipid concentration suppressed autophagosome/lysosome fusion up to 70% of that observed in untreated fractions or from animals under a normal regular diet. Furthermore, hepatic transcription levels of certain key autophagy genes could be suppressed in high fat diet fed mice, which seemed to involve the FoxO1-mediated transcriptional regulation [156, 162]. Finally, abnormal activation of protease, such as calpain, in fatty liver can significantly reduce the protein level of key autophagy molecules, including Atg5, Atg7 and Beclin 1, leading to a compromised autophagy function [154].

How autophagy may affect the pathogenesis of fatty liver condition is not quite clear. However, one of the main features of fatty liver is the excessive accumulation of fatty acids. Free fatty acids can be detrimental to hepatocytes.

The esterified form sequestered in lipid droplets (LD) would be considered non-harmful, although de-esterification can occur, which would increase cellular free fatty acids level. Removal of lipid droplet may favor the equilibrium toward the formation of lipid droplets. Autophagosomes can transport the content of lipid droplets the lysosome in which lipids are degraded by the lysosomal acid lipase. This process is known as lipophagy [153]. Lipophagy is a type of selective autophagy processes but it is not clearly how autophagosomes recognize lipid droplets. Colocalization of an autophagosome marker, LC3 and lipid droplet can be demonstrated in vivo and in vitro [140, 146, 153, 163]. Hepatic TG level in either alcoholic or non-alcoholic fatty liver disease models can be reduced by activating autophagy, or is elevated when autophagy is inhibited [140, 146, 153].

Autophagy may also promote clearance of damaged mitochondria, a select autophagy process known as mitophagy, to protect against disease progression. This may be particularly relevant in alcoholic fatty liver disease in which mitochondrial damage is more apparent [164]. It is found that autophagy induced by acute ethanol administration did not influence much the turnover of long-lived proteins [140]. But mitophagy is clearly present based on the colocalization of an autophagosome marker, LC3, and the mitochondria in a lysosome function-dependent manner. Damaged mitochondria are prone to free radical generation and promote cellular injury. Mitophagy could thus protect against this type of cellular injury.

The benefits of autophagy in protecting against ALD and NAFLD suggest that it may be possible to pharmacologically elevate or restore autophagy function to improve the liver status. Indeed, applications of clinical available agents, such as rapamycin and carbamazepine, in mouse models of ALD and NAFLD have demonstrated the anticipated benefits [146]. These findings provide a basis for the future exploration of this approach in clinic.

1.2. Materials and Methods

1.2.1 Animal Experiment

All animal experimental protocols were approved by the Institutional Animal Care and Use Committee of Indiana University (IACUC). Animals were housed under approved conditions in a secured animal facility at the Indiana University School of Medicine with 12 hour light dark cycle. Bid knockout mice were generated in our lab. Wild type mice were purchased from Jackson Animal Laboratory. At 8 weeks of age, mice were placed on normal chow diet, high fat diet (diet D12492, Research diets) for different durations. Animals were provided ad libitum access to these diets.

1.2.2 Immunoblotting

Mice liver was dissected and 250 mg of liver tissue was homogenized in NP-40 lysis buffer containing 1% NP-40, 50mM Tris-Hcl (pH 7.5), 150mM NaCl, 0.05% SDS, 1mM aprotinin, 20ug/ml PMSF, 1.7ug/ml Aprotinin, 2.5ug/ml Leupeptin, 1ug/ml Pepstatin A and supplemented with 1 tablet per 10 ml Complete Mini Protease Inhibitor Cocktail (Roche, Mannheim, Germany). Mice liver tissue was dounced for 15 times using tight (B) pestle of a glass homogenizer. Liver lysate was kept in pre-chilled Eppendorf tube on ice for 40 min. After centrifugation at 15 000 × g for 15 min at 4°C, the supernatant was stored at −80°C until further

us. Protein concentration were measured by BCA method. Immunoblots with SDS-PAGE electrophoresis system were performed as previously described. Gel Running buffer contains 25 mM Tris Base, 192 mM Glycine, 0.1% SDS at PH 8.2. Transfer buffer contains 25 mM Tris Base, 192 mM Glycine and 20% methanol (v/v). Transfer condition: 7 volt overnight/ 20 volt 2.5h. First antibody was dissolved in 5% Skimmed milk in TBS buffer or 5% BSA in TBS buffer. 2nd antibody from Jackson Laboratory was used at 1:5000 dilution. P-P70S6K antibody: Cell Signaling 9234 used in dilution of 1:1000. T-P70S6K antibody: Cell Signaling 9202 used in dilution of 1:1000. P62/SQSTM1 antibody: MBL PM045 used in dilution of 1:1000. LAMP1 antibody: U of Iowa 1D4B used in dilution of 1:1000. Atg7 antibody: Cell Signaling 2631 used in dilution of 1:1000. Beclin1 (BECN1) antibody: Santa Cruz S11427 used in dilution of 1:1000. Actin antibody: Sigma A5441 used in dilution of 1:5000. TFEB: Abcam 113372 used in dilution of 1:1000. Blots were developed by Immobilon Chemiluminescent HRP substrate (Millipore). Image was acquired by Kodak 4000 image station system.

1.2.3 Immunostaining and Bodipy Staining

Briefly, slides containing 5μm cryosection prepared from frozen liver tissue was soaked in PBS and subjected to antigen retrieval using Citrate buffer pH 6.0. Slides were blocked with 5% serum/PBS containing 0.1% Triton X (PBS-Tx) for 1 h and then incubated with primary antibody diluted in 5% serum/PBS-Tx for 2 h at room temperature or overnight at 4^{o}C. Sections were washed in PBS-Tx,

following by incubation with fluorescence conjugated secondary antibody and nuclear staining by using Hoechst 33342 (1μg/ml). Fluorescent images were obtained using a Nikon Eclipse TE 200 immunofluorescence microscope. TFEB immunofluorescent antibody: Santacruz SC11009 was used in dilution of: 1:200. For Bodipy staining, liver tissue were fixed in 4% PFA for 4h, fixed tissues were subjected to gradient sucrose washing (5%-20%). Liver tissues were than fixed in OCT and subjected to cutting by Indiana University Health Pathology Laboratory. Bodipy (493/503) was dissolved (0.1mM) in 0.4% Triton X-100 and stained for 10 min.

1.2.4 Histology

Different tissues from mice were harvested, washed with ice-cold PBS, and fixed in 10% formalin overnight and transferred to 70% ethanol the next day. Tissue blocks were processed by Indiana University Health Pathology Laboratory. Histochemical analysis was carried out on 4-um-thick sections using hematoxylin and eosin (H&E) and images were taken by Nikon Eclipse E200 microscope.

1.2.5 ALT, Triglyceride and Cholesterol measurement

Serum glutamic-pyruvic transaminase (SGPT) or alanine aminotransferase (ALT) were measured by ALT (SPGT) reagent kit (Pointe Scientific, Canton, MI).Briefly, serum was diluted for five times and samples were read in 340nm absorbance at

37C. Plasma triglyceride and cholesterol level were measured by Triglyceride/ Cholesterol kit (Pointe Scientific, Canton, MI).

1.2.6 Hepatic Triglyceride Measurement

80mg of frozen liver tissue were powdered under liquid nitrogen and incubated for 1 hour at room temperature with shaking to extract the lipid phase in total of 1ml of chloroform-methanol mix (2:1). After addition of 200ul of H2O, samples were vortexed and centrifuged for 5min at 3000g. The lower lipid phase was collected and dried in hood overnight. The lipid pellet was resuspended in 60ul of tert-butanol and 40ul of a Triton X-114-methanol (2:1) mix. Triglycerides were than measured using the Pointe Scientific Triglycerides kit (Pointe Scientific, MI)

1.2.7 Lysosome Enzyme Activity Assay

Briefly, Liver tissue were homogenized using lysis buffer: Cathepsin B/D/E (0.1 M Sodium acetate 0.1 M Sodium chloride, pH 4.0), lysosomal acidic lipase (0.2 M Sodium acetate, Tween-80 0.1ul/ml, pH 5.5), and acidic phosphatase using assay kit (Sigma CS0740). Protein concentration of each sample were measured for standardization. Substrate and reaction buffer for each enzyme were added to reaction mix and incubate at 37^{o}C for 45 min or 90 min (lysosomal acidic lipase). Plate were read in Tecan 96-well plate reader. Acidic phosphatase: absorbance

OD405, Cathepsin D/E: Ex: 365nm, Em: 440nm, Cathepsin B: Ex: 365nm, Em: 440nm, Lysosomal acidic lipase: Ex: 327nm, Em: 449nm at 90min.

1.2.8 Human Patient Study

Liver biopsy samples from NAFLD clinically diagnosed patients in Indiana University Health were collected in Division of Gastroenterology and Hepatology. Clinical data acquisition was approved by Office of Research Administration of Indiana University. TFEB antibody: Abcam 113372 used in dilution of 1:100

1.2.9 Gene Expression Analysis: Real-time PCR

Liver tissue total RNA was extracted with GeneJET RNA purification kit (Thermo Scientific). Briefly, 30mg of frozen tissue were lysed by lysis buffer provided by kit, 600 ul of proteinase K were added and subsequently centrifuged for 12000g. Next, 450ul of ethanol were used and lysates were subjected for series washing by washing buffer provided by kit for RNA purification. RNA quality and concentration/amount was /quantified by A260/A280.

Next, 5ug of RNA was reverse transcrived by M-MLV reverse transcriptase (Invitrogen), procedures were followed by manual from the supplier. For RT PCR amplification of target genes, Applied BioSystem and AmpliTaq Fast DNA polymerase were used for 40 cycles, temperature and duration were set

according to the manual. ---Analysis was performed by the 2ΔΔCT method. QPCR results were normalized against gene PPIA

Primer sequences used for the amplification are as follows:

ATP6V0D2 Fw - 5'-AAGCCTTTGTTTGACGCTGT-3'

Rv - 5'-TTCGATGCCTCTGTGAGATG-3'

Cathepsin B (CTSB) Fw-5'-AAAAAGGCCTGGTTTCAGGT-3'

Rv-5'-GGGAGTAGCCAGCTTCACAG-3'

Cathepsin D (CTSD) Fw-5'-TCAGGAAGCCTCTCTGGGTA-3'

Rv-5'-CCCAAGATGCCATCAAACTT-3'

Lysosomal Acidic Lipase (LIPA) Fw-5'-AAGGTCCCAGACCAGTTGTG-3'

Rv-5'-TGTGCTTCAGAGACCAGGTG-3'

Acid Phosphatase (ACP2) Fw-5'-GAGCCTGTCATACCCAAGGA-3'

Rv-5'-AACATGGTGGTAGCCAGGAG-3'

1.2.10 Statistical Analysis

Data were expressed as mean±SE. Differences between two treatment groups were compared by t test. When more than two groups were compared, on way ANOVA analysis was used. Results were considered statistically significant when $P<0.05$. All analyses were performed with Sigma Stat 3.5.

1.3 Results:

1.3.1 The mTOR Activity Oscillates Under the Sustained Hyper-nutrition Condition.

Excessive nutrition uptake is perhaps the most common cause of metabolic syndrome and non-alcoholic fatty liver disease (NAFLD). mTOR, as one of the most important molecules responsive to cellular nutrient status, is known to play a role in the development of NAFLD. We reasoned that its activity was likely changing in response to the change in nutrient supply. To examine this hypothesis, we fed mice with high fat diet for up to 32 weeks and collect samples at varies time points to examine the mTOR activity in correlation with hepatic steatosis.

When activated, mTOR phosphorylates p70S6 kinase as its main target. The mTOR activity could be indicated by level of the phosphorylated p70S6 kinase (pp70S6K). A higher mTOR activity was reflected by a higher level of pp70S6K normalized by the level of total p70S6K. Conversely, a reduced mTOR activity was indicated by a lower level of pp70S6K. When pp70S6K level, as measured by immunoblotting essay (Fig 1A) and densitometry (Fig 1B), was plotted against the duration of HFD feeding, a damping oscillation pattern was observed (Fig 1C). pp70S6K was steadily increased in the first 3 weeks of HFD feeding, but became reduced by 6 weeks and bottomed out at 10 weeks. However, pp70S6K

level was increased again at 16 week of feeding, reduced again at 24 weeks, and returned to a higher level by 32 weeks. This oscillation pattern, however, is reduced in magnitude over the time. Therefore it is mathematically known as the damping oscillation. In order to further confirm the oscillation pattern of mTOR activity, we also stained the liver sections obtained from mice fed with regular diet or HFD for 3wk or 10wk for phospo-S6. As shown in Fig 1D, the phosphorylated S6, which is a target of p70S6K downstream of mTOR first increased in 3wk but then suppressed on the10wks samples.

1.3.2 TFEB is Activated in an Oscillation Pattern Under the Sustained Hyper-nutrition Condition.

Transcription Factor EB (TFEB) is a master transcription factor for lysosome function and biogenesis. More importantly, TFEB itself can be directly phosphorylated by mTOR at specific sites and becomes trapped in the cytosol, unable to activate its target genes [72]. Using the same groups of mice that were studied for mTOR activity (Fig 1), we conducted TFEB immunostaining on the cryosections of the liver (Fig 2A). As indicated in the quantification analysis, the percentage of cells with nucleus TFEB location, also showed a dynamic oscillation pattern (Fig 2B), but in a direction opposite to that of p70S6K phosphorylation. TFEB was more likely found in the nucleus of mice fed with regular diet but it moved out to the cytosol when mTOR was activated, e.g. at 3wk and 16wk of high fat diet feeding. TFEB was back to the nucleus when mTOR was suppressed, i.e. at HFD 10wk. Interestingly, the percentage of cells with TFEB-positive nuclei after 10wks of high fat diet treatment was even higher than that in mice given regular diet (Fig 2B), implicating that other possible regulations of TFEB may exist. Nucleus location of TFEB also showed a pattern of damping oscillation (Fig 2C). To test whether this dynamic change of TFEB location had any physiological impact, we also measured the expression of representative lysosomal enzyme genes by RT-PCR (Fig 2D). Correlated with TFEB location, the expression of three genes, lysosomal acidic lipase, cathepsin D and acidic phosphatase had all dynamic pattern. Another lysosomal membrane

protein gene, ATP synthase A6, didn't show similar pattern. Its expression was lowest in 10wks and started to recover in 16wks after HFD feeding, indicating a possible delayed regulation by TFEB.

1.3.3. Lysosomal Functions Oscillate during Long-term High Fat Diet Feeding.

Consistent with the nucleus location of TFEB and the lysosomal gene expression, the activities of cathepsin B, cathepsin D/E, lysosomal acidic lipase and acidic phosphatase all oscillated in the same (Fig3A-D).

Another major function of TFEB is to regulate lysosome biogenesis. Thus, we examined the level of a major lysosomal marker LAMP-1 by immunoblotting analysis (Fig3 E). Densitometry analysis (Fig 3F) indicated that expression of LAMP-1 also showed a dynamic change at different time of high fat diet treatment.

Because mTOR negatively regulates TFEB function, the oscillation of the lysosome activity was the opposite in direction of that of mTOR activity. However, reduced mTOR activity can in turn leads to the suppression of mTOR activity as the action of mTOR requires a normal lysosomal function (see introduction). Thus we think the change in lysosome enzyme activity not only regulate the lysosome degradation capability, but also contribute to the damping oscillation pattern of mTOR in Fig 1.

1.3.4. Autophagy Degradation is Dynamically Regulated.

Autophagy process is one of the major downstream events regulated by the mTOR complex 1. It can be directly suppressed by mTORC1 activation. Autophagy function has also been shown to be both altered by and contributed to NAFLD development. Autophagy's contribution to NAFLD is mainly mediated by the lipophagy process [153]. But autophagy process can also be affected by excessive lipids in the cell. Previous studies have shown that the autophagy process either was activated [165] or suppressed [159], leaving some controversies in findings. It was not known how autophagy may be affected by high fat diet. We thus examined the autophagy activation and degradation at different time points. GFP-LC3 mice were fed with regular diet or high fat diet for different times. Chloroquine (CQ) was given (i.p) 16 hours before sacrifice to suppress the lysosome function and thus autophagic degradation in the liver. As shown in Fig 4A and B, autophagosomes were represented by GFP-LC3 dots. The number of GFP-LC3 dots per cell was increased after high fat diet treatment. However, further treatment with CQ did not give rise to a significantly higher increase, as would be expected in an activation status. In contrast, the increment of the increase following CQ treatment in the high fat group was smaller than that in the regular diet (Fig 4B), which was not due to the aging of the mice since mice at the same age but fed with regular diet did shown a significant increase in GFP-LC3 dots upon CQ treatment (Fig 4A, C). The incremental changes between these groups were the base for us to calculate the level of autophagy

activation and autophagy degradation capability (see Figure 4 legend for the detailed description of the formula). The result showed that activation of autophagy was suppressed through the duration of high fat diet (Fig 4D). However, the capability of the degradation of autophagosome was suppressed at 0.5, 3wk and 16wk, but recovered at 1wk and 10wk of high fat diet feeding. The gain in the degradation occurred at 10wk (Fig 4E), in parallel with the lysosomal function. Notably, several autophagic molecules did not alter significantly in the expression during the same course (Fig 4F), suggesting that the change of autophagy degradation is mainly due to the change in lysosome function.

1.3.5. Degradation of Lipid Droplets by Lipophagy during NAFLD Development.

Autophagy, more specifically, lipophagy, has been shown to be important in lipid degradation by the autophagosome-lysosome pathway [166]. Promotion of autophagy in NAFLD could ameliorate the disease [146]. As we have discussed in Figure 4, the autophagy degradation capability was reduced but periodically rebounded. We wanted to understand whether this oscillation pattern in long term high fat diet treatment had same effects on fatty liver development. Therefore, we examined the lipid content of the liver at different times after high fat diet with or without CQ treatment. Cryosections of the liver were stained and the intrahepatic lipid droplets were quantified (Fig 5A, B). Generally, autophagic degradation relies on the intact function of lysosome, inhibition of the lysosome function with CQ would suppress lipophagy leading to an increase in LD numbers. We found that after CQ treatment, the lipid droplet numbers were increased but to different degrees in mice with high fat diet treatment for different durations. Thus, the degradation of lipid droplet was relatively small in amount on 0.5wk, 1wk high fat diet regimen, but fell to nearly zero on 3wk regimen, which was observed again by 10wk but decreased again by 16wk of feeding (Fig 5C). Notably, those changes shared the same trend with autophagy degradation (Fig 4E), and lysosomal function (Fig 3). These findings indicated that autophagy degradation capability directly impacted lipid amount within the hepatocytes.

As a further confirmation of the finding made with the Bodipy staining method, we measured the level of hepatic TG in the same group of mice. Consistent with the staining, hepatic TG showed same dynamic changes at different time points of high fat diet treatment (Fig 5D).

Severe steatosis, can lead to steatohepatitis and liver injury, the next stage of NAFLD, steatohepatitis. In order to check whether autophagy degradation affects liver injury, we measured serum ALT level. As shown in Fig 5E, CQ co-treatment exacerbated the injury. The trend correlated well with that of autophagy degradation and lysosome function in that there was more injury at 10wks, but less injury at 3 and 16wk of high fat diet treatment that was affected by autophagy or lysosome function. These data suggest that the dynamic of autophagy in high fat diet regimen regulates the dynamic development of NAFLD at the early stage.

1.3.6. The Subcellular Location of TFEB Location Correlates Highly with NAFLD and Obesity in Human.

We found that TFEB exhibited dynamic translocations in and out of the nucleus under the sustained hypernutrient condition in mice (Fig2), which was inversely correlated with the mTOR activity (Fig1) but positive correlated with hepatic lipid droplet degradation (Fig 5). We hypothesized that the subcellular location of TFEB could be a sensitive marker for hepatic steatosis in human patients as well. Thus we collected, and stained with an anti-TFEB antibody on liver biopsy samples from patients who had been diagnosed of NAFLD or NASH. Indeed, we found that TFEB location in hepatocytes was negatively correlated with the severity of steatosis, which was scored using NAFLD scoring system published by Non-alcoholic Steatohepatitis Clinical Research Network [167] (Fig 6A-B). Those patients with low steatosis scores had a higher percentage of hepatocytes that stained positive for nuclear TFEB, whereas patients with high steatosis score had a lower percentage of hepatocytes with nuclear TFEB staining. More interestingly, the correlation was stronger when patients younger than 35 years old were excluded. Excluding the young patients, the correlation coefficient reaches -0.91 (Fig 6C).

We also studied the correlation of TFEB nuclear location with BMI, which assesses the severity of obesity. Surprisingly, we found that TFEB nuclear location was only mildly correlated with BMI, which become more strongly

correlated under the circumstance when younger patients and a patient who had discordant obesity and steatosis were excluded (Fig 6D and E). We then compared the TFEB staining pattern with other clinical parameters. TFEB nuclear location was negatively correlated with serum cholesterol (Fig 6F), but had no correlation with serum TG, ALT or AST (Fig 6G, H, I). Consistent with the TFEB study in the mouse model of NAFLD, these results suggest that TFEB is potentially a sensitive marker for steatosis, especially in high nutrition/obesity induced steatosis in middle-aged and elderly patients. But it may not be correlated with liver injury or steatohepatitis, a later stage of NAFLD.

1.3.7. Suppression of mTOR Activity Promotes TFEB Translocation to the Nucleus and Rescues the Lysosome Function in the Fatty Livers.

Previous reports have shown that mTOR can directly suppress TFEB by phosphorylation [72]. In order to check whether TFEB nucleus location is due to mTOR activation under high fat diet regimen, we pharmacologically suppressed mTOR activity using rapamycin. We specially designed an administration strategy so that rapamycin was given at the time point when mTOR was highly activated, i.e. at 3wk or 16wk after High fat diet treatment. As shown in Fig 7A, both dosage of 2mg/kg and 4mg/kg successfully suppressed mTOR's ability to phosphorylate p70S6K and 4EBP1. At the same time TFEB was translocated to the nucleus in a dose dependent manner (Fig 7B and C). To further confirm the translocation and dephosphorylation of TFEB by mTOR, we performed immunoblotting assay. As shown in Fig 7D, more TFEB was found in the nuclear fraction of the rapamycin-treated mice. There was a mobility shift of the nuclear TFEB in the 4mg/kg group, which was consistent with the molecule being dephosphorylated, likely due to mTOR suppression.

We then explored whether the suppression of mTOR had physiological consequences. We found that the mRNA expression of several representative TFEB target lysosomal enzymes: lysosomal acidic lipase, cathepsin D, acidic phosphatase and ATP synthase was increased following rapamycin administration, only the ATP synthase didn't show dose dependent manner,

probably meaning saturation at 2mg/kg dosage (Fig7E-H). Consistently, the activities of cathepsin B, cathepsin D/E and lysosomal acidic lipase activities had recovered in a dose dependent manner (Fig 7I-L). However, the activity of acidic phosphatase didn't further recover at the 16wk time point for which the reason was unknown.

We thus confirmed that at 3wk and 16wk of HFD treatment, lysosomal function was impaired due to mTOR activation, which could be reserved by the inhibition of mTOR.

1.3.8. Overexpression of Wild Type or mTOR resistant TFEB Mutant Improves Lysosomal Functions, Hepatic Fat content and Liver Injury in 3wk High Fat Diet Mice.

The above study indicated that by disrupting mTOR activity with rapamycin, we can reactivate TFEB and improve lysosomal functions. To further test whether improved lysosmal function can lead to reduced hepatic steatosis, we over-expressed TFEB in the mouse livers using adenoviral vectors.

As TFEB has been found to be phosphorylated at specific site and be retained in the cytosol by mTOR, we used not only wild type TFEB but also a site-specific mutant S211A TFEB, which is resistant to mTOR phosphorylation [168]. We have made S211A TFEB adenovirus and expected it would have a higher ability to regulate lysosome activity. We injected the virus at the first day of high fat diet treatment and collected samples three weeks later. By western blotting assay. We confirmed that both WT and mutant TFEB had been successfully expressed in the mice liver (Fig 8L). We then compared lysosomal enzyme activities in WT-TFEB, S211A-TFEB and control mice. As we have expected, TFEB S211A -injected mice had the highest level of cathepsinB, cathepsin D/E, lysosomal acid lipase and acidic phosphatase activities, whereas the enzyme activity levels in mice receiving WT- TFEB were also increased (Fig 8A-D). As regards to phenotypic changes, administration of either WT or mutant TFEB resulted in decreased body weight (Fig 8E). However, only administration of mutant TFEB

resulted in decreased liver weight and thus the liver weight/body weight ratio, (Fig 9F, G). Similarly, liver steatosis level, as indicated by hepatic triglyceride, also decreased in mice receiving wild type TFEB and partially in mice receiving mutant TFEB (Fig 9H). Mutant TFEB also had the strongest protection of liver injury in NAFLD development, as indicated by in serum ALT level (Fig 8I). We didn't observe any differences in serum triglyceride level (Fig 9K). Mutant TFEB had also lowered the serum cholesterol level (Fig 8J).

These findings have implicated that TFEB could improve hepatic lysosomal activities and delay NAFLD development induced by high fat diet treatment in mice.

1.3.9. Overexpression of TFEB Improves Lysosomal Functions, Hepatic Fat content and Liver Injury in 16wk High Fat Diet Fed Mice.

To examine the effect of TFEB overexpression in mice given high fat diet for a longer term, we gave WT TFEB to mice fed with high fat diet for 16wk. As shown in Fig 9A-D, cathepsinB, cathepsin D/E, lysosomal acid lipase and acidic phosphatase all recovered, although not statistically significant in acidic phosphatase. In addition, the body weight, liver weight and liver weight/body weight ratio were all lower in TFEB-injected mice (Fig 9E-G). Liver steatosis was protected by WT TFEB overexpression, as indicated by hepatic triglyceride measurement (Fig 9H) and H-E staining (Fig 9I). Serum cholesterol and triglyceride (Fig 9J, K) were also decreased, indicating that dyslipidemia was protected by WT TFEB expression as well. Overexpression of TFEB could thus improve lysosome function, hepatic steatosis and liver injury (Fig 9L).

1.3.10. Consistent Activated RagA Mutant Inhibited TFEB Translocation, TFEB Activity, Lysosomal Function and Liver Function.

The above studies showed that enabling TFEB activity by either suppressing mTOR or over-expressing TFEB, particularly the mTOR-resistant TFEB, could enhance lysosomal function and improve hepatic steatosis. We then examined the hypothesis that a sustained mTOR activity would lead to a more severe suppression of TFEB and exacerbate hepatic steatosis. To achieve this goal, we gave high fat diet - fed mice with an adenovirus carrying a consistently activated HA-tagged RagA mutant, $RagA^{GTP/GTP}$. As mentioned in the Introduction part, mTORC1 interacts with, and its activity depends on, Rag proteins. Expression of $RagA^{GTP/GTP}$ in cells renders the mTORC1 activation independent of amino acid activation and could thus constitutively activate mTOR in nutrient-depleted conditions. $RagA^{GTP/GTP}$ adenovirus was injected to mice by tail vein after 6 weeks of high fat diet treatment and the mice were sacrificed at 10wk after another 4 weeks of high fat diet treatment. The total high fat diet feeding time was 10 wks, the time points when mTOR activity was low (Fig 1).

As shown in Fig 10A, we first confirmed that exogenous $RagA^{GTP/GTP}$ was successfully expressed in the livers, by immunoblotting analysis using anti-RagA and anti-HA antibodies. mTOR activity was consequently elevated, with a high level of phosphorylation of p70S6K and 4EBP1, compared to the vector-only group. As anticipated, TFEB was retained in the cytosol in virus-injected mice,

instead of in the nucleus as in the control group (Fig 10B). To determine whether activation of mTOR had the effect on lysosomal function, we measured mRNA expressions of lysosomal acidic lipase, cathepsin B, cathepsin D and acidic phosphastase and found all were suppressed following virus injection (Fig 10C-F). Similarly, the activities of cathepsinB, lysosomal acidic lipase and acidic phosphatase were also impaired in the $RagA^{GTP/GTP}$ group (Fig 10G-I)

We then studied if constitutive activation of mTOR at 10wks had any effects on NAFLD development. As we expected, in virus-injected group, the liver weight and the liver/body weight ratio were higher (Fig 8J-L). The levels of hepatic triglyceride amount and serum ALT were also increased (Fig 8M-N), compared with the control group. These findings indicate that by re-activating mTOR at the time point of 10wk of high fat diet feeding, we can promote hepatic injury and steatosis.

1.4 Discussion:

Activation of mTOR is believed to be related to cell growth and proliferation. Whether the activation of mTOR is persistent in the duration of high fat diet feeding has not been characterized. This question is meaningful because activation of mTOR can cause pathological changes to cells, organs, and the body [10]. In this part of study, we have shown that mTOR can be down-regulated in high nutrition status. mTOR was activated soon after high fat diet started and reached the peak activation at 3wks. After 6 to 10wks of feeding, mTOR activity has reduced and returned to almost base line. Later during the continuous high fat diet stimulation, mTOR activities had gone through several oscillations again and finally reached to a quite low level in mice fed with high fat diet for 32 wks.

mTOR activation relies on intact lysosomal function. Major genes of lysosome biogenesis and enzyme activity are transcriptionally controlled by TFEB. Meanwhile, TFEB can be directly phosphorylated and suppressed by mTOR in the cytosol. Thus, TFEB plays important role in mTOR activity. We have shown in Figure 2 that the subcellular location of TFEB also oscillates during high fat diet regimen, in a direction opposite to that of mTOR oscillation (Fig 11B). As we expected, expression of downstream genes and activation of lysosomal enzyme also changed along with the change of the location of TFEB. This interesting

phenomenon demonstrated a link between mTOR activation and lysosome activity during long term high fat feeding (Fig 11 A).

Oscillation mTOR activation has been observed in an early study [169]. Under the starvation condition, mTOR is suppressed and autophagy is activated. However, mTOR can be reactivated by prolonged starvation. Reactivation of mTOR is autophagy-dependent and requires the degradation of autophagosome contents in lysosomes. This finding implies a mechanism in which mTOR activity is dependent on lysosome. Thus lysosome dysfunction can affect mTOR activation. A self-feedback regulatory loop of mTOR is composed of mTOR, TFEB, lysosome activity. When activated by high fat diet, mTOR suppresses TFEB by phosphorylation and subsequently impairs lysosomal activities. When the lysosomal function is impaired, mTOR would be in turn de-activated (Fig 11B). Once the mTOR activity is down-regulated, TFEB is released and promotes lysosomal function, which would allow mTOR reactivation once again. Interestingly, the magnitude of the reduces over the time, oscillation pattern of mTOR indicating that the activity of mTOR finally returns to the baseline. This pattern has been reported in physical sciences as a natural response of a system to a change from equilibrium. The response of mTOR activation in high fat diet regime is not an "on/off" events but rather a process of the body to equilibrate the outside stimulation to a more stable status. The damping oscillation pattern has been also observed in NF-κB activation followed by the stimulation of TNF-alpha [170].

Evolutionarily, human beings have acquired the ability to store excessive nutrients in the form of fat for future use when in starvation. Thus, pathways related to catabolic metabolism shuts down and anabolic metabolism is activated, such as mTOR in high nutritious status. This evolutionary acquirement has its advantage in times when food is restricted. However, in times when food is in surplus, persistent anabolic activation can be harmful. Excessive fat storage can be found in liver, muscle and other non-fat storing tissues. Here, our study indicate that anabolic metabolism mediated by mTOR can be down-regulated through the TFEB-lysosome mechanism.

Early development of steatosis is critical in the pathogenesis of NAFLD, both in terms of diagnosis and treatment. Here in this study, we have also discovered a potential sensitive marker for early NAFLD diagnosis. TFEB staining is negatively correlated with the traditional steatosis score. As the staining pattern of TFEB can be easily quantified, this may become an effective way to access severity of steatosis. It is worth to be noticed that the application of TFEB in diagnosis may be only effective in diet/obesity induced NAFLD in middle aged to elderly patients, as in young patients and patients with non – obesity NAFLD steatosis does not seem to correlate with TFEB location. The early and effective treatment of NAFLD has not been well developed [171]. We found that overexpression of mutant and WT TFEB in mice can significantly improve steatosis and metabolic syndrome, which could be a potential target in the treatment.

Furture studies should be focused on other consequences of mTOR oscillation related to metabolism, such as SREBP1, which is important for lipid synthesis. Because mTOR also controls metabolism related to cell growth, whether these phenotype show a similar pattern of change remains to be explored.

1.5 Figures and Figure Legend

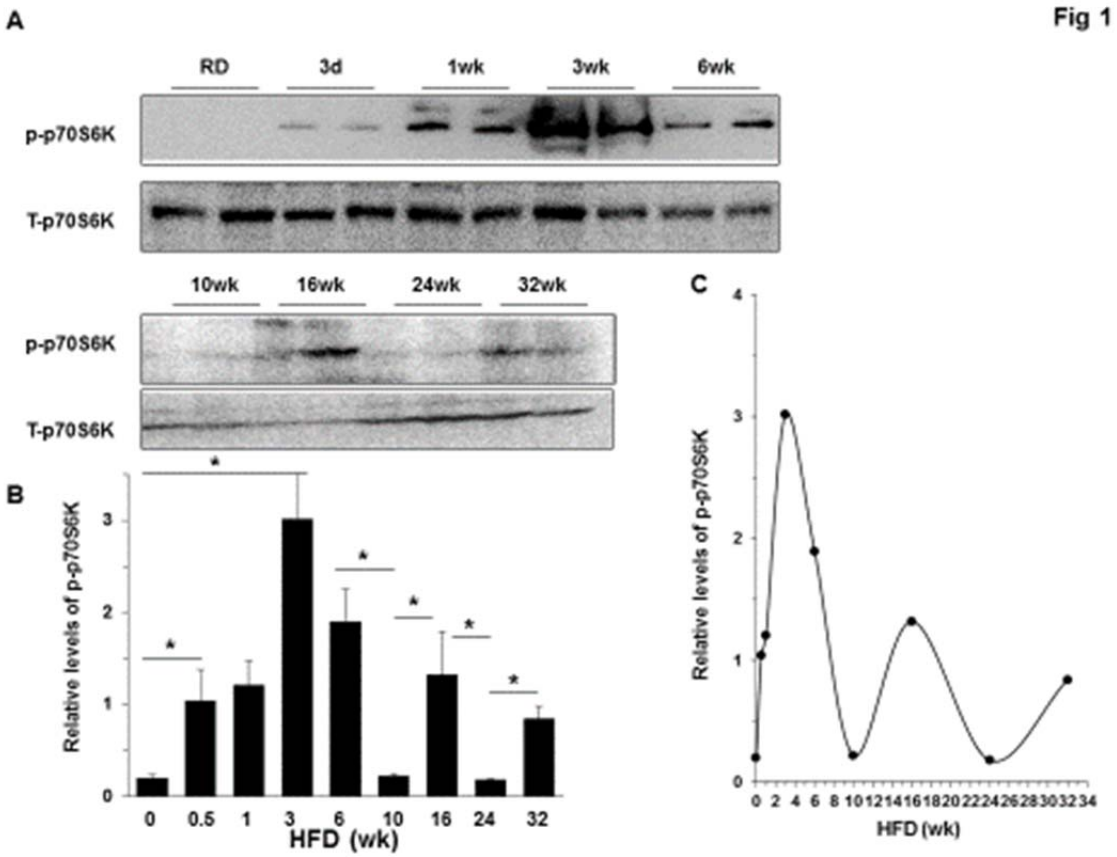

Figure 1: The mTOR activity oscillates under the sustained hyper-nutrition condition.

(A) GFP-LC3 mice were fed with HFD for the indicated durations and the mTOR activity (phospho-p70S6 kinase level) in the liver was analyzed by immunoblot assay. Each lane represents one individual mouse. (B) Densitometry analysis were performed for phosphor-p70S6 kinase (p-p70S6K) in each group. The value (mean + SEM) is normalized with the level of total p70S6 kinase (T-p70S6K). (C) The relative levels of p-P70S6K were plotted against the time. A damping oscillation pattern can be observed.

n=4-6 per group, *: $p<0.05$

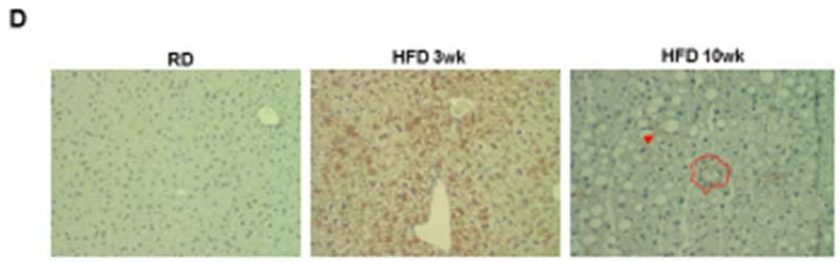

Figure 1: The mTOR activity oscillates under the sustained hyper-nutrition condition.

(D) phospho-S6 expression were analyzed by Immunohistochemistry staining in the liver tissue of C57BL wild type mice fed with HFD for the indicated time point. Magnification X100. Representative images were shown.

n=4-6 per group, *: $p<0.05$

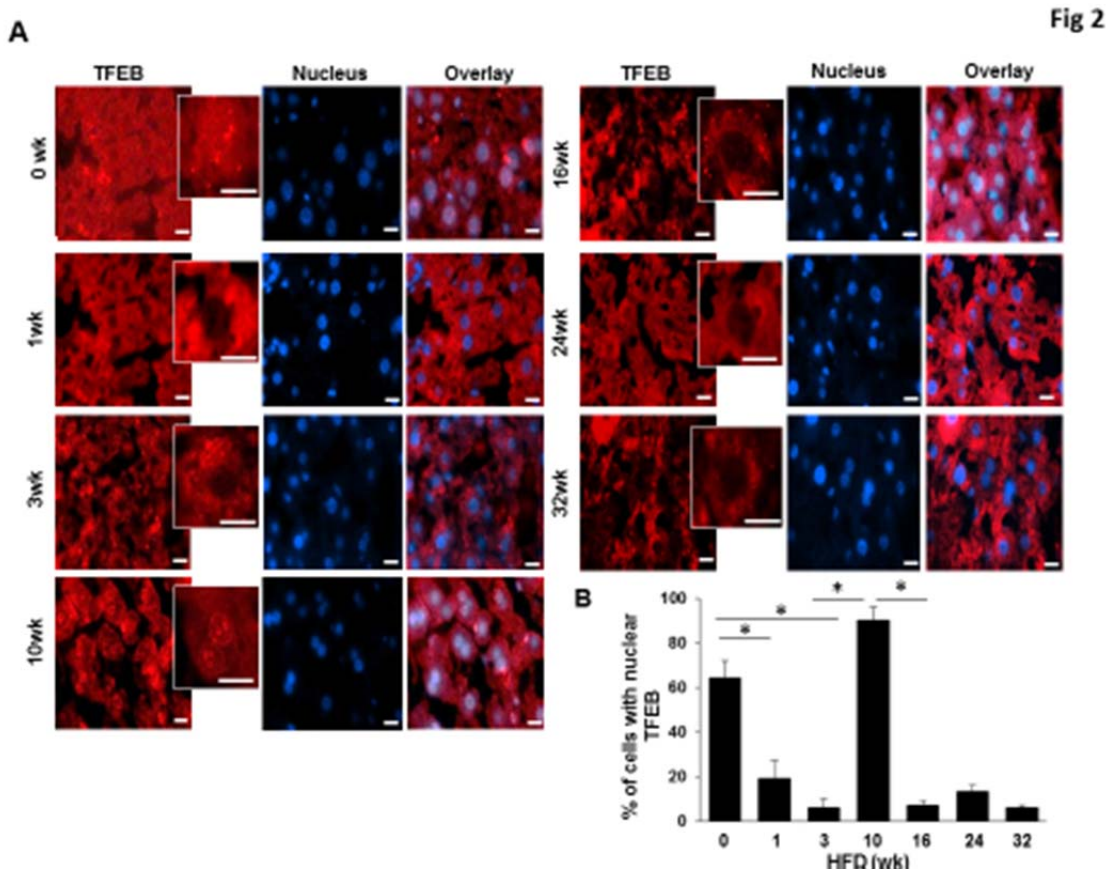

Figure 2: TFEB is activated in an oscillation pattern under the sustained hyper-nutrition condition.

(A) GFP-LC3 transgenic mice were fed with HFD for the indicated durations. The cryosection of the liver tissues were stained with anti-TFEB and Hoechest 33328 (for the nucleus). Insets show representative hepatocyts at a higher magnification. (B) The percentage of cells with TFEB-positive nuclei was quantified. (mean+ [SEM])

n=4 per group, scale bar=10um, *: $p<0.05$

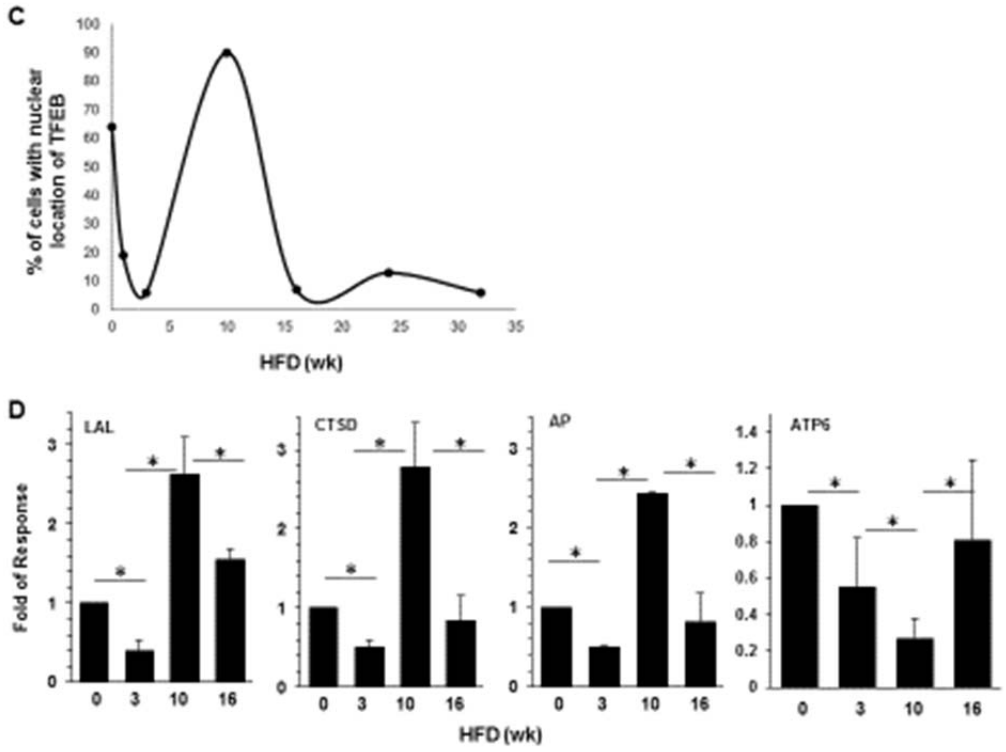

Figure 2: TFEB is activated in an oscillation pattern under the sustained hyper-nutrition condition.

(C) The percentage of cells with TFEB-positive nucleus was plotted against the feeding duration. (D) The mRNA levels for the TFEB targets were analyzed by RT-PCR in the same group of mice fed with high fat diet for different times. LAL: lysosomal acidic lipase; CTSD: cathepsin D; AP: acidic phosphatase; ATP6: ATP synthase subunit 6.

n=3 per group, *: $p<0.05$

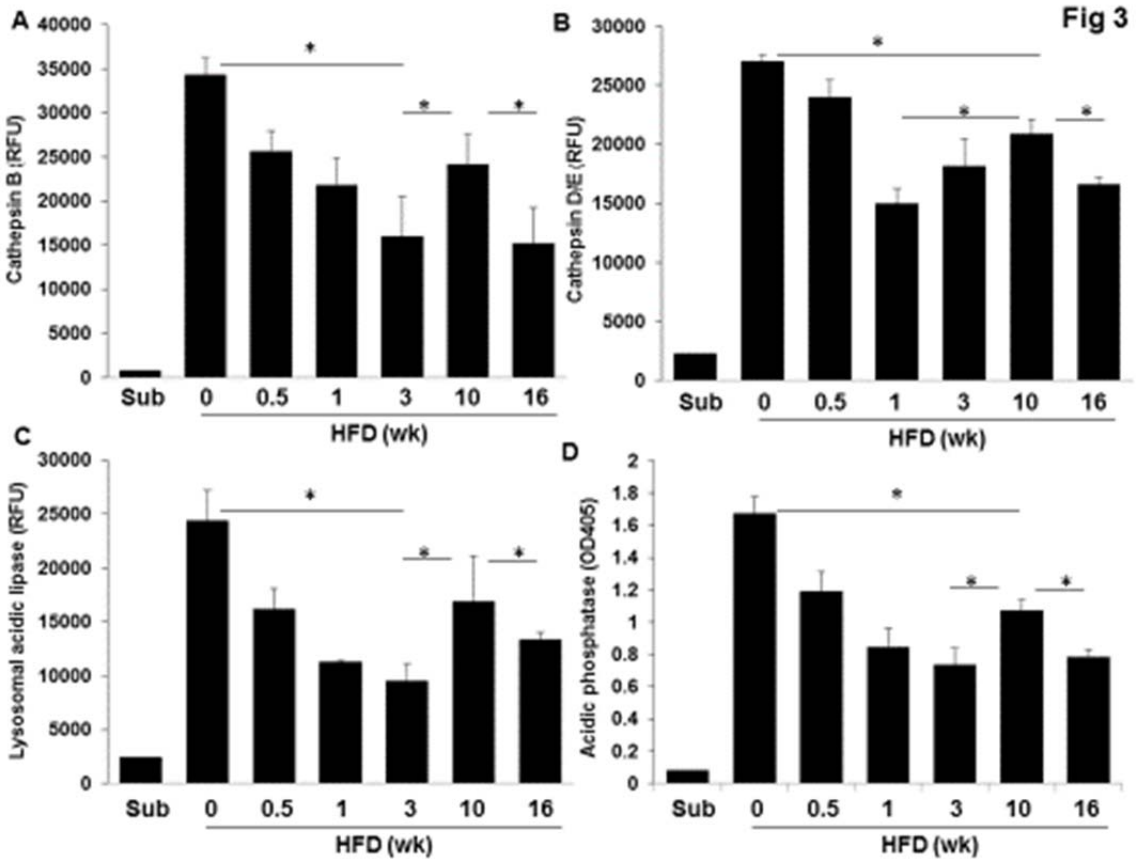

Figure 3: Lysosomal functions oscillate during long-term high fat diet feeding.

GFP-LC3 transgenic mice were fed with HFD for the indicated durations. Livers were analyzed for the activity of cathepsin B (A), cathepsin D&E (B), lysosomal acidic lipase (C), acidic phosphatase (D). (mean+standard error of mean[SEM])

n = 4 per group, ∗: $p < 0.05$

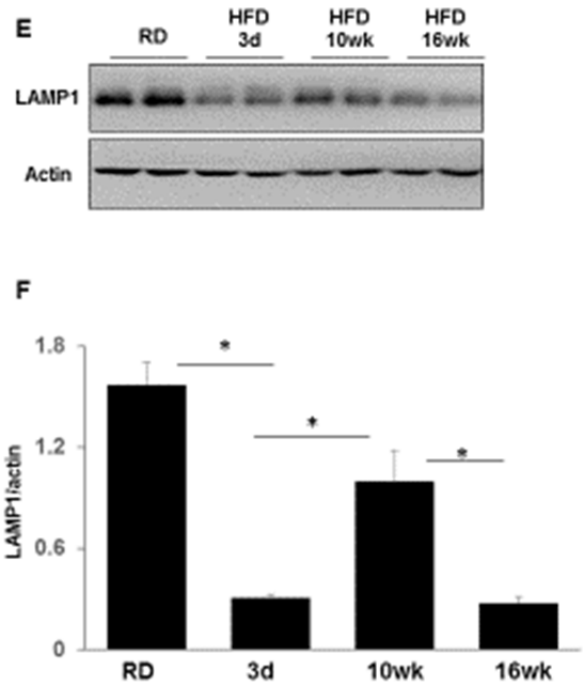

Figure 3: Lysosomal functions oscillate during long-term high fat diet feeding.

(E): Expression of LAMP1 in the livers of high fat diet fed mice was analyzed by immunoblotting assay. Each lane represents an individual mouse (F): Densitometry analysis of LAMP1 expression in the same groups of mice.

n = 3 per group, ∗: $p < 0.05$

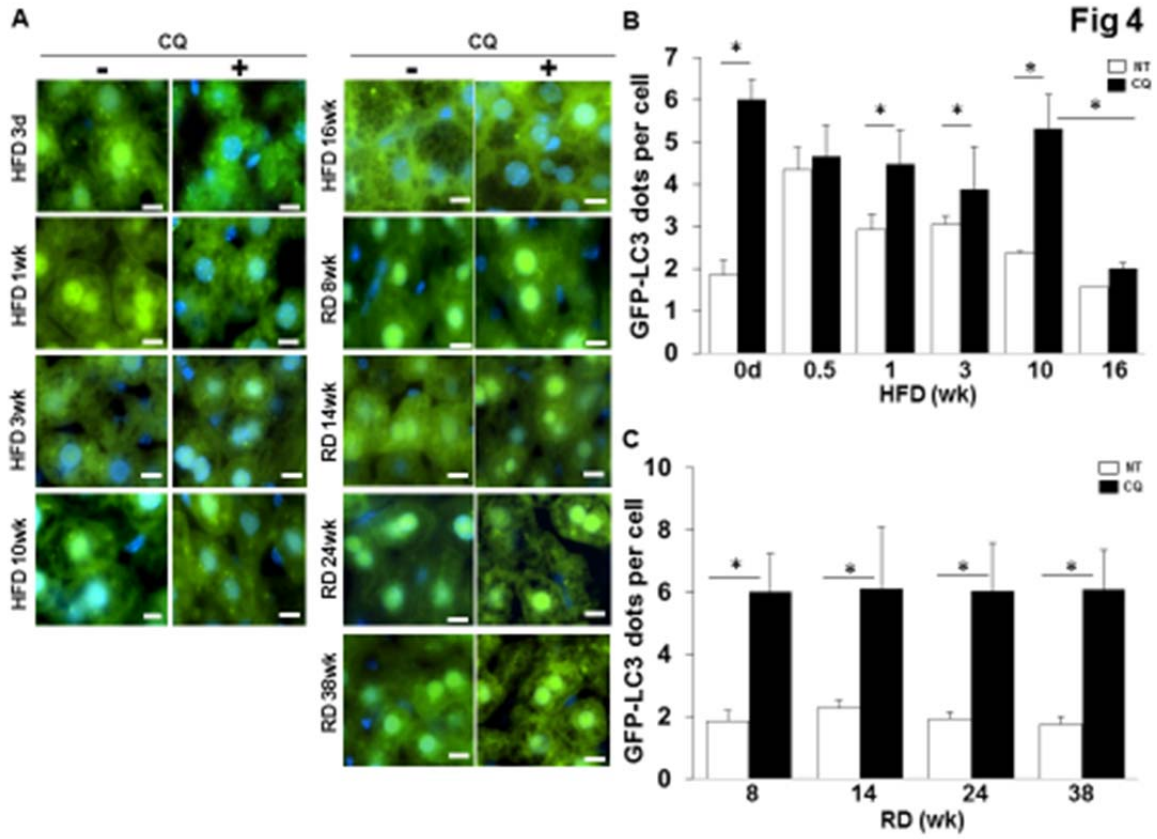

Figure 4: Autophagy degradation is dynamically regulated.

(A) GFP-LC3 transgenic mice were fed with regular diet or high fat diet for the indicated duration, with or without a treatment with CQ (60 mg/kg, ip) for 16 h before sacrifice. Liver cryosections were prepared and images were obtained by fluorescent microscopy. Green GFP-LC3 puncta represent autophagosomes. (B) GFP-LC3 puncta per cell (mean+SEM) were quantified from each animal. (A and C) GFP-LC3 transgenic mice were fed with a regular chow diet for the indicated duration, with or without a treatment with CQ. GFP-LC3 puncta (mean+SEM) were quantified from each animal.

Scale bar: 10 um. n = 4–6 per group, *: $p<0.05$

Fig 4

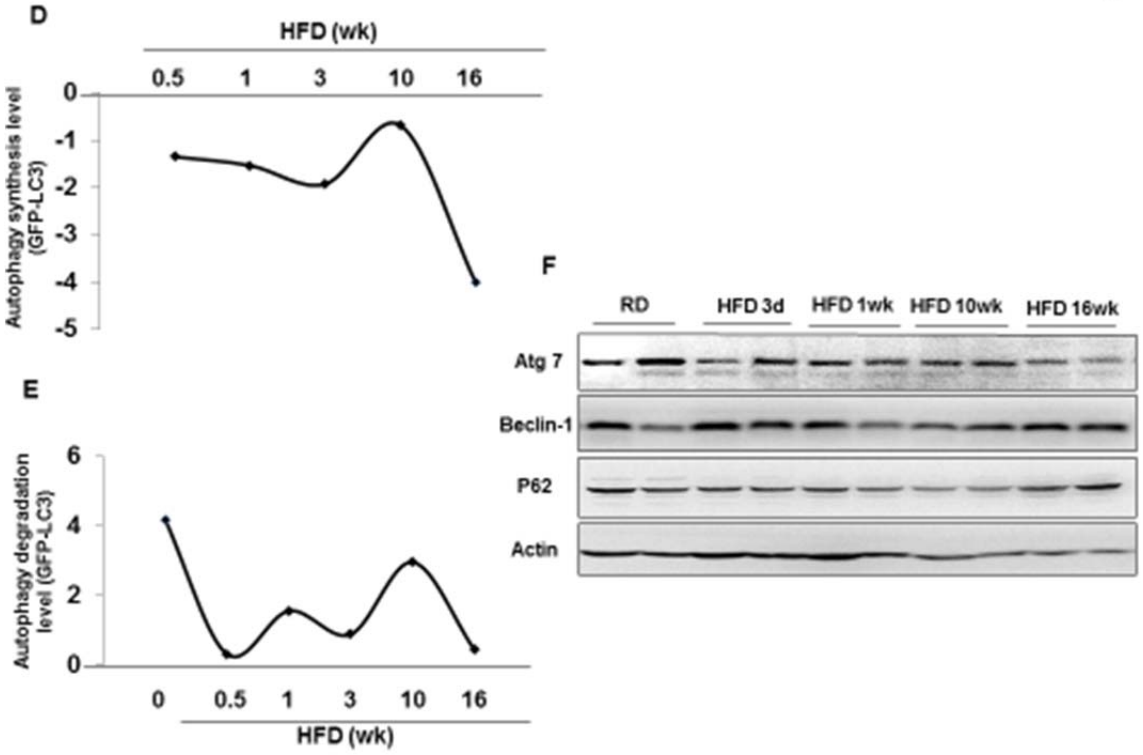

Figure 4: Autophagy degradation is dynamically regulated.

(D-E) Autophagy synthesis (D) and degradation (E) were calculated based on GFP-LC3 puncta/cell. The values were then plotted against the feeding duration. The number of GFP-LC3 dots level in the following groups are subjected to the subtractive operations as indicated. Calculation of degradation: HFD/CQ - HFD. Synthesis: HFD/CQ – RD/CQ (F) Autophagy related proteins were analyzed by immunoblot essay.

n = 4–6 per group

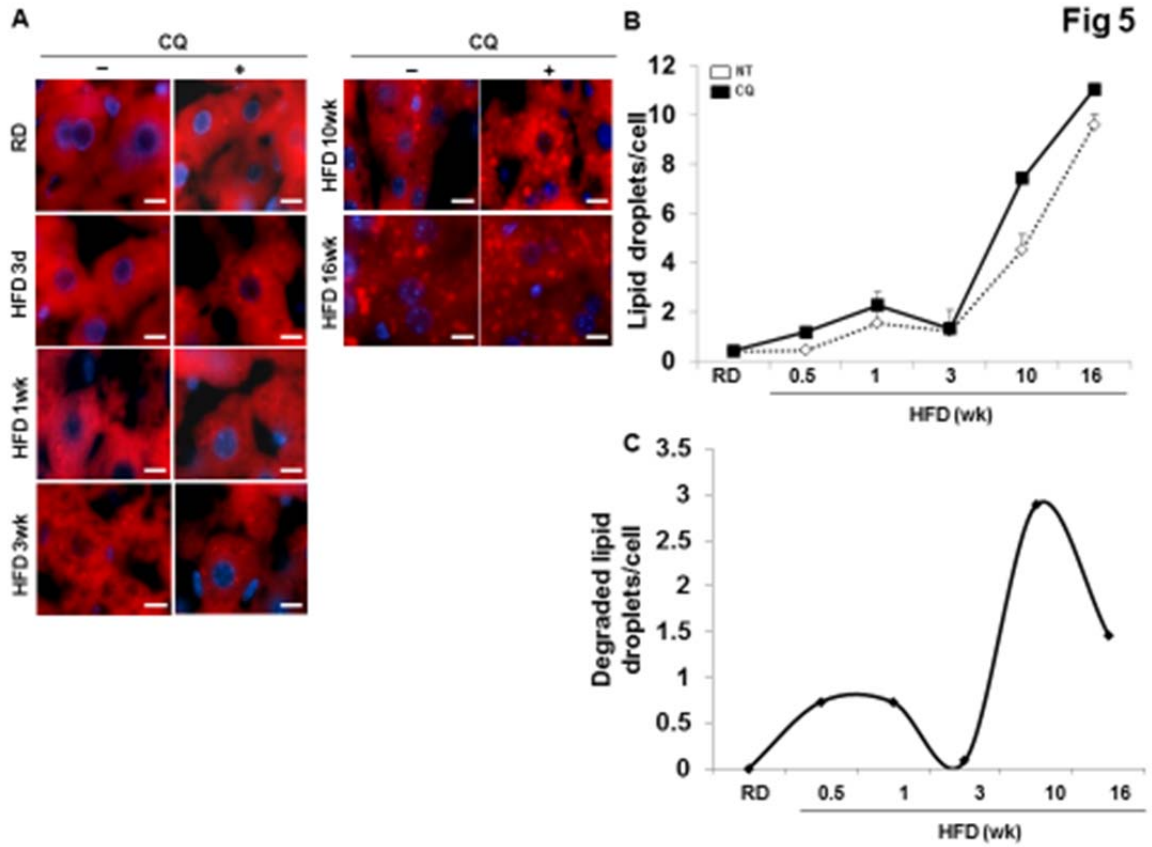

Figure 5: Degradation of lipid droplets by lipophagy during NAFLD development.

(A-B) GFP-LC3 transgenic mice were fed with HFD for the indicated durations. The cryosections of the liver were stained with Bodipy (493/503) for lipids droplets (A), which were quantified (mean+SEM) (B). (C) Degradation of lipid droplets were calculated by subtracting the number of lipid droplets in high fat diet group from that of lipid droplets in high fat diet/CQ group. (mean+SEM).

Scale bar: 10 μm. n=3-6 per group, *: $p<0.05$

Fig 5

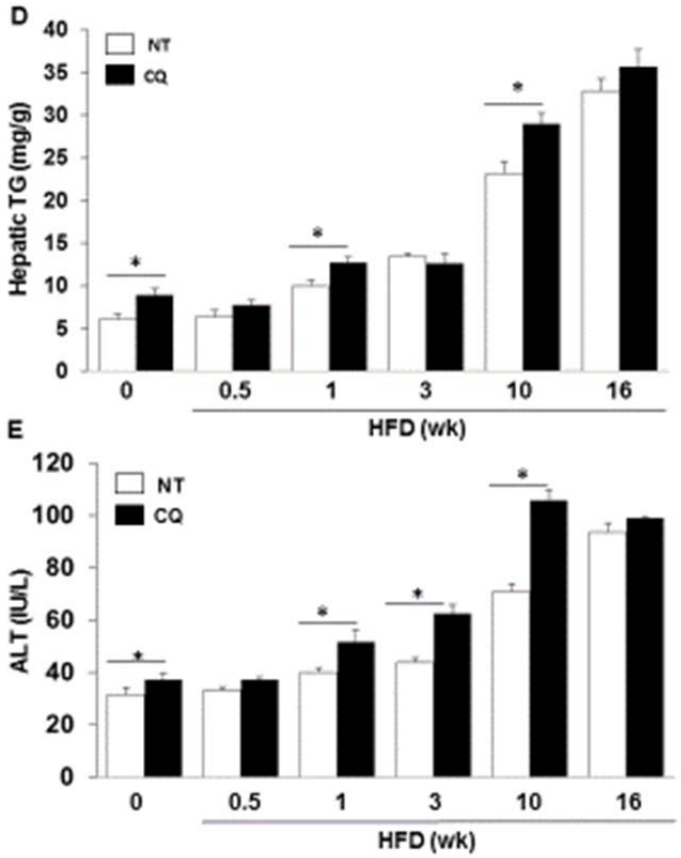

Figure 5: Degradation of lipid droplets by lipophagy during NAFLD development.

(D) Hepatic triglycerides were measured in the same group of mice (mean+SEM). (E) Liver injury were assessed by the serum alanine transaminase (ALT) measurement in the same group of mice (mean+ SEM).

n=3-6 per group, *: $p<0.05$

Fig 6

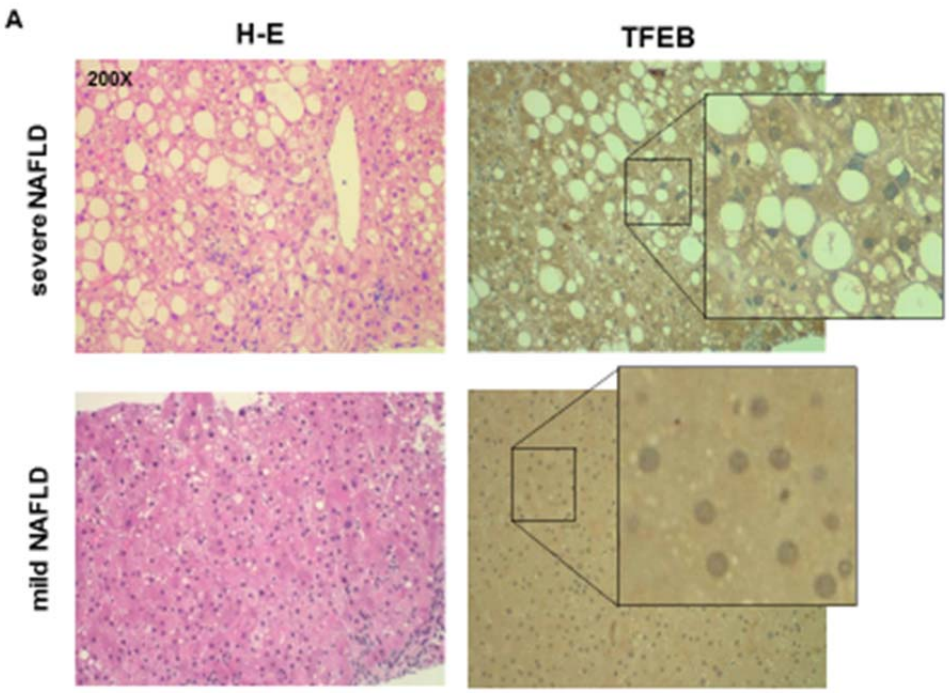

Figure 6: The subcellular location of TFEB correlates highly with NAFLD and obesity in human.

(A) The liver biopsy sample of NAFLD patients were stained with H-E or with anti-TFEB antibody. Representative mild and severe cases were shown (200X). Insets show enlarged images.

Patient No. n=15-19

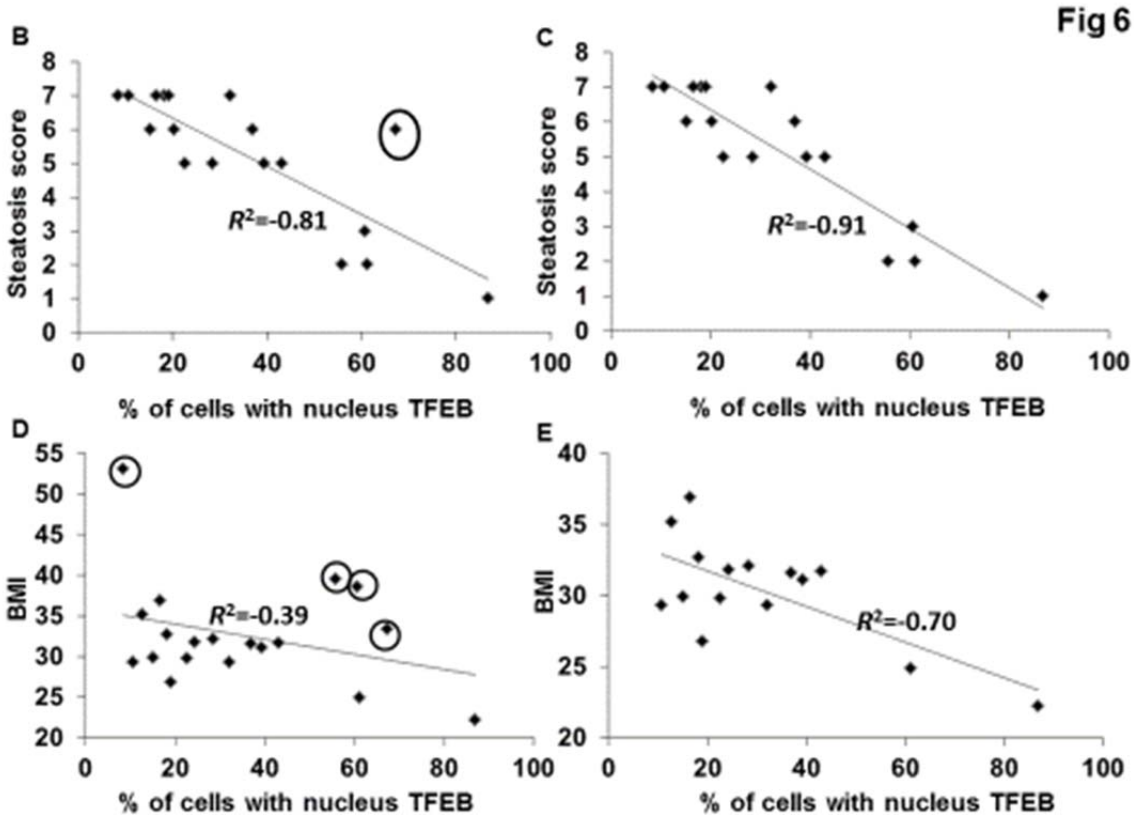

Figure 6: The subcellular location of TFEB correlates highly with NAFLD and obesity in human.

(B) Correlation of steatosis score and percentage of cells with TFEB positive nucleus. (C) Correlation of steatosis score and percentage of cells with TFEB positive nucleus excluding clinically significant outliers. (D): Correlation of BMI and percentage of cells with TFEB positive nucleus. (E): Correlation of BMI and percentage of cells with TFEB positive nucleus excluding clinically significant outliers. Circled symbols in B and D represent patients who were outliers and excluded in panel C and E, respectively.

Patient No. n=15-19

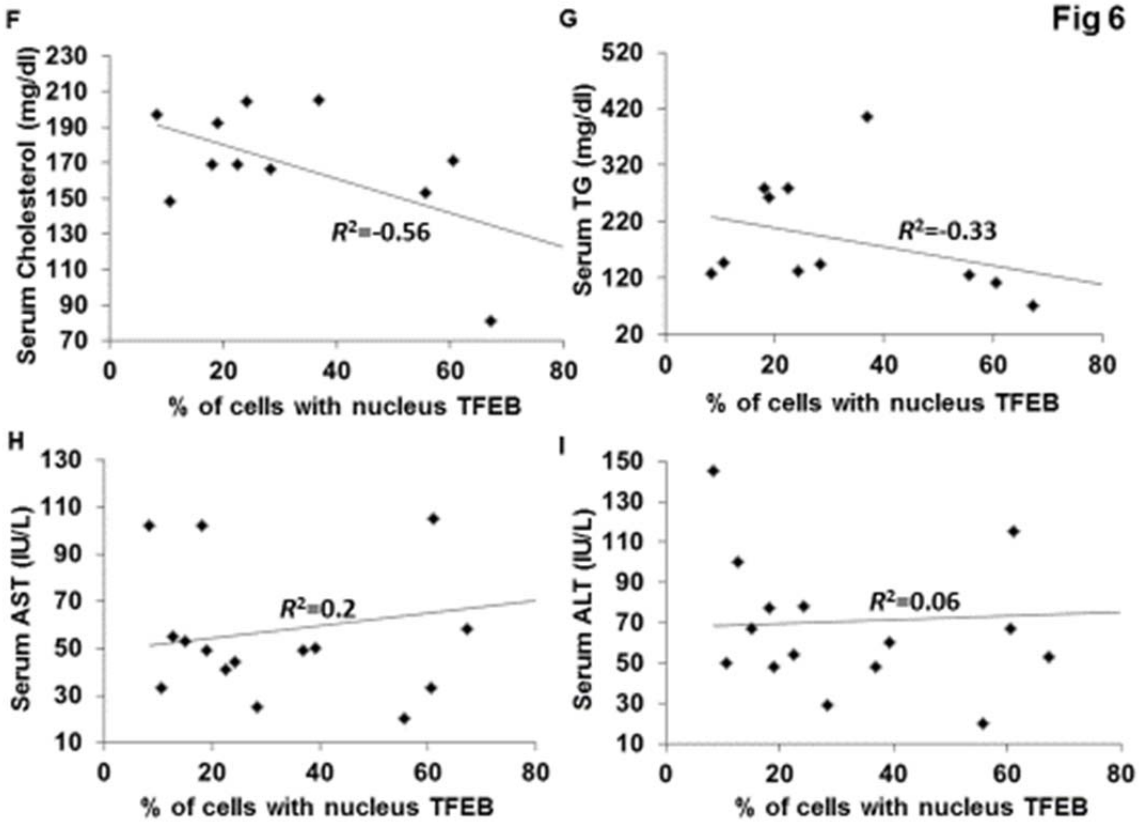

Figure 6: The subcellular location of TFEB correlates highly with NAFLD and obesity in human.

(F): Correlation of serum cholesterol and percentage of cells with TFEB positive nucleus. (G): Correlation of serum triglyceride and percentage of cells with TFEB positive nucleus. (H): Correlation of serum AST and percentage of cells with TFEB positive nucleus. (I): Correlation of serum ALT and percentage of cells with TFEB positive nucleus.

Patient No. n=15-19

Fig 7

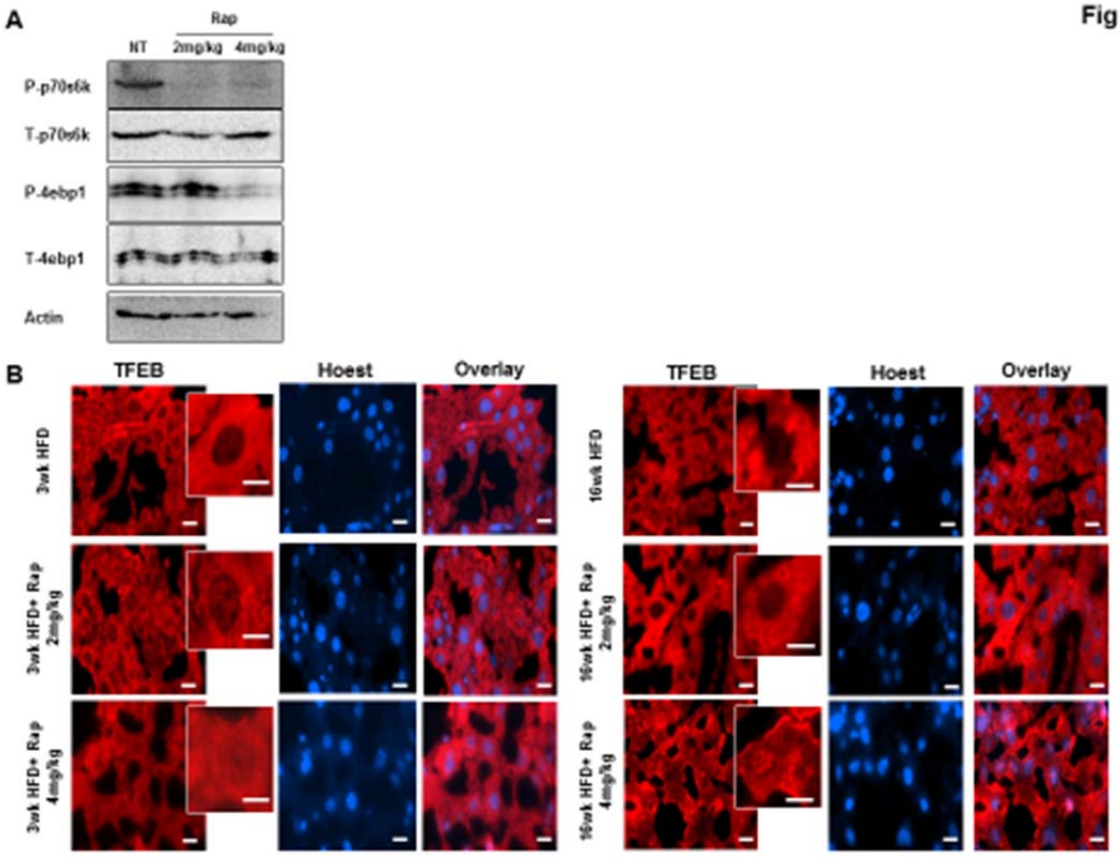

Figure 7: Suppression of mTOR activity promotes TFEB translocation to the nucleus and rescues the lysosome function in the fatty livers.

(A) mTOR activity was analyzed in the liver tissues from individual from mice following rapamycin (Rap) treatment. (2mg/kg, 4mg/kg) 16 hour before sacrifice. (B-C) GFP-LC3 transgenic mice were fed with HFD for the indicated durations, rapamycin were given as in A. Cryosections of the liver were stained with anti-TFEB and Hoechest 33328 for the nucleus. Cells with TFEB positive nucleus were quantified (mean+SEM).

Scale bar: 10 um, n=3 per group, *: $p<0.05$

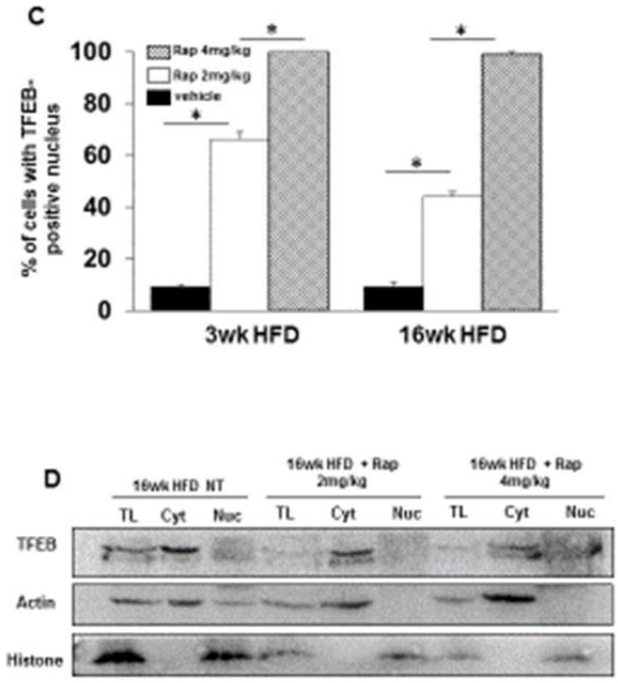

Figure 7: Suppression of mTOR activity promotes TFEB translocation to the nucleus and rescues the lysosome function in the fatty livers.

(B-C) GFP-LC3 transgenic mice were fed with HFD for the indicated durations, rapamycin were given as in A. Cryosections of the liver were stained with anti-TFEB and Hoechest 33328 for the nucleus. Cells with TFEB positive nucleus were quantified (mean+SEM). (D) Liver tissues from the same group of mice were processed to separate the nucleus and the cytosol fractions. The TFEB level was analyzed by immunoblot essay in each of the fraction.

n=3 per group, *: $p<0.05$

Fig 7

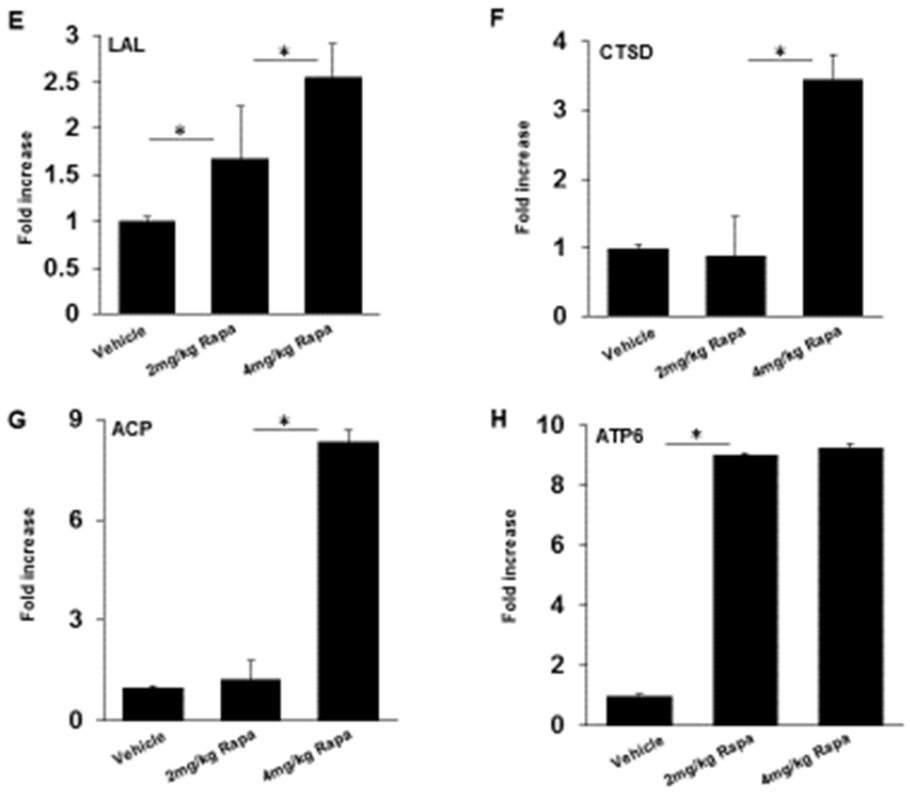

Figure 7: Suppression of mTOR activity promotes TFEB translocation to the nucleus and rescues the lysosome function in the fatty livers.

(E-H) The mRNA level of TFEB targets were quantified in the same group of mice by RT-PCR. (E) lysosomal acidic lipase, (F) cathepsin D, (G) acidic phosphatase, (H) ATP synthase subunit 6.

n=3 per group, *: $p<0.05$

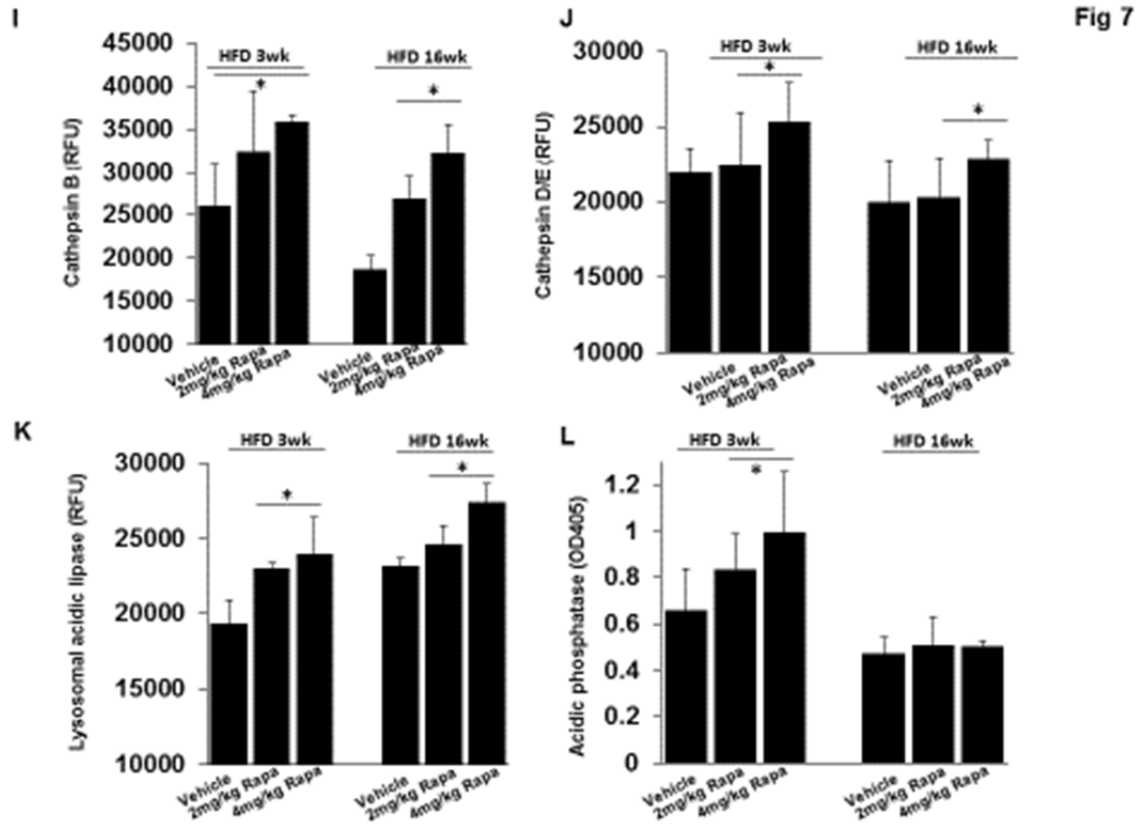

Figure 7: Suppression of mTOR activity promotes TFEB translocation to the nucleus and rescues the lysosome function in the fatty livers.

(I-L) Lysosomal activity were measured by the enzyme activity assay in the same group of mice, (I) cathepsin B, (J) cathepsin D/E, (K) lysosomal acidic lipase, (L) acidic phosphatase.

n=3 per group, *: $p<0.05$

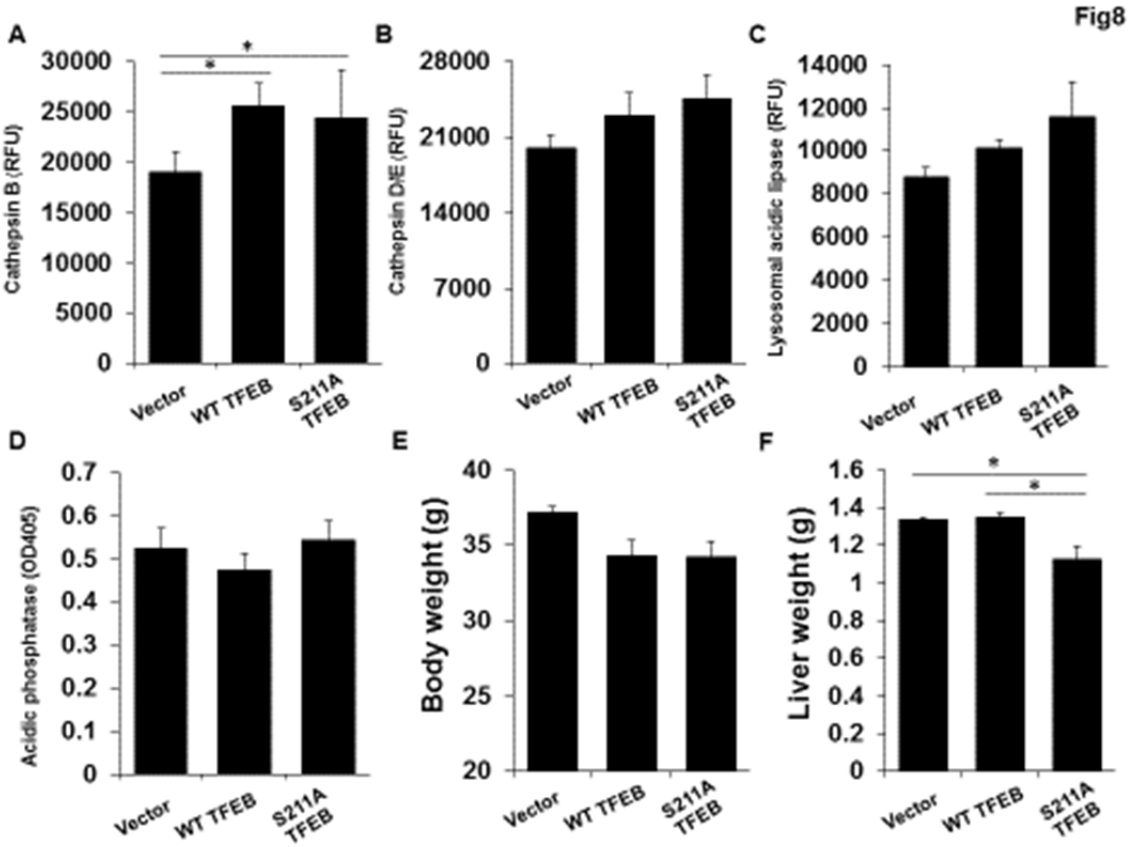

Figure 8: Overexpression of wild type and mTOR resistant TFEB mutant improves lysosomal functions, hepatic fat content and liver Injury in 3wk High Fat fed diet mice.

GFP-LC3 transgenic mice were fed with regular chow diet before Ad- TFEB (WT), Ad-TFEB (S211A) and Ad-vector were given i.v. Mice were then fed with high fat diet for 3wks. (A-D) lysosomal enzyme activity were analyzed in each group of the mice. (A) cathepsin B, (B) cathepsin D/E, (C) lysosomal acid lipase and, (D) acidic phosphatase. (L): Immunoblotting analysis of liver lysate from each mice. The following parameter were determined: (E) body weight, (F) liver weight.

n=3-6 per group, *: $p<0.05$

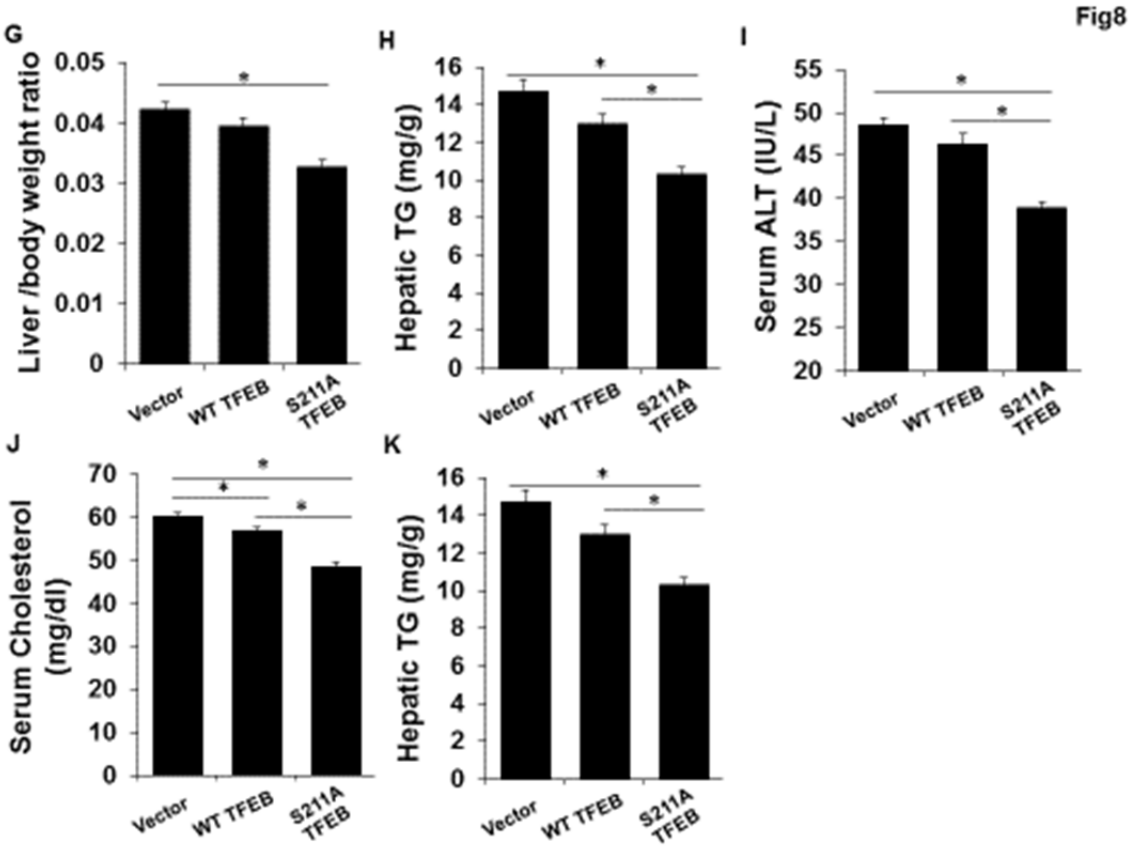

Figure 8: Overexpression of wild type and mTOR resistant TFEB mutant improves lysosomal functions, hepatic fat content and liver Injury in 3wk High Fat fed diet mice.

(G) liver/body weight ratio, (I) serum ALT, (K) serum triglyceride, (J) serum cholesterol (H) hepatic triglyceride.

n=3-6 per group, *: $p<0.05$

Fig8

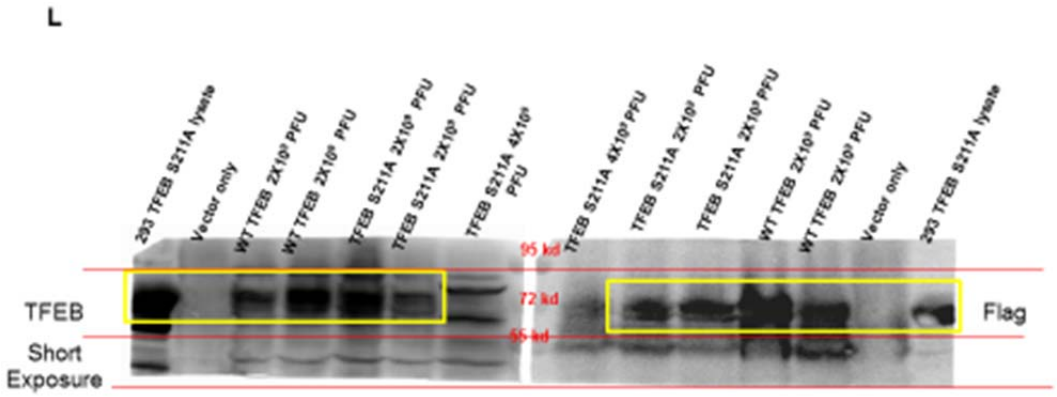

Figure 8: Overexpression of wild type and mTOR resistant TFEB mutant improves lysosomal functions, hepatic fat content and liver Injury in 3wk High Fat fed diet mice.

(L) Expression of TFEB in treated mice was assessed with immunoblotting assay.

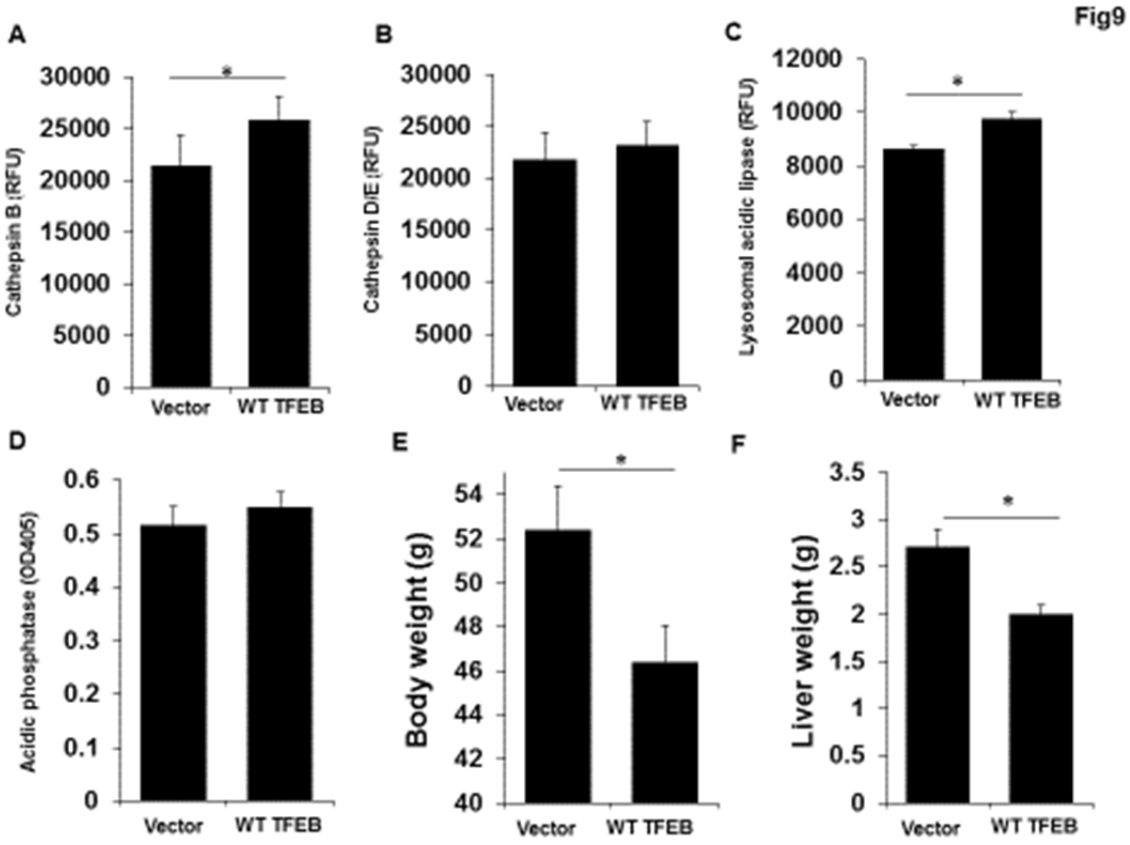

Figure 9: Overexpression of TFEB improves lysosomal functions, hepatic fat content and liver Injury in 16wk high fat diet fed mice.

GFP-LC3 transgenic mice were fed with high fat diet for 12wks, Adenovirus expressing TFEB or the vector were injected through tail vein and mice were fed for another 4wks before the experiment. Mice were sacrificed and the following parameters were determined: (A) body weight, (B) liver weight, (C) liver weight/body weight ratio, (D) serum triglyceride, (E) serum cholesterol, (F) hepatic triglyceride.

n=3-6 per group, *: $p<0.05$

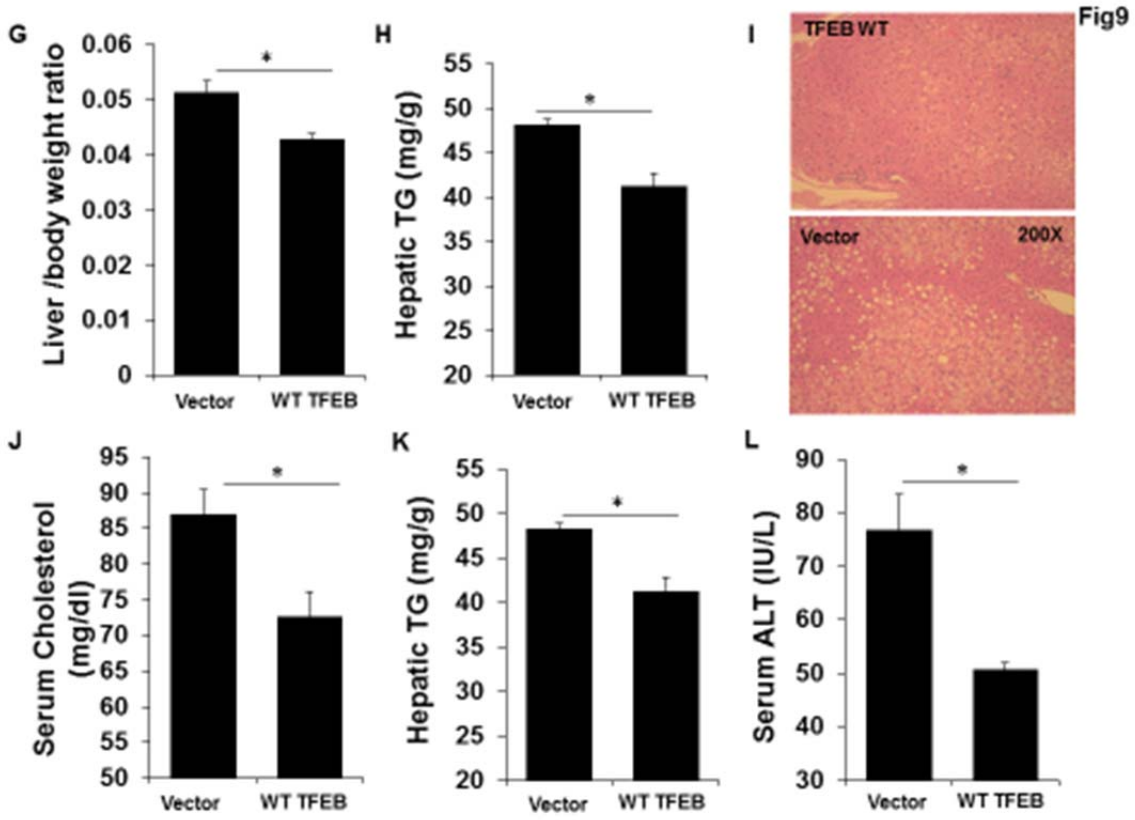

Figure 9: Overexpression of TFEB improves lysosomal functions, hepatic fat content and liver Injury in 16wk high fat diet fed mice.

(G) serum ALT. (A-D) lysosomal enzyme activity were analyzed in each group of the mice. (A) cathepsin B, (B) cathepsin D/E, (C) lysosomal acid lipase, and (D) acidic phosphatase. (L) H-E staining of liver tissue of TFEB or vector treated mice. Representative image are shown (X200).

n=3-6 per group, *: $p<0.05$

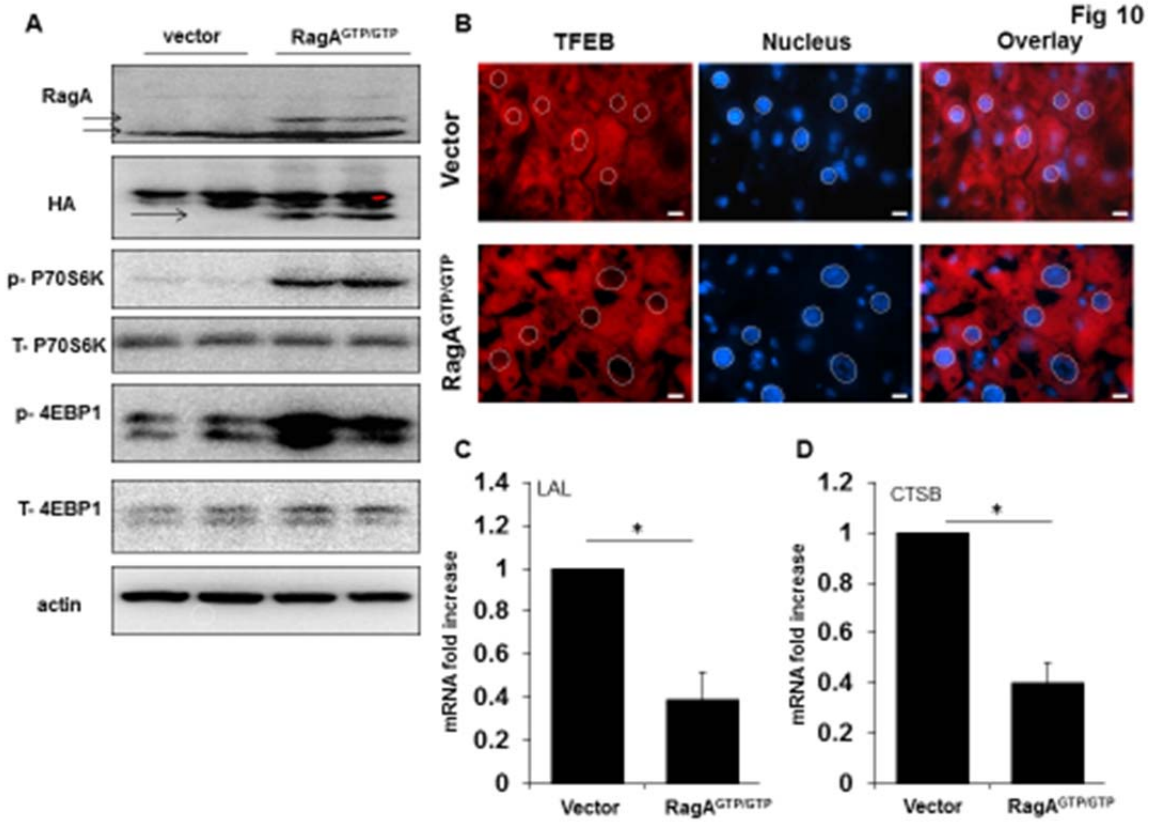

Figure 10: Constitutively activated RagA mutant inhibited TFEB translocation, TFEB activity, lysosomal function and liver function.

GFP-LC3 transgenic mice were fed with high fat diet for 6wks and then given adenovirus expressing a HA-tagged constitutively activated RagA mutant ($RagA^{GTP/GTP}$), or the control vector. Mice were then given high fat diet for another 4wks before experiment. (A) Livers were analyzed by Immunoblotting for RagA expression. (B) Cryosections of the livers were prepared and stained with anti-TFEB and Hoechst 33328 for the nucleus (dotted circles). (C-F) RT-PCR analysis of the expression of lysosomal enzymes: (C) lysosomal acidic lipase, (D) cathepsin B.

Scale bar: 10um, n=3 per group, *: $p<0.05$

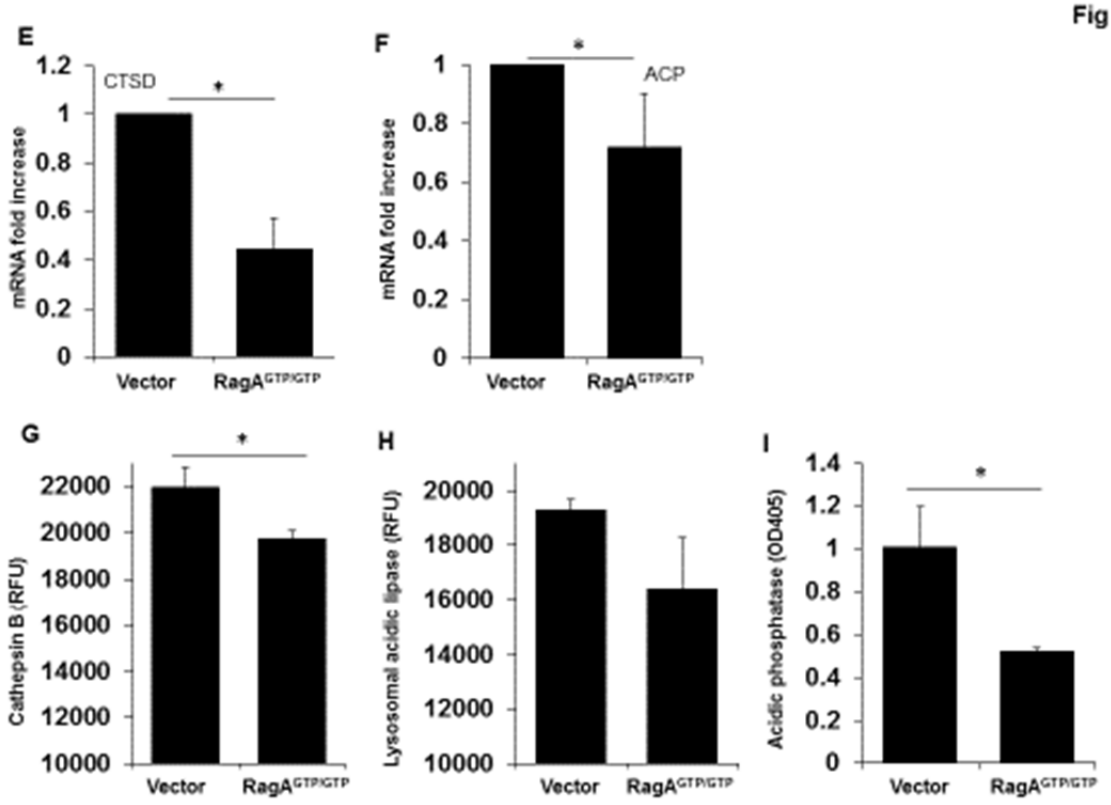

Figure 10: Constitutively activated RagA mutant inhibited TFEB translocation, TFEB activity, lysosomal function and liver function.

(C-F) RT-PCR analysis of the expression of lysosomal enzymes: (E) cathepsin D, and (F) acidic phosphastase. (G-I) Lysosomal enzyme activities were analyzed in each group of mice (G) cathepsinB, (H) lysosomal acidic lipase, (I) acidic phosphatase. (J-N) Phenotypic analysis of each group of mice: (J) body weight, (K) liver weight, (L) liver weight/body weight ratio (M) hepatic triglyceride and (N) serum ALT.

n=3 per group, *: $p<0.05$

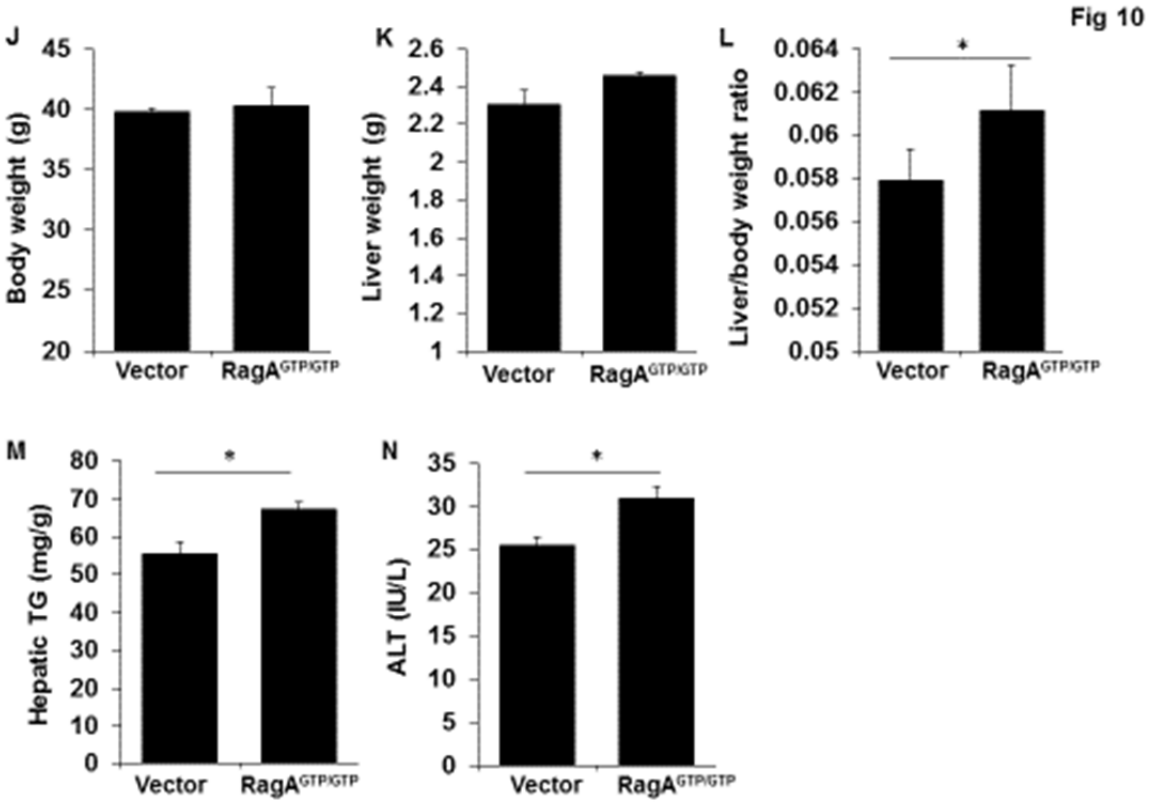

Figure 10: Constitutively activated RagA mutant inhibited TFEB translocation, TFEB activity, lysosomal function and liver function.

(J-N) Phenotypic analysis of each group of mice: (J) body weight, (K) liver weight, (L) liver weight/body weight ratio (M) hepatic triglyceride and (N) serum ALT.

n=3 per group, *: $p<0.05$

Fig 11

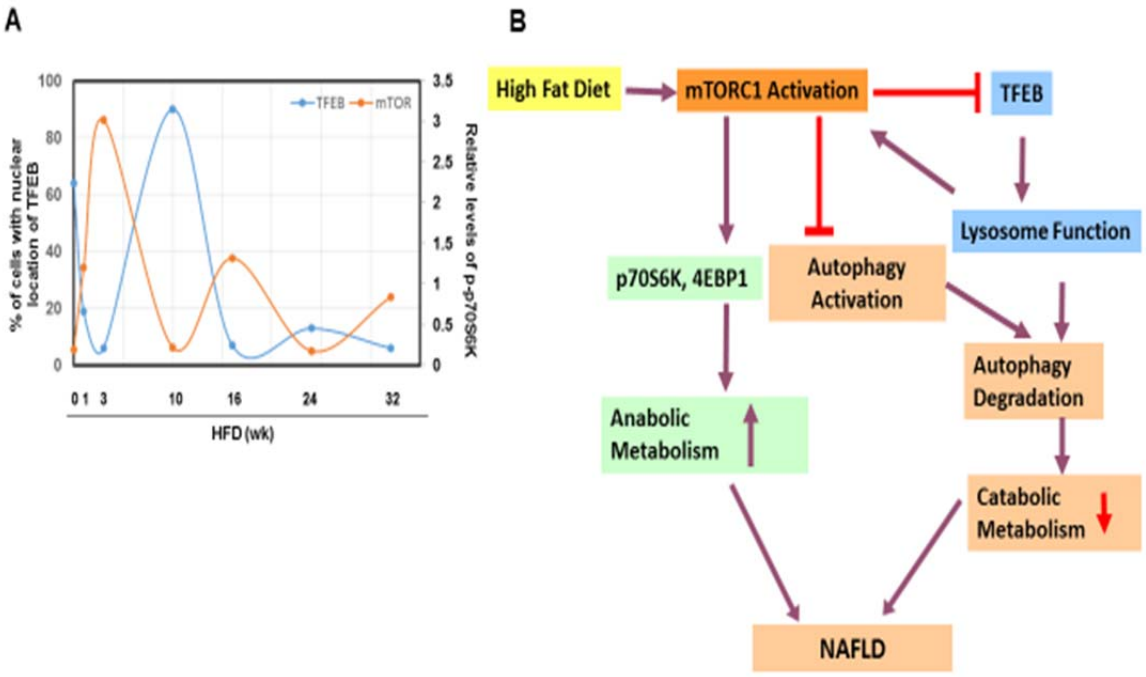

Figure 11: Schematic Model of mTOR – TFEB Self-regulatory Loop.

(A) mTOR and TFEB activity are oscillating in opposite direction. (B) Signaling model of mTOR-TFEB-lysosome self-regulatory loop and its downstream effects.

Part II. The function of Bid in NAFLD and obesity

1.1 Introduction

1.1.1 Bid and its function

1.1.1.1 Introduction

Bid, or: BH3-interacting domain death agonist, is a member of the Bcl-2 family proteins that regulate apoptosis by controlling the permeabilization of the outer mitochondrial membrane (OMM). This family of proteins is composed of anti-death members, such as Bcl-2 and Bcl-xL, and pro-death members, such as Bid, Bax and Bak. Structurally, this family of apoptotic regulators can be subdivided based on the number of sequence homology domain with the anti-apoptotic protein Bcl-2. Most anti-apoptotic proteins, such as Bcl-XL and Bcl-w, share four regions of homology with Bcl-2 (BH domain 1–4). The multi-domain pro-apoptotic proteins, Bax and Bak, contain the BH domain 1–3. Most other pro-apoptotic Bcl-2 family proteins, including Bid, Bim and Bad, contain sequence homology only in the BH3 domain and hence are referred to as BH3-only proteins [172].

Bid is mainly post-translationally activated in response to apoptotic stimuli. It transduces the apoptotic signals to the multi-domain pro-death molecules Bax and/or Bak at the site of mitochondria, which induce the release of apoptogenic

factors and a number of other events, leading to caspase activation and cell death. This constitutes the activation of the mitochondrial death pathway. Bid is widely studied in terms of its activation in the cytosol and its subsequent actions at the mitochondria. While the pro-death activity is the first function defined for Bid, Bid is proven to have alternative functions promoting cell proliferation and DNA repairs [173]. These properties of Bid render it to be an unique and fascinating molecule to be investigated to understand how an apoptotic protein affect cells death and more generously, cell functions.

1.1.1.2 The Structure and Transcriptional Regulation of Bid

Bid was discovered in 1996 [174]. Its function in apoptosis was first determined in lymphoma cell lines [175]. Bid was subsequently identified as by two other laboratories [176, 177] as a substrate of caspase-8 [178]. Most importantly, these studies found that cleaved Bid could translocate from the cytosol to the mitochondria and induce the release of cytochrome c from the mitochondria. Its ability to interact with the multi-domain pro-death molecules, Bax or Bak, is a very distinguished feature of this molecule among the Bcl-2 family proteins [173].

Both the human and mouse Bid genomic structures have been determined [179, 180]. In the mouse, the Bid gene is located at chromosome 6. Human Bid is located in a syntenic region, chromosome 22q11.2. The molecule is 22 KD and contains eight α-helices, with two central hydrophobic helices (helices 6 and 7) forming a hairpin structure that is surrounded by the remaining six amphipathic

helices. The BH3 domain of Bid (amino acids 90–98), which comprises a region of sequence homology to other Bcl-2 proteins and is required for interaction with both pro-apoptotic Bax and anti-apoptotic proteins such as Bcl-2 [174], is located in Helix 3. Bid also contains a large unstructured loop (amino acids 42–79) that separates Helices 2 and 3. This loop contains a variety of sites that are subjected to post-translational modifications, which regulate Bid localization and its apoptotic function. Finally, structural comparison of Bid with multi-domain anti-apoptotic proteins, including several viral proteins, suggests that Bid (as well as Bax and Bak) contains a redefined BH4 region at the N terminus, a feature previously believed to be shared only by anti-apoptotic proteins [181].

Transcriptionally, Bid can be positively regulated by TP53 [182]. Functional p53-binding elements have been found in both human and mouse Bid genomic loci upstream of the first coding exon. The p53-binding element of human Bid is 85% identical to the consensus p53-binding element. Specific protein-DNA complex could be formed and the binding element was proved to be functional in a transactivation assay only in the presence of wild type p53, but not in the presence of a tumor-derived mutant p53. Furthermore, over-expression of p53 could induce the upregulation of Bid mRNA levels both in cell lines and in mice. This upregulation of Bid might be important to p53-mediated apoptosis following the administration of DNA damaging agents such as adriamycin and 5-FU so that Bid-deficient fibroblasts were more resistant to these agents [182].

Transcriptional down-regulation of Bid had also been reported. The promyelocytic leukemia zinc finger (PLZF) protein affects myeloid cell growth and is involved in some acute promyelocytic leukemia. It could transcriptionally suppress the expression of Bid [183]. A high-affinity PLZF-binding site element has been identified about 2 Kb upstream of the transcription start site in the human Bid gene [183].

1.2.1.3 Post-translational Modification of Bid and Its Pro-apoptotic Function.

Caspase 8 cleavage of Bid is the major mechanism that regulates Bid migration to the mitochondrial membrane. Caspase 8 is an initiation caspase, which is normally activated following the engagement of death receptors, such as Fas, TNF-R1 and TRAIL. The death receptor apoptosis pathway or the extrinsic pathway had been thought to involve only the caspase cascade in which caspase 8 activates the downstream effector caspases, such as Caspase-3. The discovery of Bid being activated by caspase indicates the involvement of the mitochondria in the death receptor apoptosis pathway. Cleavage by Caspase 8 releases the inhibition mediated by the N-terminal p7 fragment of Bid, thus increasing the number of exposed hydrophobic residues and facilitating the binding of p15 truncated Bid (tBid) to the mitochondrial membranes [184]. Consistent with hydrophobic interactions holding the p7 N-terminal and the p15 C-terminal fragments of Bid together, incubation with octyl glucoside is required to separate the fragments when purified Bid is cleaved with recombinant caspase-8 [185]. However, some recent data reveal that in the presence of

membranes, the p7 and p15 tBid fragments spontaneously dissociate following cleavage, allowing tBid to insert into the mitochondrial membrane. Therefore, It is presumed that in the presence of a membrane target, caspase-8-cleaved Bid undergoes a conformational change that displaces the p7 fragment and exposes sufficient additional hydrophobicity to drive insertion of the tBid fragment into the membrane [172]. The ordered series of steps required for outer membrane permeabilization are: (1) tBid rapidly binds to membranes, where (2) tBid interacts with Bax, causing (3) Bax insertion into membranes and (4) oligomerization, culminating in (5) mitochondrial outer membrane permeabilization (MOMP) [186]. Cleavage by caspase-8 also exposes Gly60 at the newly formed N-terminus of tBid, which allows N-myristoylation to occur subsequently [185]. This secondary post-translational modification significantly increases the ability of tBid to interact with membranes and therefore enhances its translocation to the mitochondria. As a consequence, myristoylated tBid is more potent than the non-modified tBid in inducing a full release of cytochrome c from the mitochondria.

It has also been reported that extrinsic caspases such as Caspase-3, activated downstream of mitochondrial permeabilization, can also cleave Bid [187], at the regulatory loop. Differences in the sensitivity to caspase-8 and caspase-3 are present, which might be significant in term of in vivo regulation [188]. However, since the cleavage of Bid by caspase-3 apparently occurs downstream of the

mitochondria activation, Bid can serve as a key link in the amplification of various apoptosis signals other than the death receptor engagement [187].

Other studies have indicated that Bid can be cleaved in a specific and limited way by other proteases such as Granzyme B and calpains. These proteases are first activated in response to a plethora of stimuli, including death receptor activation, cytotoxic T cell attack, ischemia/reperfusion injury and lysosome damage. These observations indicate that Bid is in general a sentinel to protease activation resulted from various injury stimuli. As such Bid serves a critical role in connecting these stimuli to the mitochondria, thus allowing the death process either to be advanced or to be amplified [173]. Finally, Bid can also be activated by lysosomal enzymes [173]. Lysosomal enzymes represent a large group of catabolic enzymes, which are found to participate in the apoptosis process. In particular, cathepsins have been shown to link to the mitochondria pathway [189, 190]. Bid has been implicated in the process as the mediator connecting lysosome to the mitochondria. Bid can be cleaved by the lysosomal enzymes at the regulatory loop [166] and the cleaved Bid is able to activate the mitochondria. A detailed study now shows that murine Bid can be cleaved by cathepsin B, H, L, S, and K, predominantly at Arg65 or Arg71 [190]. However, the aspartic protease cathepsin D is not found to be able to cleave Bid [190].

Another important modification related to Bid function is its phosphorylation. In Bid, there are two potentially phosphorylated residues (Thr59 and Ser65) in the

vicinity of the caspase-8 cleavage site [172]. Phosphorylation of Thr59 severely inhibited cleavage of Bid by caspase-8, whereas phosphorylation of Ser65 had no effect [188]. Phosphorylation of Thr59 was achieved by casein kinase II, and presumably other cellular kinases. Similarly, phosphorylation of murine Bid (at Ser61 and Ser64) by casein kinase I and II also attenuated cleavage by caspase-8 cleavage [191]. Because cleavage of Bid is an essential prerequisite to its binding to membranes, phosphorylation effectively prevents Bid from translocating to the mitochondria.

It is worth to mention that the mitochondrial recruitment of Bid also relies on the facilitation of MIMP/MTCH2 (mitochondrial carrier homologue 2/Met-induced mitochondrial protein). MTCH2 is a tBid-interacting protein. It is a surface-exposed outer mitochondrial membrane protein. Knockout of MTCH2/MIMP in embryonic stem cells and in mouse embryonic fibroblasts hinders the recruitment of tBID to mitochondria, the activation of Bax/Bak, MOMP, cytochrome C release and apoptosis. Moreover, conditional knockout of MTCH2/MIMP in the liver decreases the sensitivity of mice to Fas-induced hepatocellular apoptosis and prevents the recruitment of tBID to liver mitochondria both in vivo and in vitro. These findings indicate that MTCH2/MIMP has a critical function in liver apoptosis by regulating the recruitment of tBID to mitochondria [192].

Cardiolipin also plays an important role in Bid interaction with the mitochondria. Cardiolipin is a unique phospholipid present in the mitochondrial inner

membranes and also the outer membranes of the contact site. Initially, Bid–cardiolipin interaction was defined in vitro using purified proteins and lipids. In cardiolipin-deficient cells, induction of cytochrome c by Bid was significantly compromised [193]. Direct evidence that Bid could interact with cardiolipin in the mitochondria was obtained by mass spectrum analysis of lipids extracted from tBid-treated mitochondria [194]. Overall, Bid–cardiolipin interaction is independent of the BH3 domain of Bid [194], but dependent on its α4–α6 helices [195]. Since tBid is only present in the outer membranes of the mitochondria [194] and cardiolipin is most enriched in the inner membranes and the contact site, people has studied on where the tBid and cardiolipin interacts with each other. Fractionation of the mitochondrial membranes finds that tBid could target to different locations of the mitochondrial outer membranes. Most tBid is present in the outer membranes of lighter density consistent with the location of Bak and the contact site. Further studies using a cardiolipin-specific dye, 10-nonyl-acridine orange (NAO), shows that it is at the contact site where tBid seems to interact with the cardiolipin [194]. This finding is consistent with the study of electron microscopy tomography, which supports the presence of tBid in the contact site[196].

1.1.2 Bid's role in the Liver, the Apoptotic and Non-apoptotic Functions

The functional role of Bid has been studied in the liver related to its pro-apoptotic function. Thus, several liver injury models in murine are triggered by the death receptor agonists. Although engagement of the death receptors could trigger apoptosis without the participation of the mitochondria pathway in the so called types I cells, the latter is required in the type II cells [197]. Type I cells have been defined to be independent of mitochondria for the induction of death receptor-mediated apoptosis, whereas Type II cells are mitochondria-dependent [198]. Hepatocytes were the first type II cells defined in vivo when it was shown that bid-deficient mice were resistant to anti-Fas antibody-induced liver injury [199].

Bid is also important for TNFα- and TNF-related apoptosis-inducing ligand (TRAIL)-initiated apoptosis. In that case, Bid is cleaved and activated on TNFα/cycloheximide stimulation [178]. The mediation of Bid in TRAIL-induced mitochondrial is critical to the killing of cancer cells [200] and to the synergistic effects of TRAIL and DNA-damaging agents [201]. A notable difference seen in TNFα-induced liver injury is that deletion of Bid impedes, but does not prevent TNFα-induced killing. This is likely due to the fact that TNFα can activate several other death effector mechanisms, among which c-Jun N-terminal kinase and Bim, another BH3-only molecule that can be activated by c-Jun N-terminal kinase, turn out to be crucial players. Combined deletion of Bid and Bim could

protect mice from lipopolysaccharide/D-galactosamine (LPS/GalN)-induced liver injury, which is also mediated by TNFα [202].

Varies other studies have shown Bid's role in different liver diseases, with possible hepatocyte apoptosis as a consequences. For example, liver ischemia-reperfusion injury [203], hepatobiliary cyst and hepatocellular carcinoma [204], liver intoxication [205] and alcoholic liver disease [206], etc. Interestingly, under physiological conditions without adverse stimulation, a small amount of cleaved Bid is found in wild-type mouse livers, which can cause cytochrome c release. However, such a condition does not lead to noticeable liver injury unless an anti-apoptotic molecule, such as Bcl-xL, is deleted, or suppressed by a pharmacological inhibitor. Further studies showed that deletion of Mcl-1, another anti-death Bcl-2 family molecule constitutively expressed in the liver, can also result in spontaneous hepatocyte apoptosis [207]. Co-deletion of Bid suppressed the spontaneous apoptosis [208]. Taken together, these studies indicated that Bid is important to hepatocyte homeostasis under both physiological and pathological conditions [209].

Previously findings have all focused on Bid's function and effect in apoptosis. However, recently, more studies have shown Bid participates in non-apoptosis functions. One study shows that Bid is important in immune response [210]. Innate immunity is a fundamental defense response that depends on evolutionarily conserved pattern recognition receptors for sensing infections or

danger signals [211]. Bid has been found related to nucleotide-binding and oligomerization domain (NOD) proteins. NODs are cytosolic pattern-recognition receptors of paramount importance in the intestine, and their dysregulation is associated with inflammatory bowel disease. The Salehs' group [212] has used genome-wide RNA interference and identified a significant crosstalk between innate immunity and Bid. Colonocytes lack of BID or macrophages from Bid KO mice are markedly defective in cytokine production in response to NOD activation. Furthermore, Bid KO mice are unresponsive to local or systemic exposure to NOD agonists or their protective effect in experimental colitis. Mechanistically, BID interacts with NOD1, NOD2 and the IκB kinase (IKK) complex and ERK signalling. Those findings have shown the connection between apoptosis and immunity via linkage of Bid.

Several other studies have focused on Bid's role in hematopoiesis [209]. Generally, hematopoietic cell quiescence maintains hematopoietic stem cell function. Quiescent cells are less vulnerable to DNA damage from exogenous toxins, the chromatin packed DNA is protected from modification by ROS. Loss of Bid in mice results in abnormal myeloid homeostasis and tumorigenesis [210, 213]. Initially, Bid knockout mice maintain hematopoietic homeostasis with normal blood counts in all lineages. After 1 year of age, Bid knockout mice display a decrease in blood counts, with anemia and thrombocytopenia. This progresses to an increase in cells of the myeloid lineage, culminating in a disorder that closely resembles chronic myelomonocytic leukemia with evidence

of significant chromosomal instability. Two groups subsequently showed that Bid is a phosphorylation substrate of the DNA damage kinases, ATM and ATR, namely ataxia telangiectasia mutated (ATM)/ataxia telangiectasia and Rad3-related (ATR) kinases. The ATM kinase was previously demonstrated to have a role in regulating the self-renewal and quiescence of hematopoietic stem cells [214]. In addition, Bid has a role in S phase checkpoint regulation following DNA damage [215]. This cell cycle checkpoint role requires phosphorylation at serine 78, but does not require the BH3 or death domain of Bid [216]. Those important findings not only have described a role for Bid in preserving genomic integrity but also have showed Bid functions at an early point in the path to determine the fate of a cell. Bid plays an unexpected role in the intra-S phase checkpoint downstream of DNA damage distinct from its proapoptotic function. New findings have indicated that Bid associates with the ATR/Atrip/replication protein A (RPA) complex and the association between ATR/Atrip and RPA is significantly diminished in Bid-deficient cells following replicative stress, another evidence suggesting that Bid has a role to maintain the DNA damage sensor complex [209]. Interestingly, exposing wild-type mice to irradiation also triggers an increase in mitochondrial Bid and an increase in mitochondrial ROS [217] suggesting that the ATM–Bid complex may affect metabolism changes in DNA damage. Taken together, these results suggest that at low levels of DNA damage ATM phosphorylates Bid to keep it away from the mitochondria resulting in low levels of ROS generated from mitochondria. Increasing the levels of DNA

damage proportionally increases the levels of mitochondrial Bid, which leads to a proportional increase in mitochondrial ROS.

In regards to the function of Bid's phosphorylation, it is well established that ATM is a nuclear kinase and it was previously demonstrated that part of the Bid protein pool is localized to the nucleus [215]. Thus, it is most likely that ATM phosphorylates Bid in the nucleus and that this phosphorylation inhibits Bid exit from the nucleus and thereby its accumulation in mitochondria. However, most recently, it is demonstrated that ATM is also localized to the mitochondria [218]. An alternative possibility is thus that ATM phosphorylates Bid at the mitochondria, leading to its retrotranslocation into the cytosol.

These findings, although in the hematopoietic systems, have unveiled some of the other non-apoptotic function of Bid. How does the ATM–Bid complex regulate the metabolic status and ROS generation from the mitochondria? As mentioned in the previous section, MTCH2 has been shown to serve as a mitochondrial receptor for Bid and is very important for Fas-induced liver apoptosis. Interestingly, MTCH2 was previously identified in a genome-wide association study as one of six new gene loci associated with body mass index (BMI) in humans [218, 219]. Body mass index is the most commonly used quantitative measure of adiposity, and adults with high values of body mass index are associated with obese. Thus, MTCH2 may also be involved in fatty acid/glucose metabolism in the mitochondria. It is logical to make a hypothesis that the

function of MTCH2 is coupled with Bid. Thus, it is possible that Bid could play a role in regulating mitochondrial function in a non-apoptotic way.

1.2 Materials and Methods

1.2.1 Animal Experiment:

All animal experimental protocols were approved by the Institutional Animal Care and Use Committee of Indiana University (IACUC). Animals were housed under approved conditions in a secured animal facility at the Indiana University School of Medicine with 12 hour light dark cycle. Bid knockout mice were generated in our lab. Wild type mice were purchased from the Jackson Laboratory (Bar Harbor, ME). At 10 weeks of age, mice were placed on normal chow diet, high fat diet (diet D12492, Research diets) or high-fat high-carbohydrate (HFHCD) diet. For HFHCD diet, mice were given high fat diet along with the drinking water enriched with high-fructose corn syrup equivalent to a total of 42 g/L of carbohydrates. Drinking solution was made by mixing in drinking water at a ratio of 55% fructose (Acros Organics, Morris Plains, NJ) and 45% sucrose (Sigma-Aldrich, St. Louis, MO) by weight. Animals were provided ad libitum access to these diets for 10-24 weeks. Body weight was recorded weekly.

1.2.2 Immunoblotting

Mouse livers were dissected and 250 mg of liver tissue was homogenized in NP-40 lysis buffer containing 1% NP-40, 50mM Tris-Hcl (pH 7.5), 150mM NaCl, 0.05% SDS, 1mM aprotinin, 20µg/ml PMSF, 1.7µg/ml Aprotinin, 2.5µg/ml

Leupeptin, 1μg/ml Pepstatin A. The buffer is supplemented with 1 tablet Complete Mini Protease Inhibitor Cocktail (Roche, Mannheim, Germany) per 10 ml. Mice liver tissue was dounced for 15 times using tight (B) pestle of a glass homogenizer. Liver lysate was kept in pre-chilled Eppendorf tube on ice for 40 min. After centrifugation at 15 000 × g for 15 min at 4°C, the supernatant was stored at −80°C until further us. Protein concentrations were measured by the BCA method. Immunoblots with SDS-PAGE electrophoresis system were performed as previously described. Gel Running buffer contains 25 mM Tris Base, 192 mM Glycine, 0.1% SDS at PH 8.2. Transfer buffer contains 25 mM Tris Base, 192 mM Glycine and 20% methanol (v/v). Transfer condition is 7 volt overnight or 20 volt 2.5h. First antibody was dissolved in 5% Skimmed milk in TBS buffer or 5% BSA in TBS buffer. Secondary antibody in conjugation HRP (Jackson Immuno-Research Laboratory) was used at 1:5000 dilution. Rabbit anti-mouse Bid antibody was made by in house and was used at the dilution of 1:500. MTCH2 antibody, (Proteintech 16888-1-AP) was used at the dilution of 1:1000, CPT1 antibody (Santa Cruz 98834) was used at the dilution of 1:500. Blots were developed using Immobilon Chemiluminescent HRP substrate (EMD Millipore, Billerica, MA). Image was acquired by Kodak 4000 image station system.

1.2.3 Indirect Calorimetry

The TSE (Chesterfield, MO) Labmaster calorimetry cage is a set of live-in cages for automated, non-invasive, and simultaneous monitoring of oxygen consumption, and CO_2 production. Eight 10wk old mice from Bid KO and WT groups were given HFD for 10wks (accumulated age 20 wks) and then placed in calorimetry cages. Each cage was maintained at 25^{o} C at the 12 hour dark-light cycle. After acclimatization individually for 72h, the O_2 consumption (VO_2, mL/kg/min), CO_2 production (VCO2, mL/kg/min), and respiratory quotient (ratio of VCO_2/VO_2) were continuously measured. VO_2 and VCO_2 were recorded every 10 min for a total of 48 h. The hourly file displays all measurements for each parameter.

1.2.4 Histology

Different tissues from mice were harvested, washed with ice-cold PBS, and fixed in 10% formalin overnight and transferred to 70% ethanol the next day. Tissue blocks were processed by Indiana University Health Pathology Laboratory. Histochemical analysis was carried out on 4-μm-thick sections stained with hematoxylin and eosin (H&E), and Trichrome C.

1.2.5 Gene Expression Analysis: with Real-time PCR

Total RNA from liver tissue was extracted with GeneJET RNA purification kit (Thermo Scientific). Briefly, 30mg of frozen tissue were lysed with the lysis buffer provided by the kit. Six hundred µl of proteinase K were then added followed by centrifugation at 12000g. Next, 450ul of ethanol were added and the precipitated pallets were washed with washing buffer provided by the kit for RNA purification. RNA quality and concentration was quantified by spectrometry at A260/A280.

Next, 5µg of RNA was used in a reverse transcription reaction using M-MLV reverse transcriptase (Invitrogen), per manufacture's introduction. For RT-PCR amplification of the target genes, cDNAs were mixed with AmpliTaq Fast DNA polymerase and other necessary ingredients. Amplification was conducted for 40 cycles using an Applied Bioscience PCR system. ---Analysis was performed using the 2ΔΔCT method. QPCR results were normalized against gene PPIA

Primer sequences used for the amplification are as follows:

PPIA Fw: 5'- CACCGTGTTCTTCGACATCA -3'

Rv: 5'- CAGTGCTCAGAGCTCGAAAGT -3'

IL-1beta Fw: 5'- GCTGCTTCCAAACCTTTGAC -3'

Rv: 5'- TGTCCTCATCCTGGAAGGTC -3'

INF-gamma Fw: 5'-GATGCATTCATGAGTATTGCCAAGT-3'

Rv: 5'-GTGGACCACTCGGATGAGCTC-3'

TGF-beta Fw: 5'-CACCGGAGAGCCCTGGATA-3'

Rv: 5'-TGTACAGCTGCCGCACACA-3'

Collagen – 1l Fw: 5'-ACGGCTGCACGAGTCACAC-3'

Rv: 5'-GGCAGGCGGGAGGTCTT-3'

TIMP1 Fw: 5'- ATTCAAGGCTGTGGGAAATG -3'

Rv: 5'- CTCAGAGTACGCCAGGGAAC -3'

IL-18 Fw: 5’- ACGTGTTCCAGGACACAACA -3’

Rv: 5’- ACAAACCCTCCCCACCTAAC -3’

PGC-1 alpha Fw: 5'-TCCTCTGACCCCAGACTCAC-3'

Rv: 5'-TAGAGTCTTGGAGCTCCT-3'

PGC1 beta Fw: 5’ –CCGAGCTCTTCCAGATTGAC– 3’

Rv: 5’ –TTCATCCAGTTCTGGGAAGG– 3’

PRC Fw: 5’ –GCTACTTCCCAGGAGCCTCT– 3’

Rv: 5’ –GGTGAAGCCTCAGGAGACAG– 3’

PPAR delta Fw: 5’ –TGGAGCTCGATGACAGTGAC– 3’

Rv: 5’ –GGTTGACCTGCAGATGGAAT– 3’

arnitine/acylcarnitine translocase (CAC)

Fw: 5’ –TGCCAGTGGGATGTATTTCA– 3’

Rv: 5’ –GTTGAAGATCCCTGCAAAGC– 3’

MTCH2: Fw: 5’ –TTTGGGCGACAAGTATGTCA– 3’

Rv: 5’ –CTTTCCCATGGACCACAGTT– 3’

1.2.6 Ketone Body Measurement

Whole blood from mice was collected through axillary artery. Serum were collected after centrifugation at 4000 rpm for 15 mins. Serum ketone body was measured with beta –hydroxybutyrate colorimetric assay kit (Cayman Chemical, Ann Arbor, MI). Absorbance was taken at 445-455 nm. To measure the ketone body in liver tissue, 400 µg of liver were dounced in1.5 ml of tissue lysis buffer provided by the kit and subjected to procedure as described above. Final concentrations were normalized to protein concentrations.

1.2.7 Ex-Vivo Fatty Acid Oxidation Rate Measurement

Live mitochondria was extracted for ex-vivo fatty acid oxidation measurement. Briefly, 250-350 mg of liver tissue from different lobes were dounced with the loose (A) pestle of a glass homogenizer for 3 times by HIM buffer containing 200mM mannitol, 70mM Sucrose, 5mM Hepes, 0.5mM EGTA. Liver lysates were centrifuged for 10min at 2000 rpm. Supernatant was collected as the mitochondria fraction and kept on ice.

Radiolabelled substrate was prepared by aliquoting radiolabled substrate (0.7uCi/recaction) into an Eppendorf tube. The organic phase dried off under air. Nonradiaolabeled palmatic acid and BSA carrier were then added. The reaction mixture contains 100 mM Sucrose, 10 mM Tris-Hcl, 5mM KH_2PO_4, 0.2 mM

EDTA, 5 mM Nicotinamide, 1 μM TricostatinA, 0.3% fatty acid free BSA, 80 mM KCl, 1mM $MgCl_2$, 2mM L-carnitine, 0.1mM Malate, 0.05 mM Co-enzymeA, 2mM ATP, 1mM DTT, adjust to pH 8.0 were made to 380ul per reaction.

A filter paper was cut to fit in the cap of Eppendorf tube and was soaked with 10ul of NaOH. This was subsquently to trap the C14 labeled CO_2 released from the oxidation reaction. Generally, 20 ul of mitochondria fraction, 12 ul of substrate (radiolabled and nonradiolabled) were added to the reaction mix which was incubated at 37C water bath. The time from tissue dissection to reaction initiation should be less than 30min to ensure mitochondria vitality for the reaction. After incubation, 200μl of percholic acid were added to each reaction tube followed by incubation of 1 hour at room temperature and centrifuge at 14000rpm to separate the radiolabeled acetyl CoA from the unoxidized fatty acid. The 200 μl of supernatant after centrifugation and the filter papers trapped with CO2 were put into separate scintillation vial containing 4ml of scintillation fluid for reading in a Packman Scintillation Counter. CPM readings were finally adjusted for protein concentration.

1.2.8 Hepatic Triglyceride Measurement

80 mg of frozen liver tissue were powdered under liquid nitrogen and incubated in total of 1ml of chloroform-methanol mix (2:1) for 1 hour at room temperature with shaking to extract lipids phase. After addition of 200 μl of H_2O, samples

were vortexed and centrifuged for 5min at 3000g. The lower lipid phase was collected and dried in a chemical hood overnight. The lipid pellet was resuspended in 60 µl of tert-butanol and 40 µl of a Triton X-114-methanol (2:1) mix. Triglycerides were than measured using the Pointe Scientific Triglycerides Assay Kit (Pointe Scientific, MI)

1.2.9 Blood Biochemistry Assay and Insulin Resistance Measurement

Serum glutamic-pyruvic transaminase (SGPT) or alanine aminotransferase (ALT) was measured with an ALT (SPGT) reagent kit (Pointe Scientific, Canton, MI).Briefly, serum was diluted five times. After reaction, samples were read at 340nm absorbance at 37^{o}C. Plasma triglyceride and cholesterol level were measured by Triglyceride/ Cholesterol kit (Pointe Scientific, Canton, MI). Serum insulin level was measured with an insulin ELISA kit (Millipore, Billierica, MA). Blood glucose level was measured using the Contour blood glucose monitoring system (Bayer, Mishawaka, IN). Insulin resistance (HOMA) was calculated by the following formula, (fasting glucose/18 mg/dl * fasting insulin * 25ng/ml)/22.5.

1.2.10 Free Fatty Acid Measurement

Serums collected from the mice were used for the free fatty acid measurement with the free fatty acid assay kit from Cayman Chemical (Ann Arbor, MI). Generally, 10µl of serum sample were used and the assay was performed at

37^{o}C. Fluorescence with an excitation wavelength between 530-540 nm and an emission wavelength between 585-595 nm were measured by a fluorescent spectrometer Infinite200 plate reader (Tecan)

1.3.11 Statistical analysis

Data were expressed as mean±SE. Differences between two treatment groups were compared by t test. When more than two groups were compared, on way ANOVA analysis was used. Results were considered statistically significant when $P<0.05$. All analyses were performed with Sigma Stat 3.5.

1.3 Results

1.3.1 Bid Knockout Mice Are Protected from High Fat Diet Induced Obesity

As we have discussed in the introduction, Bid protein plays an important role in apoptosis initiation via the mitochondria pathway. Recently, various findings have shown Bid also functions in DNA homeostasis, hematopoietic stem cell metabolism ROS generation and cell proliferation [209, 217]. There was other findings that have shown that MTCH2, Bid carrier protein, is one of the gene loci whose polymorphism associated with obesity in human [219]. We hypothesized that Bid may have a new function in regulating metabolism via its interaction with the mitochondria in a non-apoptotic condition.

To test our hypothesis, we gave wild type (WT) and Bid-deficient (KO) mice regular chow diet, high fat diet or high fat high carbohydrate diet and measured their body weight gains. We confirmed that the Bid protein was successfully deleted in Bid-deficient mice (Fig S1). To our surprise, we found that Bid KO mice have significantly smaller body weight gain following either high fat diet or high fat high carbohydrate diet (Fig 1A, B). The high fat diet regimen seemed to yield a larger difference between the WT and KO mice. However, the body weight was not significant changed in regular chow diet group (Fig 1A, B), indicating that obesity protection by Bid deletion is diet specific. We also calculated the percentage of body weight gain to rule out any possible baseline

variations. Under the regular diet, 6wk to 10wk old mice gained body weight naturally as a normal growth process. WT mice started to gain more weight, but less so, than the Bid KO mice in the subsequent 0-8wk and 8-16wk, respectively (Fig 1C). This suggested the different growth rates between the two groups, although the body weight gain did not differ noticeably in the full grown-ups. However, under the high fat diet and high fat high carbohydrate diet, the WT mice consistently showed a higher body weight gain through the whole course.

The lack of rapid increase in body weight following high fat diet and high fat high carbohydrate diet in Bid KO mice overall lead to a lower body mass index (BMI), a clinical marker of obesity (Fig 1D). We conducted the F2 segregation assay to study whether the effect of Bid deletion is dominant or recessive. As showed in Fig S2A, the body weight in the Bid heterozygous mice following high fat diet was no different than that in WT mice, indicating that the effect of Bid deletion is a recessive feature. Yet the effect could be clearly observed in all Bid KO mice, suggesting that it is a single gene event. It is worth to note that the smaller body weight gain by Bid KO mice was only seen in male mice, but not in female mice (Fig S3). We think the sex discrepancy may be due to the fact that a high level of estrogen in female counteracts the effect of Bid knockout, many findings have shown that estrogen affects fat metabolism and mitochondrial function [220, 221]. We also found that Bid deletion did not affect obesity caused by leptin deficiency (Fig S4). Bid-deficient mice were crossed to OB/OB mice, and the body weight of OB/OB mice and OB/OB/Bid KO mice were monitored for 20 weeks. There were

no significant body weight differences. This finding indicates that deletion of Bid is only impact on obesity caused by hyper-nutrients (high fat diet).

Most body weight gain under hyper-nutrients is due to significant adipose tissue accumulation. Thus, we studied if the smaller body weight gain in Bid KO is due to a less fat accumulation. Indeed, both epigonadal adipose tissue weight and its ratio with the whole body weight were lower in Bid KO mice following high fat diet or high fat high carbohydrate treatment (Fig E, F, S2B). Histological analysis indicated a smaller size of adipocytes in Bid KO adipose tissue, suggesting a smaller fat-content. Thus, there were fewer WT adipocytes than Bid-deficient adipocytes in a given microscopic field (Fig 1G-H).

1.3.2. Bid Knockout Mice Are Protected from Hyper-nutrients-Induced Metabolic Syndrome

Clinically, obesity causes multiple metabolic disturbances. As we have showed in Fig 1, Bid KO can protect high fat diet and high fat high carbohydrate diet - induced body weight gain. We thus studied whether Bid KO also protected against the development of metabolic syndrome in high fat diet and high fat high carbohydrate diet regimes.

As shown in Fig 2A, fasting glucose level was lower in Bid KO following 16wk of high fat diet or high fat high carbohydrate diet treatment, although statistical significance was only achieved in high fat diet regimen. It is possible that, high carbohydrate diet caused severe diabetes, which masked the protective effect of Bid KO [222]. The insulin level was significantly lower in Bid KO mice after either diet treatment (Fig 2B). The assessment of insulin resistance is based on the level of fasting glucose and fasting insulin, which leads to the calculation of the HOMA value. The HOMA value was lower in Bid KO mice (Fig 2C), indicating a lower insulin resistance level. Serum cholesterol levels (Fig 2C), but not serum triglyceride levels (Fig 2B), were lower in Bid KO group in high fat diet and high fat high carbohydrate diet, Hypercholesterolemia is one of the most common indications of atherosclerosis and risk factors of coronary artery disease. It is worth to note that Bid KO could potentially protect the development of coronary artery disease by lowering serum cholesterol.

In a long-term study (24wk) with only high fat diet treatment (Fig S5), we found that the fasting glucose level was not as high as in the 16wk group (compare Fig S5A and Fig 2A), although Bid –deletion still led to a lower glucose level than that in the wild type and Bid heterozygous mice. Serum cholesterol level remained significantly lower in Bid KO mice (Fig S5B). The levels of triglycerides were increased in all groups of mice at 24wk (Fig S5C) compared to those at 16wk (Fig 2E). At this time point, the protective effect of Bid deletion was revealed. Serum triglyceride level was significantly lower in Bid KO mice than the WT mice or the Bid heterozygous mice (Fig S5C).

1.3.3. Bid Knockout Mice Are Protected from Steatosis, Steatohepatitis and Liver Fibrosis.

Liver is the largest organ in the body and carries most of the metabolism functions. High fat diet can cause liver steatosis [223] whereas high fat high carbohydrate diet can also trigger steatohepatitis and early stage of fibrosis [167]. All these lead to the development of NAFLD, which is an important contributor to the metabolic syndrome. Since deficiency of Bid protects against diet induced obesity and metabolic syndrome. We would like to study how Bid deficiency may affect NAFLD development in mice under high fat diet and high fat high carbohydrate diet regimes.

We found that Bid deletion had a strong protection against steatosis development in both diet regimes as assessed by histology (Fig 3A) or by the level of hepatic triglyceride (Fig 3B). Severe liver steatosis could lead to steatohepatitis where there is severe liver injury. We found Bid KO could protect liver injury induced by high fat diet and high fat high carbohydrate diet treatment measured by serum ALT level (Fig 3C, Fig S5D).

High fat high carbohydrate diet gives rise to a more severe liver phenotype, which is not only characterized by a more severe steatosis (Fig 3B), a more severe liver injury (Fig 3C) but also the development of hepatic fibrosis (Fig 3D). The expression of inflammatory cytokines (Fig 3E-G) and fibrogenic molecules:

Collagen 1l, TGF-beta, TIMP (metallopeptidase inhibitor 1) (Fig 3H-J) were all significantly increased. However, deletion of Bid led to a significant reduction of hepatic fibrosis and the expression of these genes in high fat high carbohydrate diet treatment (Fig 3D-J).

Steatosis, steatohepatitis and liver fibrosis/cirrhosis and hepatocellular carcinoma are sequential pathologies in NAFLD, in which fibrosis is a step before the pathogenesis become irreversible. Bid may thus prompt the pathogenesis of NAFLD and deletion of it may have a significant beneficial effect.

1.3.4. Bid Knockout Mice Have Higher Whole Body Metabolic Rate in vivo

Our data indicate Bid knock out can protect against obesity, metabolic syndrome and NAFLD (Fig 1-3). The mechanism leading to this interesting phenotype was unknown and could potentially imply a new molecular function of the Bid protein. As the size of adipocyte in Bid KO mice were much smaller in high fat diet and high fat high carbohydrate diet treatment groups (Fig 1G, H), we hypothesized that the phenotype of Bid KO mice could be related to an altered fat metabolism and/or energy expenditure.

We conducted calorimetry analysis on WT and Bid KO mice fed with high fat diet for 10wk (Fig 4C and D). We found that both O_2 consumption and CO_2 generation were higher in Bid KO mice than in WT mice (Fig 4A-C). Bid KO mice consistently consumed more O_2 without the differences between the day time and the night time (Fig 4A). The respiratory exchange ratio, a ratio of the amount of CO_2 produced above that of O_2 consumed, was lower in high fat diet fed Bid KO mice (Fig 4D). Respiratory exchange ratio, also known as respiratory quotient, is an indicator of the type of energy source (carbohydrate or fat) being metabolized to supply the body with the energy. A lower respiratory exchange ratio means that the Bid KO mice tended to use more fat as their energy source, which may explain the lower fat content in the adipose tissue of the Bid KO mice. Consistent with a higher metabolic rate, the heat generated from Bid KO mice in high fat diet treatment was also increased. Notably, the food consumption

between the WT and Bid KO mice was equivalent in the 16wk high fat diet feeding period (Fig 4F).

Calorimetry data thus indicated that Bid KO mice had a higher whole body metabolic rate and tended to burn more fat.

1.3.5. Deficiency of Bid Leads to a Higher Expression of Genes That Promote Energy Expenditure.

The above studies showed that Bid deletion could promote fatty acid metabolism. We thus examined the expression of genes important for this process in Bid KO mice. PGC-1 alpha (Fig 5E,J) PGC-1 beta (Fig 5A,F) , PGC1-related coactivator (PRC) (Fig 5B,G) gene expressions were all had a higher hepatic expression in Bid KO mice liver, suggesting a higher mitochondrial biogenesis and metabolism [224] with higher mitochondrial biogenesis and function [225]. Gene expression of PPAR delta was also increased in Bid KO mice, implying an elevation of the expression of its downstream fatty acid oxidation rate related genes. Notably, we found that carnitine-acylcarnitine translocase (CAC) expressed at a higher level in Bid KO mice. CAC is the enzyme facilitates fatty acid translocation through mitochondrial membrane. In the metabolic pathway of fatty acid oxidation, Carnitine palmitoyltransferase I (CPT1) is the rate limit enzyme which facilitates transportation of free fatty acid across mitochondrial membrane. Previous findings using in vivo model have showed tBid could inhibit CPT1 [226]. We observed an increased in the liver isoform of the CPT1 gene (LCPT1), although not statistically significant. Most significantly, the highest level of the expression of the genes in Bid KO livers was further enhanced following high fat diet treatment. Taken together, Bid deficient mice could have a higher fatty acid oxidation capability, which is further enhanced under the high fat diet condition.

1.3.6. High Fat Diet Induces Full Length Bid Translocation, Insertion to Mitochondrial Membrane and Destabilize MTCH2.

Bid, when cleaved into a truncated form (tBid) in the presence of apoptotic signal, can translocate to the membrane of mitochondria to trigger cytochrome c release [173]. We found in this study that high fat diet treatment of WT mice promoted the translocation of full length Bid to mitochondria (Fig 6A-B). Increased mitochondrial presence of the full length Bid under high fat diet condition was accompanied with its binding protein MTCH2 being reduced in the mitochondrial membrane (Fig 6A). Interestingly, mitochondrial MTCH2 was decreased in Bid KO livers in both regular diet and high fat diet conditions, suggesting that MTCH2 might be destabilized by the loss of Bid and/or the high fat stimulation. Reduction of mitochondrial MTCH2 was also observed in Bid -/- MEFs (Fig S6A), suggesting that Bid deletion is sufficient to affect MTCH2 level. On the other hand, RT-PCR analysis of MTCH2 suggested its RNA level was only slightly increased under either regular diet or high fat diet (Fig S6B, C). As certain polymorphism of MTCH2 have been reported to have a close genetic association with the obesity [219], and MTCH2 KO mice have shown lean phenotype under high fat diet treatment (personal communication with Dr. A.Gross, Weizmann Institute of Israel), our finding is potentially interesting in that the lean phenotype of Bid KO could possibly due to the reduction of MTCH2. In contrast, CPT-1 expression level was higher in high fat diet condition and was even higher when Bid is not present (Fig 6A, Fig S6A). This finding was consistent with the RT-PCR

analysis (Fig 5F) and implied an elevated fatty acid oxidation in the presence of high fat diet and/or Bid deletion.

We next tested whether the full length of Bid detected in mitochondrial fraction was inserted into the membrane or just loosely attached to it. As shown in Fig 6C, a strong alkaline condition could not remove all full length Bid from the mitochondrial membrane. This finding showed that a portion of full length Bid had a strong binding with, or had inserted into mitochondrial membrane, which may provide Bid functionally stable environment for its metabolic function.

1.3.7. Mitochondria in Bid KO Livers Have Higher Fatty Acid Oxidation Rate

Our data from calorimetry study and the gene expression study suggested that Bid deletion caused an increased metabolic rate, with a potential increased use of fatty acid as the energy source. Furthermore, there was an increased presence of Bid in the mitochondria following high fat diet treatment, suggesting that Bid may have regulatory effects on mitochondrial function, such as beta-oxidation. It had been reported that apoptotic condition, tBid can suppress mitochondrial fatty acid oxidation flux by malonyl-CoA-independent inhibition of CPT1 [226]. We thus decided to directly measure and compare fatty acid oxidation rate in hepatic mitochondria prepared from WT and Bid KO mice fed with high fat diet.

During fatty acid beta-oxidation, long chain fatty acids need to first transport through the mitochondrial membrane with the facilitation of CPT1 in the outer-membrane and Carnitine palmitoyltransferase II (CPT II) in the inner-membrane. Fatty acids are then oxidized to multiple acetyl-CoAs, which enter into the Kreb cycle to generate ATP as the final product, with CO_2 as the byproduct [227]. Alternatively, acetyl-CoAs are converted to the ketone body and exported mainly occurring in the liver.

We first prepared liver homogenates from mice fed with high fat diet for 10wks and added C^{14} labeled palmitic acid as the beta-oxidation substrate. After the

incubation for 60min or 120min, we quantified the production of C^{14} – Actyl-CoA and CO_2 as the measurement of beta-oxidation. Mitochondria from WT livers showed an increased Actly-CoA production from 60min to 120min, while CO_2 production remained steady. An increased C^{14}-acetylCoA level was observed in Bid KO mice mitochondria (Fig7A), although it was somewhat unexpected that a much higher C^{14}-CO_2 level was also generated in Bid KO mitochondria (Fig7B). These results suggested that fatty acid oxidation in Bid KO mitochondria moved through the Kreb cycle to generate the final product, CO_2. Consistently, we did not observe any differences in ketone body generation between WT and Bid KO mitochondria (Fig S7).

The elevated beta-oxidation in Bid KO mitochondria was inhibited by exogenous Bid when purified recombinant Bid protein was added to Bid KO liver homogenate. Both C^{14} – Actyl-CoA and C^{14} -CO_2 were dose-dependently decreased to the level produced by the WT homogenate (Fig 7C-D). The inhibitory effect was reversed by a pharmacological inhibitor of Bid, BI6C9. Adding BI6C9 at difference doses led to the recovery of fatty acid oxidation rate that was suppressed by exogenous recombinant Bid protein (Fig 7C-D). These findings thus confirmed that the fatty acid oxidation rate could be modulated by Bid.

Enhanced fatty acid oxidation in the liver would need a higher supply of free fatty acid, mainly from adipose tissue, although also from the liver. Fatty acids

released from adipose tissue need to be transported to the liver through the circulation. Therefore, we measured the free fatty acid level in the serum of Bid KO and WT mice. As shown in Fig S8, there were higher concentrations of free fatty acid in Bid KO mice under regular diet and under short term high fat diet (5wk). However, there was more free fatty acids in WT mice in longer term of high fat diet treatment (15wk). These findings may be explained that fatty acid level in the blood is affected not only by the beta-oxidation but also the metabolic disturbances which is more severe in the WT mice.

1.4 Discussion

In this part of the study, we have demonstrated a new function of Bid, which is not related to its traditional function in apoptosis. Bid seems to be a susceptible factor for diet - induced obesity, metabolic syndrome, and hepatic steatosis and fibrosis. There are some unique features in this Bid function. First, this effect is more prominent in high fat diet regime and in high fat high carbohydrate diet regime, and shows least effect under regular diet. High fructose uptake may mask the effect of Bid, or render the contribution of Bid irrelevant to obesity development. Second, the effect of Bid is not seen in leptin deficiency induced obesity, suggesting that the contribution of Bid is relatively smaller when obesity is caused by an overwhelming uptake of food. Third, Bid's contribution in high fat diet - induced obesity is minimal in female mice, which suggests that estrogen may counteract the effect of Bid, perhaps at the mitochondrial level. Fourth, the contribution of Bid is genetically dominant and only homozygous deletion could remove this effect.

Evolutionally, animals and human being, tend to store excessive nutrients. High fat diet intake may overwhelm catabolic metabolism such as by downregulating the rate limiting enzyme CPT-1 in fatty acid oxidation pathway. Our findings give a potential mechanism of how fatty acid oxidation rate might be reduced in high fat diet regime. Full length Bid probably participates in this process. The majority of the previous studies of Bid have focused on its role in apoptosis. It is known

that when death receptors are engaged, Bid is cleaved by caspase-8 and the truncated Bid, known as tBid, is translocated to the mitochondrial membranes. However, in this study, we have shown that full length Bid is found in the mitochondrial membrane under the high fat diet condition, which could be related to its new function in suppressing fatty acid oxidation. Translocation of full length Bid seems to be trigged by high fat diet. It has been reported that tBid can interact with a lipid component, caridolipin, in mitochondrial membrane during apoptosis [194, 228]. Considering that mitochondrial membrane is composed of lipids, we speculate that high fat diet may alter lipid composition in the mitochondrial membrane that may stabilize inserted full length Bid on it. The actual mechanism of full length Bid translocation has yet to be determined.

Bid may inhibit beta-oxidation once it is on the mitochondrial membrane. CPT-1 is the rate limiting step of beta-oxidation and Bid could thus inhibit beta-oxidation via this mechanism. It may inhibit CPT-1 either functionally or via reduction of the protein level. CPT-1 level is increased in Bid -/- cells. Previous findings using an in vitro model have also shown that tBid could inhibit CPT1 [226]. Further, under apoptotic signal, tBid can suppress mitochondrial fatty acid oxidation flux by malonyl-CoA-independent inhibition of carnitine palmitoyltransferase-1[226].

How may full length Bid affect CPT-1? We suggest that Bid may do so by interacting with MTCH2, which belongs to the family of mitochondrial carrier proteins. Other members of this family include ANT (adenosine nucleotide

translocator), which is important for transporting ADP and ATP in and out of the mitochondrial membrane.

It has been reported that translocation of tBid to mitochondrial membrane needs the help of its carrier protein MTCH2 [192]. We have shown that there is a dramatic decrease of MTCH2 in the mitochondria of Bid KO mice, suggesting that Bid can promote the stability of MTCH2 in the mitochondria. There are additional reasons for us to raise the hypothesis that Bid could possibly have its function mediated by MTCH2. First, certain single nucleotide polymorphism of MTCH2 has been associated to human obesity development [219]. Second, MTCH2 knockout mice have a lean phenotype and metabolic change similar to that found in Bid KO mice reported in this study (personal communication with Dr. A Gross, Weizmann Institute, Israel). We thus can hypothesize that full length Bid, when present in the mitochondrial membrane under certain condition, e.g. in high fat diet treatment, could affect MTCH2 stability on mitochondrial membranes, which leads to a negative effect on CPT-1 and transportation of free fatty acids into the mitochondria. Future studies will be focused on seeking direct evidence to prove or disprove this hypothesis.

In this study, we have also found that there were significant differences in the expression of a set of genes that are involved in the mitochondrial biogenesis and mitochondrial function which is elevated in the absence of Bid. The difference is found in the regular diet treatment, but is enhanced in the high fat

diet regime. It is not clear how absence of Bid could cause or re-program the expression profile of these genes. It is possible that the enhanced beta-oxidation in Bid-deficient hepatocytes may trigger this positive re-enforcement for mitochondria function, which in turn would also contribute to the lean phenotype of Bid deletion in high fat diet regime.

In conclusion, we have shown a new function of Bid protein in this study, a function that relates to metabolism. Previous studies have found that Bid can promote cell death and proliferation, and can participate in DNA repair and in innate immunity. Thus, Bid has a very broad effect on cellular functions under a diverse set of conditions, which may dictate the specific role of Bid in specific cellular locations.

1.5 Figures and Figure Legend

Figure 1

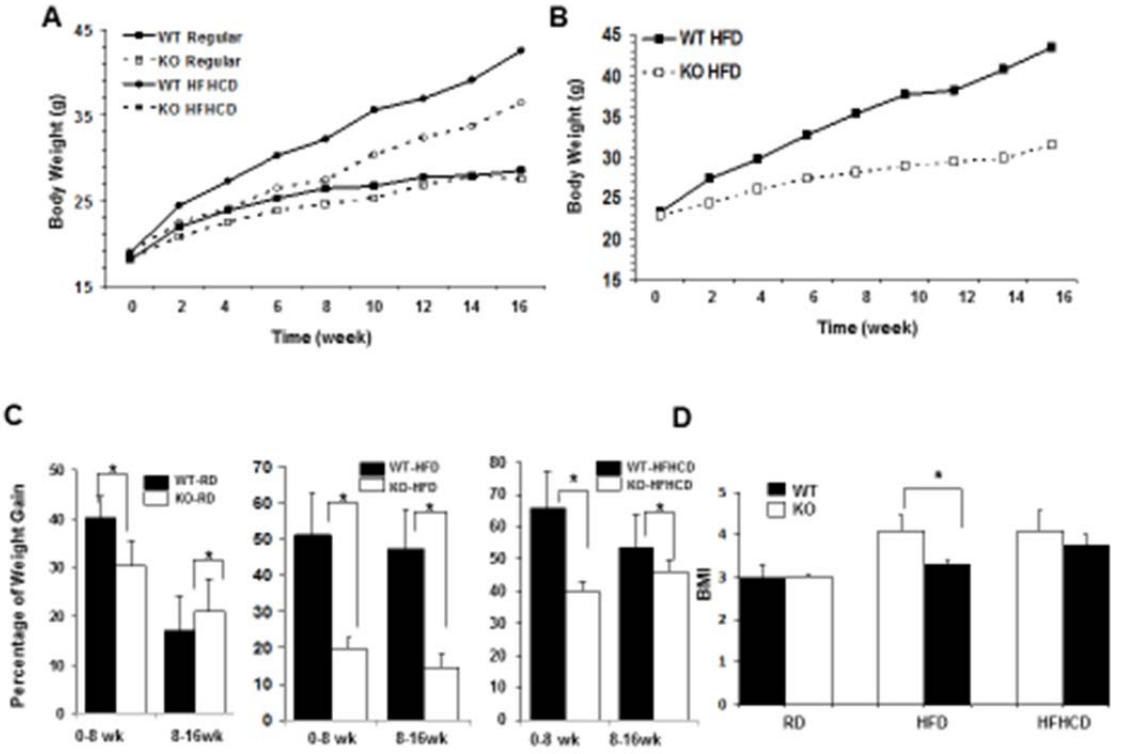

Figure 1: Bid knockout mice are protected from high fat diet induced obesity.

(A-B): Male 10wk old WT and Bid KO mice were fed with regular chow diet (RD), high fat diet (HFD) or high fat high carbohydrate diet (HFHCD) for 16wks (A-B). Body weight were measured every 2 weeks. (C): Body weight gain was expressed as the percentage of starting body weight. (D): Body mass index (BMI) were calculated as weight divided by the square of the nose-to-anus length.

n=5-8 per group, *: $p<0.05$

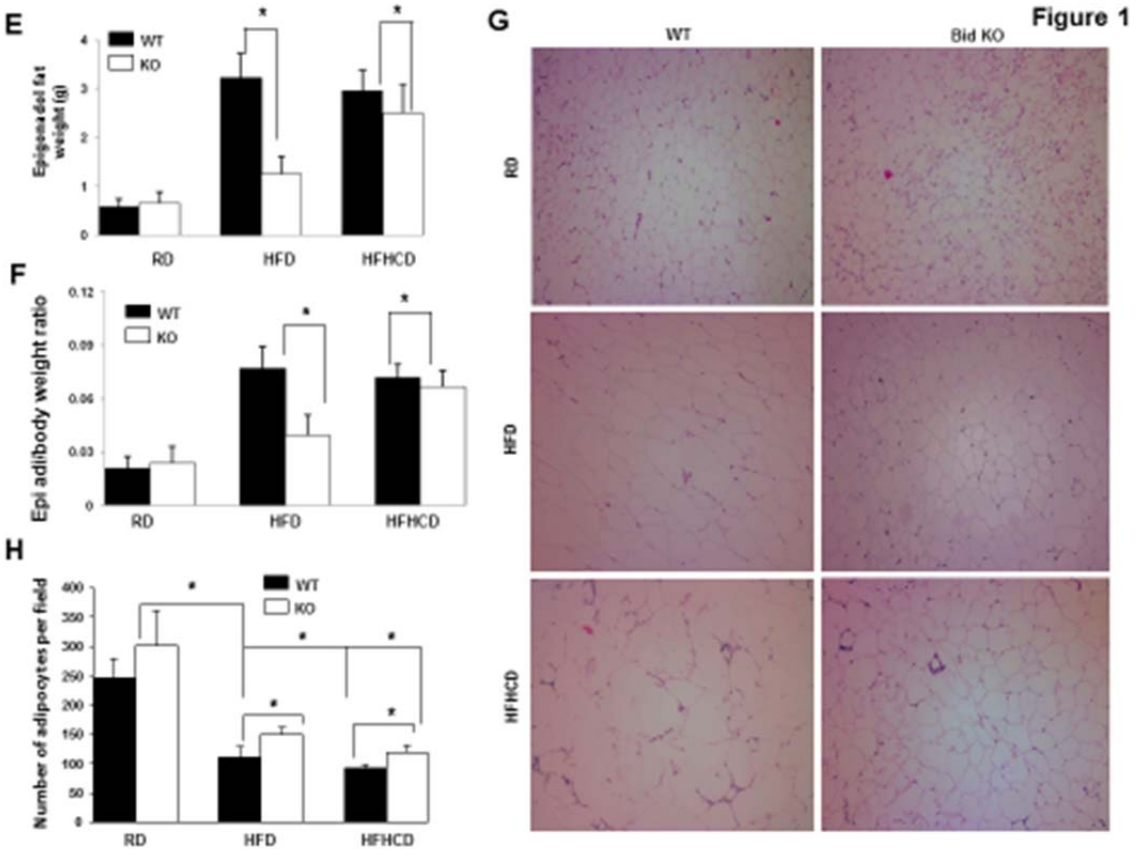

Figure 1: Bid knockout mice are protected from high fat diet induced obesity.

(E): Epigonadol tissue were obtained from one testis of each mouse and the weight was measured. (F): The ratio of epigonadol tissue and body weight ratio was determined. (G): H-E staining of the epigonadol tissue in each group of mice 100X. (H): The number of adipocytes per 100X field was determined.

n=5-8 per group, *: $p<0.05$

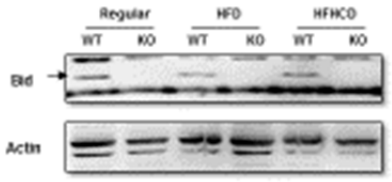

Figure S1: Expression of Bid in WT and Bid KO mice.

Male 10wk WT and Bid KO mice were fed with regular chow diet (RD), high fat diet (HFD) or high fat high carbohydrate diet (HFHCD) for 16wks. Liver tissue were homogenized and analyzed by immunoblotting assay.

Figure S2

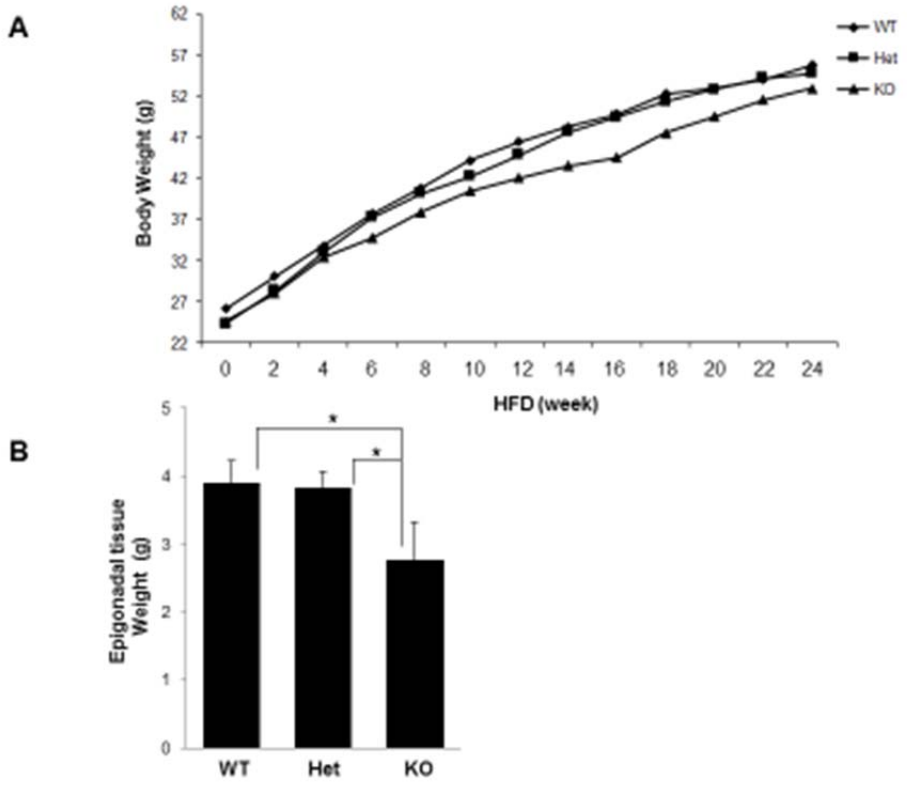

Figure S2: Bid-heterozygous male mice were not protected from high fat diet induced obesity.

(A): Male WT, Bid heterozygous (Het) and Bid knockout (KO) mice were fed with high fat diet for 24wks. Body weight were measured every 2 weeks. (B): Unilateral epigonadol adipose tissue were obtained and weight were measured.

n= 5-8 per group, *: $p<0.05$

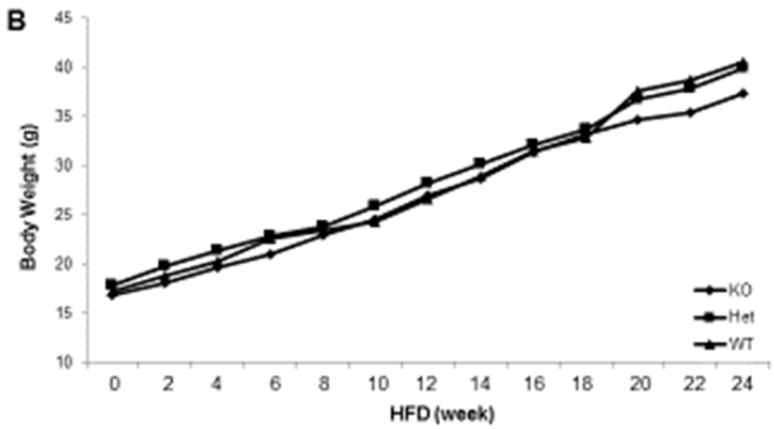

Figure S3: Female Bid KO mice were not protected from high fat induced obesity.

Female WT, Het and Bid KO mice were fed with high fat diet for 24wks. Body weight was measured every two weeks.

n= 5-8 per group

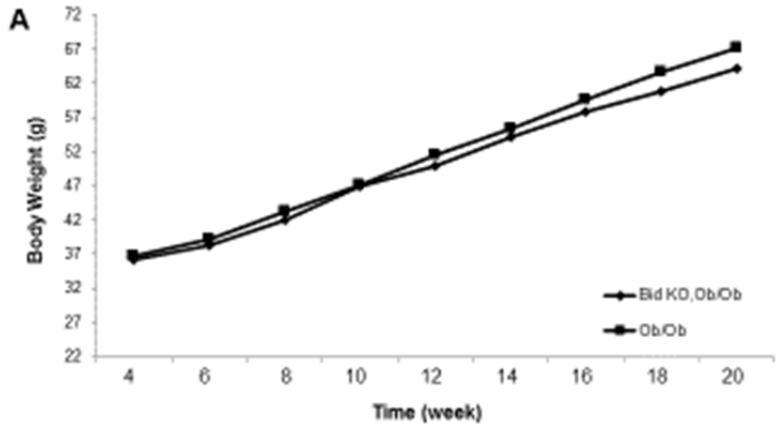

Figure S4: Bid deletion does not protect against obesity induced by leptin deficiency.

(A) Male Bid KO and Ob/Ob/Bid KO mice were fed with regular chow diet for 20wks and body weight were measured every two weeks.

n= 5-8 per group.

Figure 2

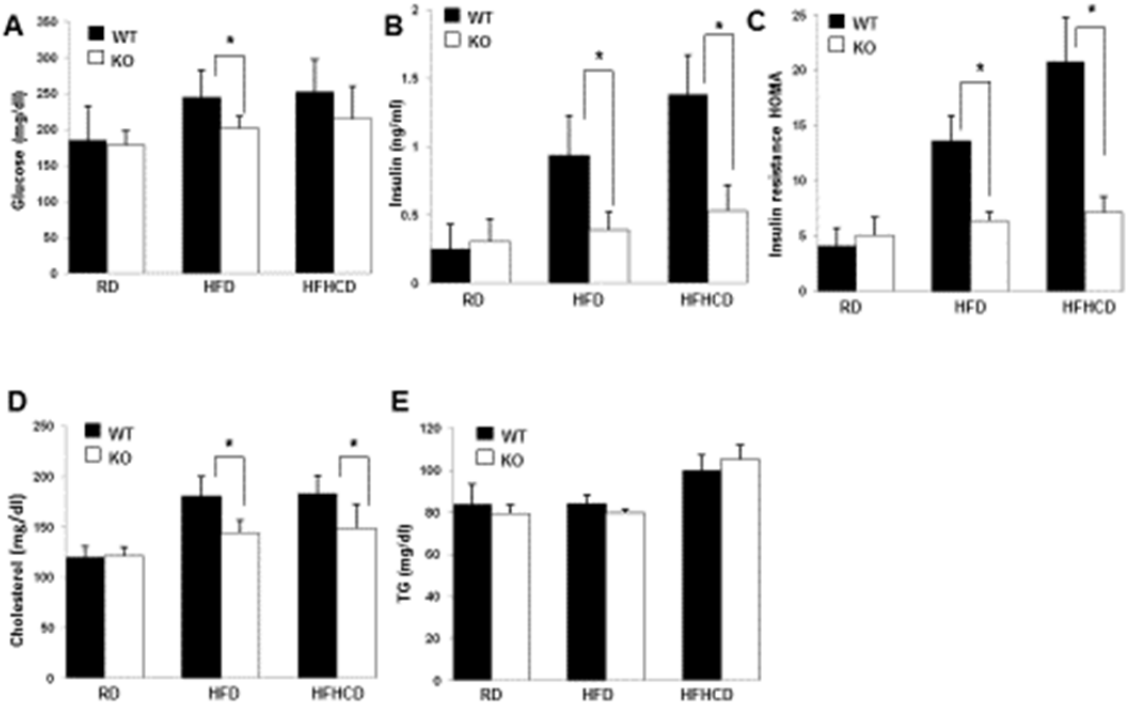

Figure 2: Bid Knockout Mice Are Protected from High Fat Diet Induced Metabolic Syndrome.

(A-E): Male Bid KO and WT mice were fed with high fat diet for 16wks. Different parameters of metabolic syndrome were measured. (A): 12 hour fasting blood glucose level, (B): Serum insulin, (C): Insulin resistance (HOMA): (fasting glucose/18 mg/dl * fasting insulin * 25ng/ml)/22.5. (D): Serum Cholesterol, (E): Serum Triglyceride (TG)

n=5-8 per group, *: $p<0.05$

Figure S5

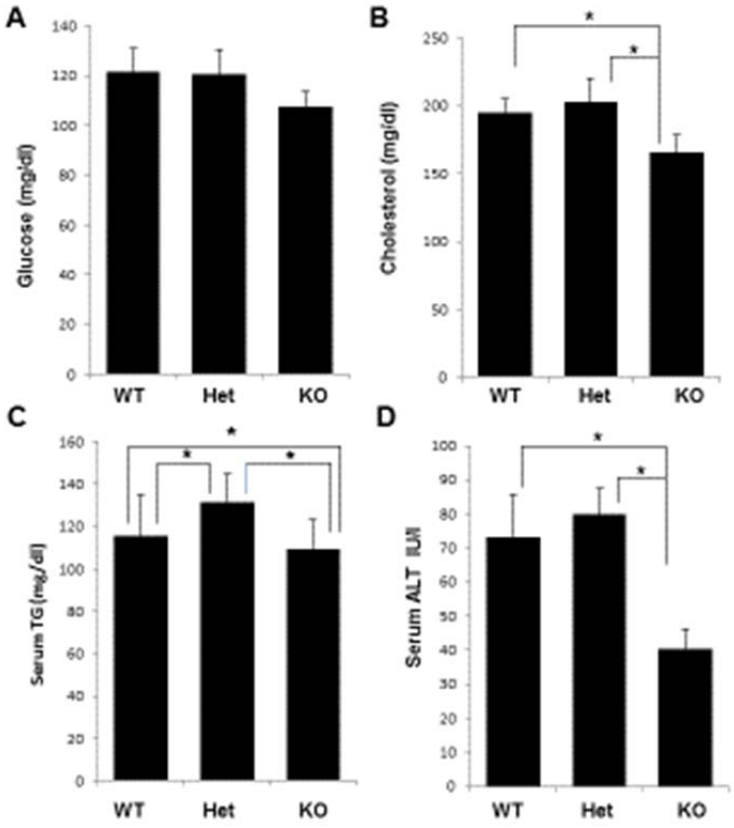

Figure S5: Heterozygous Bid mice were not protected from high fat diet induced metabolic disturbances.

(A-D): Male wild type (WT), Bid heterozygous (Het) and Bid knockout (KO) mice were fed with high fat diet for 24 wks. The following parameters were measured (A) blood glucose level, (B) serum triglyceride (TG), (C) serum cholesterol, (D) serum ALT (alanine transaminase).

n= 5-8 per group, *: $p<0.05$

Figure 3

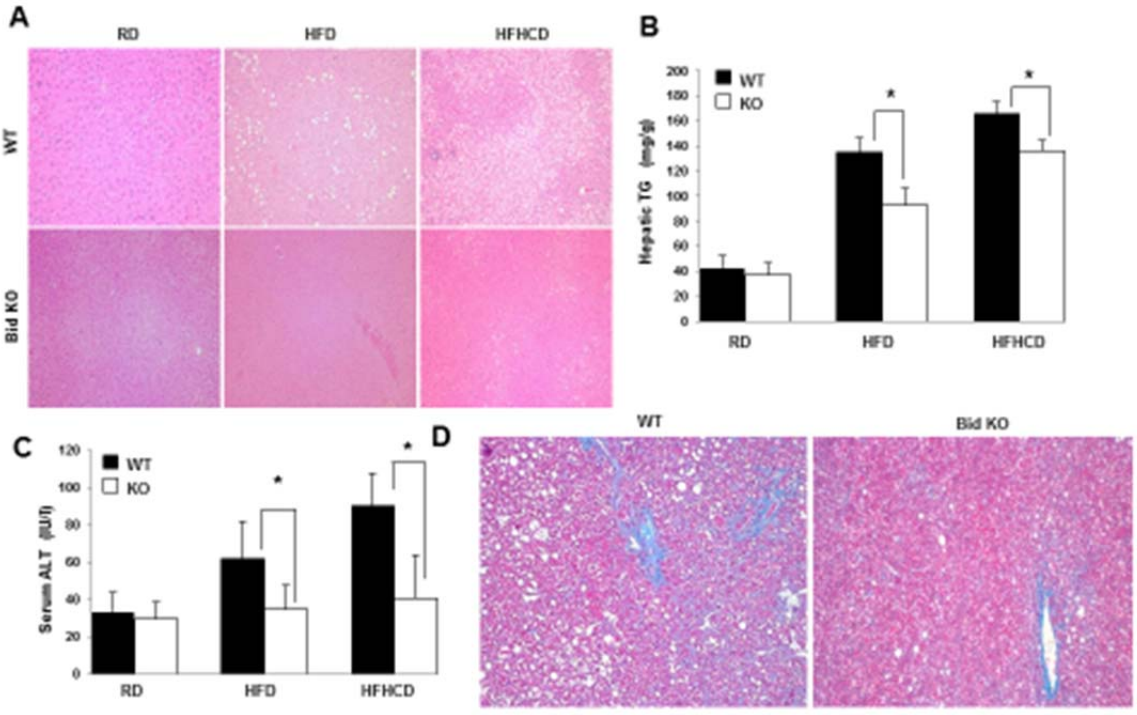

Figure 3. Bid knockout mice are protected from steatosis, non-alcoholic steatohepatitis and hepatic Fibrosis.

(A-C): Male WT and Bid KO mice were fed with regular diet (RD), high fat diet (HFD) and high fat high carbohydrate diet (HFHCD) for 16 weeks. Hepatic steatosis was examined by H-E staining (A) and measurement of Hepatic triglyceride (TG) (B) and serum alanine transaminase (ALT) (C). (D-J): Male WT and Bid KO mice were fed with high fat high carbohydrate diet for 16 weeks, and hepatic fibrosis was examined by Trichrome C staining (D).

n=5-8 per group, *: $p<0.05$

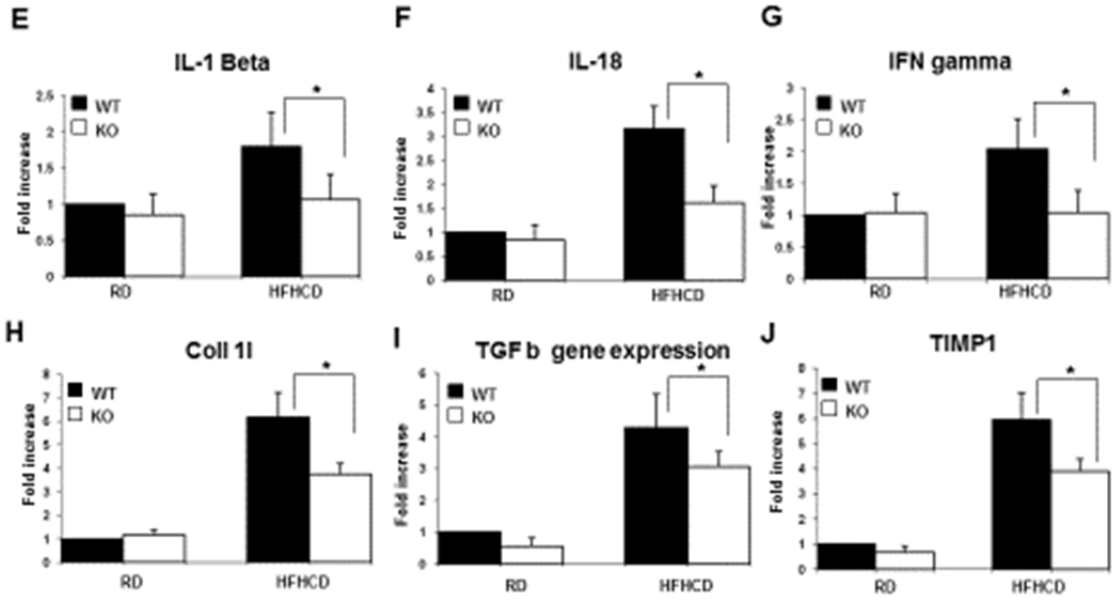

Figure 3. Bid knockout mice are protected from steatosis, non-alcoholic steatohepatitis and hepatic Fibrosis.

Male WT and Bid KO mice were fed with high fat high carbohydrate diet for 16 weeks and RT-PCR analysis of the following genes. (E): IL-1 beta, (F): IL-18, (G): IFN gamma, (H): Collagen 1I, (I): TGF-beta, (J): TIMP metallopeptidase inhibitor 1 (TIMP1).

n=5-8 per group, *: $p<0.05$

Figure 4

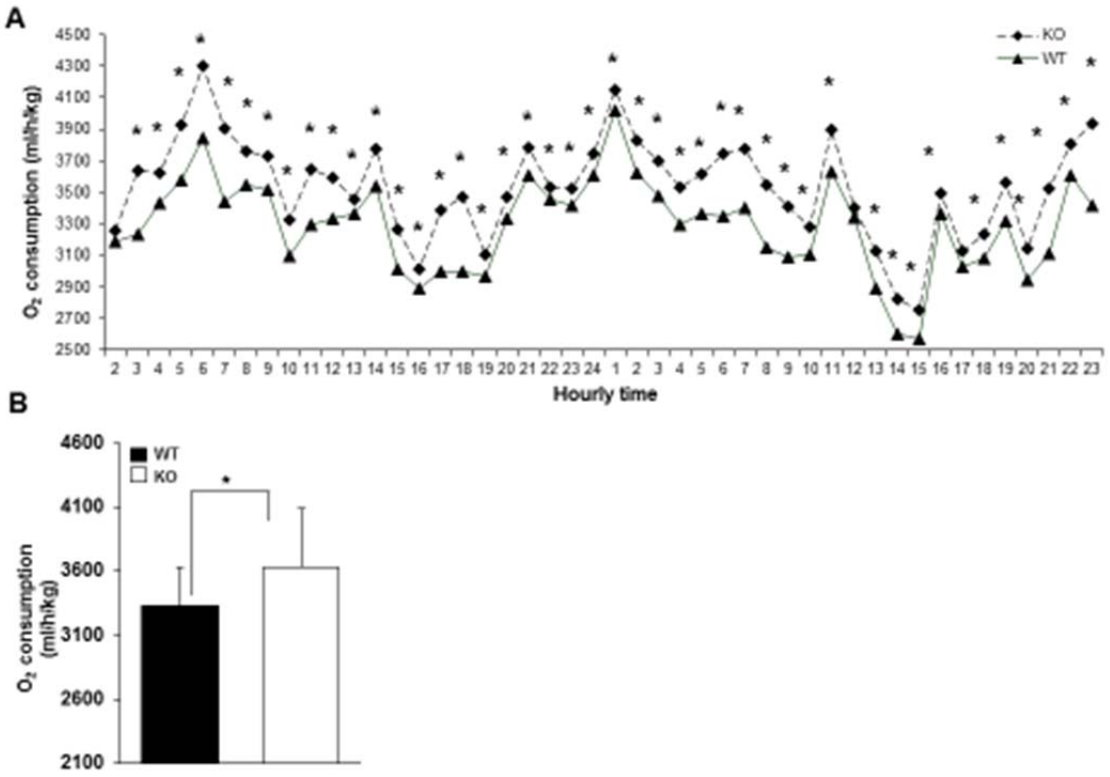

Figure 4: Bid Knockout mice have a higher whole body metabolic rate in vivo.

(A-E): Male WT and Bid KO mice were fed with high fat diet for 10wks and subjected to in vivo calorimetry analysis. (A): Hourly O_2 consumption in 48 hours, data shown hourly. (B): Average O_2 consumption in 48 hours.

n=4 per group, *: $p<0.05$

Figure 4

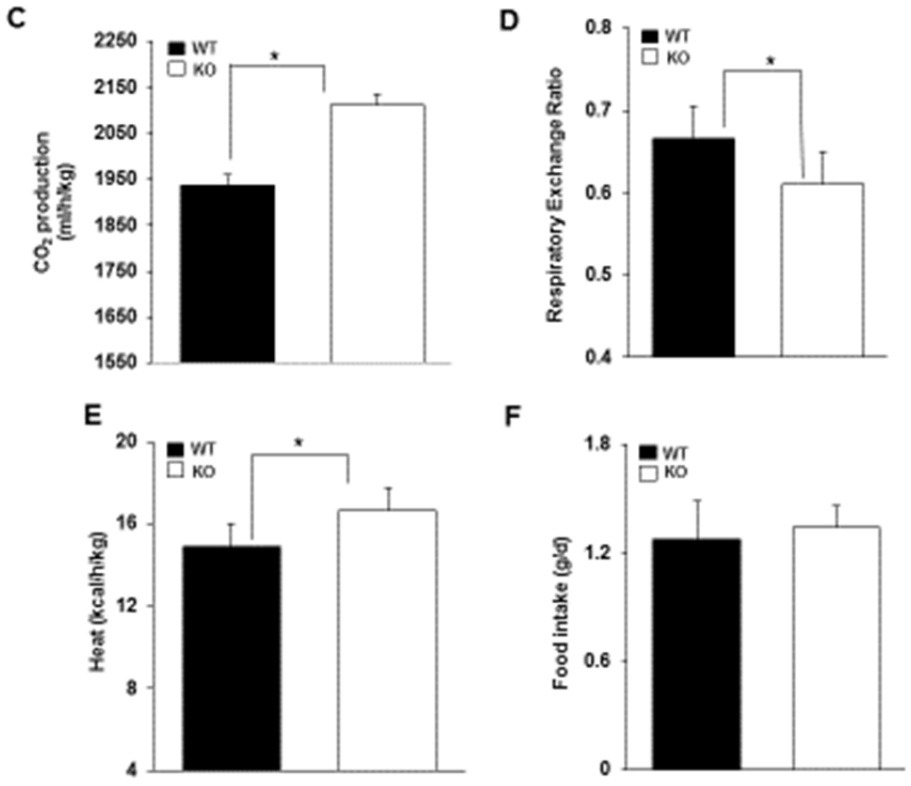

Figure 4: Bid Knockout mice have a higher whole body metabolic rate in vivo.

Male WT and Bid KO mice were fed with high fat diet for 10wks and subjected to in vivo calorimetry analysis. (C): Average CO_2 generation in 48 hours. (D): Average respiratory exchange ratio in 48 hours. (E): Average heat generation in 48 hours. (F): Male WT and Bid KO mice were fed with high fat diet for 16 weeks, food consumption were measured every 4 days. Average daily food intake was determined.

n=4 per group, *: $p<0.05$

Figure 5

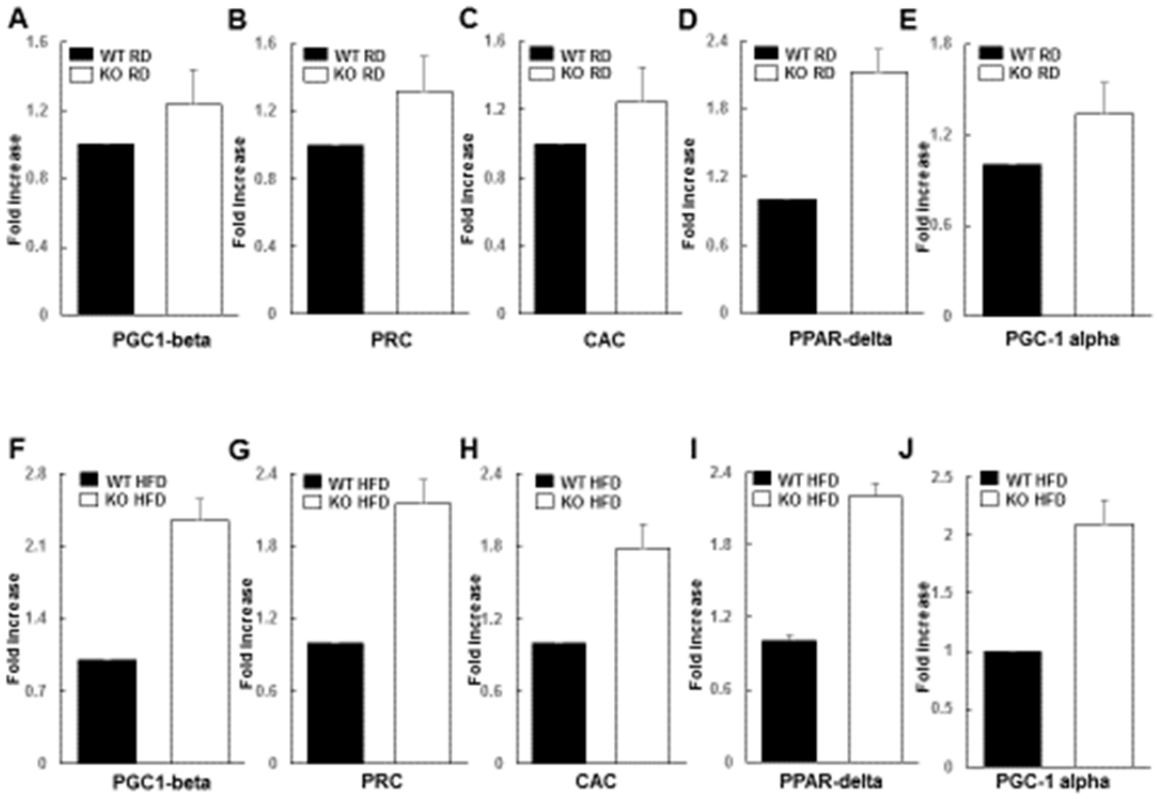

Figure 5: Deficiency of Bid leads to a higher expression of genes that promote energy expenditure.

Male 10wk old WT and Bid KO mice were fed with regular chow diet (RD) or high fat diet (HFD) for 16wks. (A-J): mRNA expression analysis by RT-PCR in liver from regular diet and high fat diet groups (A, F): Peroxisome proliferator-activated receptor gamma coactivator 1-beta (PGC1-beta). (B, G): PGC-1-related coactivator (PRC). (C, H): Carnitine-acylcarnitine translocase (CAC). (D, I): peroxisome proliferator-activated receptor (PPAR-delta). (E, J): Peroxisome proliferator-activated receptor gamma coactivator 1-beta (PGC-1 alpha)

n=4 per group

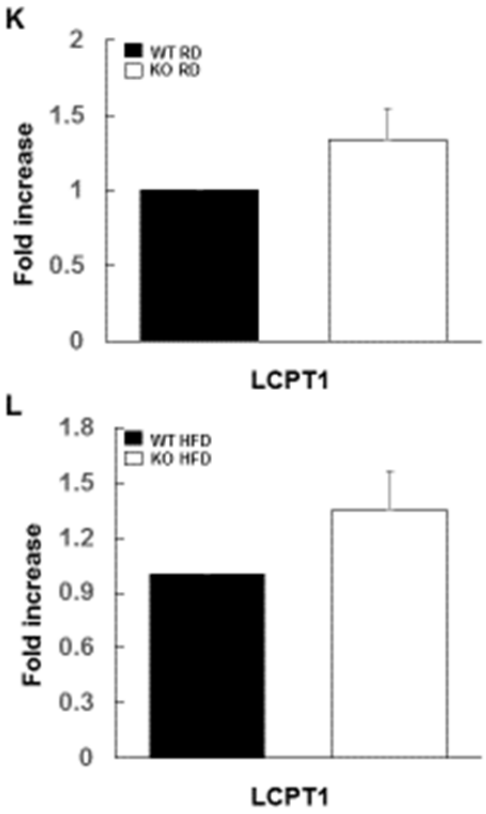

Figure 5: Deficiency of Bid leads to a higher expression of genes that promote energy expenditure.

Male 10wk old WT and Bid KO mice were fed with regular chow diet (RD) or high fat diet (HFD) for 16wks. (K, L): carnitine palmitoyltransferse I (LCPT1).

n=4 per group

Figure 6

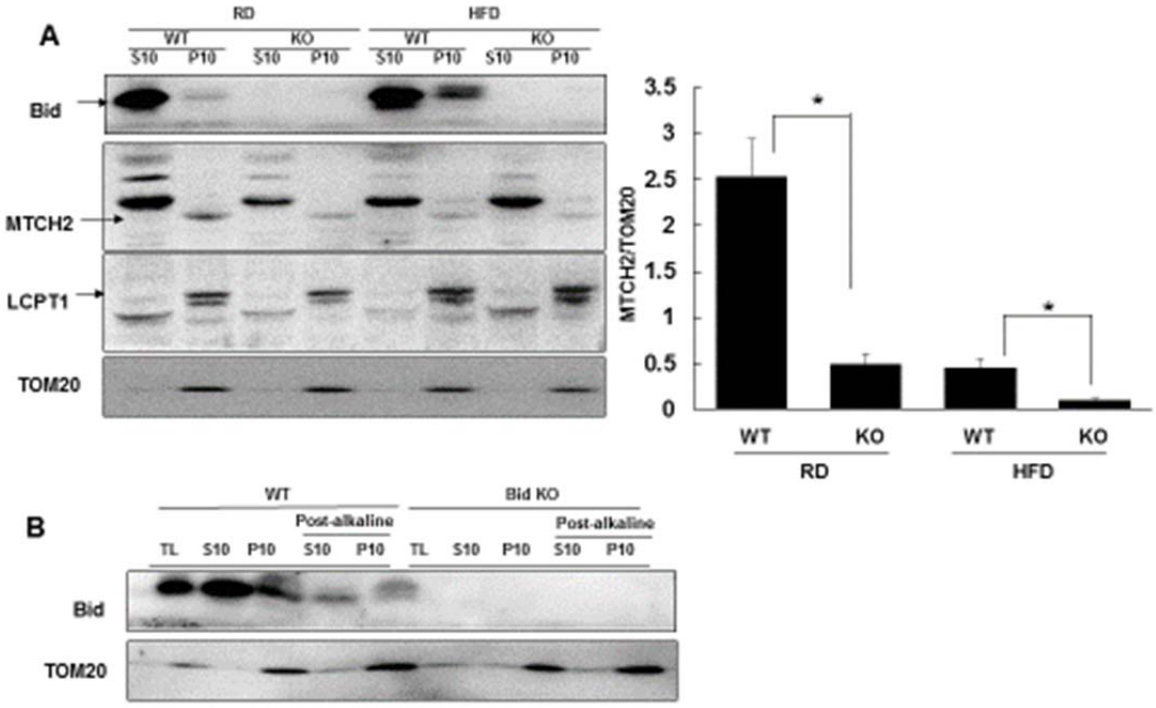

Figure 6: High fat diet induces full length Bid translocation, insertion to mitochondrial membrane and destabilize MTCH2.

(A): WT and Bid KO mice were fed with high fat diet or regular diet for 10 weeks. Homogenates of the liver were separated to the cytosol (S10) and mitochondria enriched (P10) fractions, which were subjected to immunoblotting assays. (B): Densitometry analysis of immunoblotting assays. (C) WT and Bid KO mice were fed with high fat diet for 10wks. The subcellular fractions S10 and P10 were prepared as in (A). A portion of the P10 fraction was further treated with 0.1M Na_2CO_3 PH11.5 for 30min on ice. The pallet (P10) and the Supernatant (S10) were recovered after alkaline treatment. All fractions were then analyzed by immunoblotting assay.

*:$p<0.05$

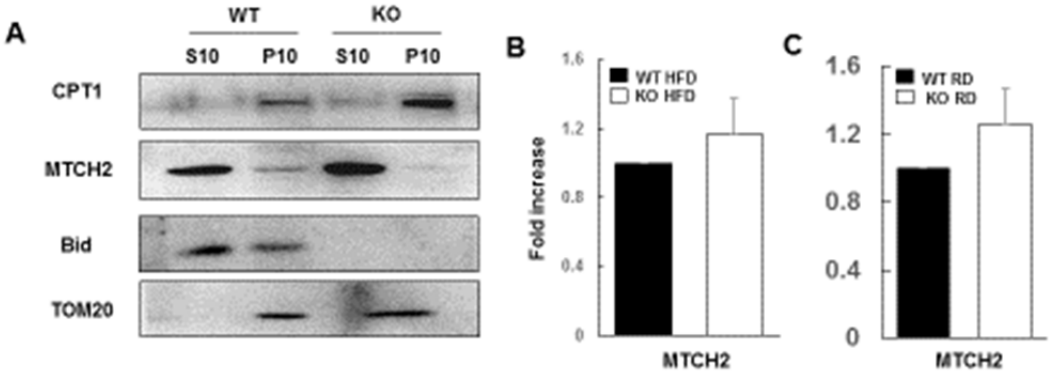

Figure S6: Expression of LCPT-1 and MTCH2 in MEF and in mice.

(A): WT and Bid KO MEFs were subjected to subcellular fractionation into the mitochondria - enriched P10 fraction and the cytosol (S10). Both fractions were analyzed by immunoblotting assay. Note MTCH2 only presents in the mitochondria – enriched P10 fraction. The signals in the S10 cytosol fraction is non-specific. (B, C): MTCH2 gene expression was analysis by RT-PCR in 10 wks of regular and high fat diet mice.

Figure 7

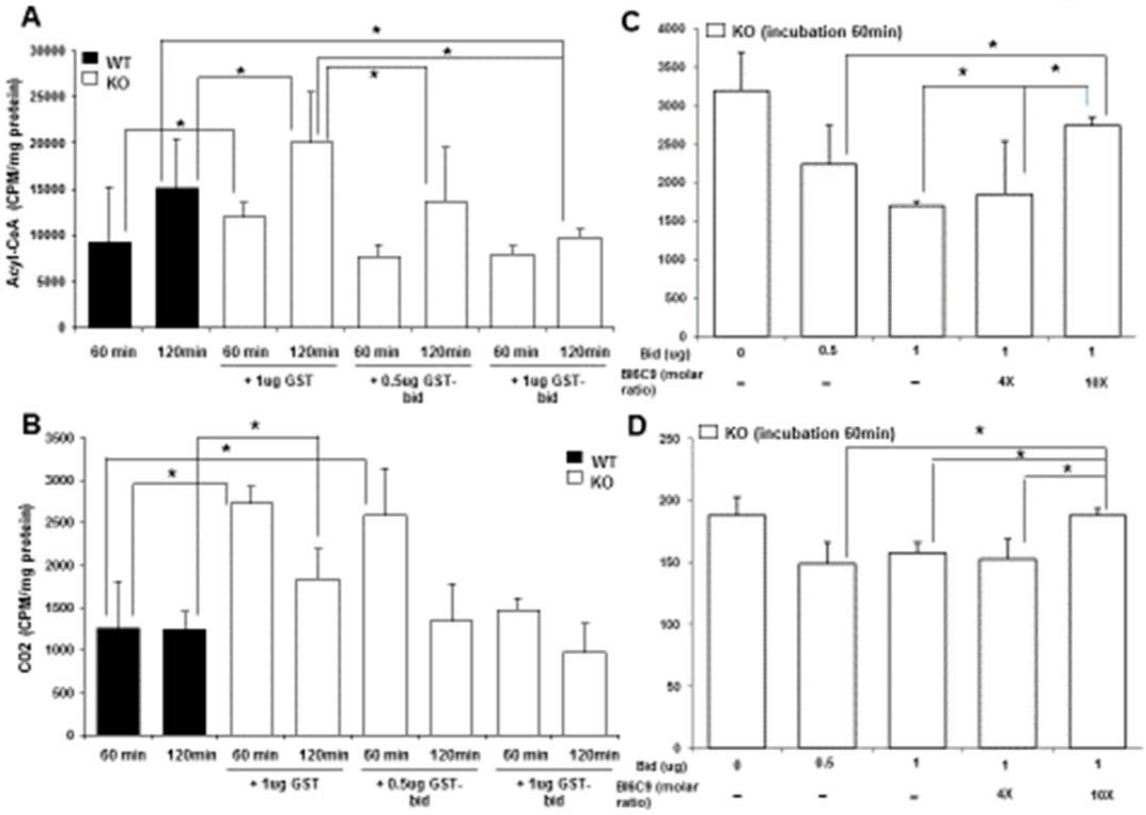

Figure 7: Mitochondrion in Bid KO mice have higher fatty acid oxidation rate and higher free fatty acid in circulation.

10wk old WT and Bid KO mice were fed with high fat diet for 10wks. Liver homogenates were prepared and subjected to ex-vivo fatty acid oxidation assay. (A, C): Measurement of C^{14}-Acyl-CoA after a 60min and a 120min reaction, GST: Glutathione S-transferases. (B, D): Measurement of C^{14}-CO_2 fatty acid oxidation after a 60 min and a 120 min reaction (C-D). A Bid inhibitor, BI6C9 was added at a 4X or 10X molar ratio against Bid. n=4 per group (A-D) *p<0.05. (E): Free fatty acid concentration in the blood was measured.

n=3 per group, *: p<0.05

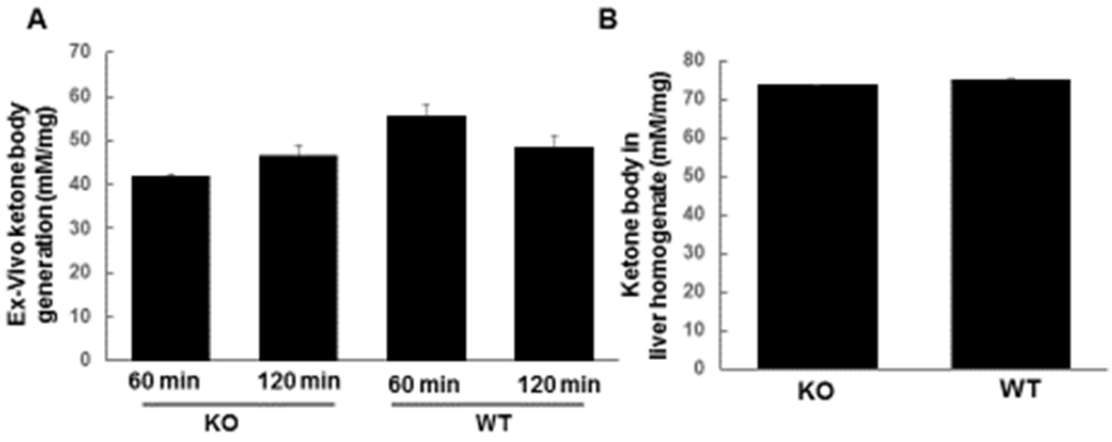

Figure S7: Measurement of ketone body in Bid KO and WT mice Liver.

(A): 10wk old WT and Bid KO mice were fed with high fat diet for 10wks. Liver homogenize were subjected to ex-vivo beta-oxidation assay. Ketone body (beta-Hydroxybutyric acid) was measured after exogenous palmitic acid added to the reaction. (B): Liver homogenates were directly subjected to the measurement of ketone body (beta-Hydroxybutyric acid).

n=3 per group.

Figure S8

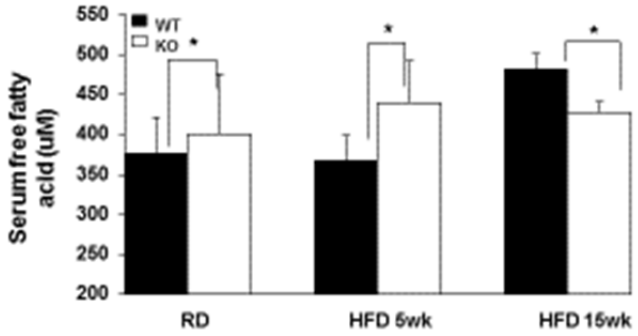

Figure S8: Serum free fatty acid concentration measurement.

10wk old WT and Bid KO mice were fed with regular diet or high fat diet for 5 or 15wks. Serum free fatty acid concentration was then measured. n=3 per group, *: $p<0.05$

Part III References

1. Laplante, M. and D.M. Sabatini, *mTOR signaling at a glance.* J Cell Sci, 2009. 122(Pt 20): p. 3589-94.
2. Albert, V. and M.N. Hall, *mTOR signaling in cellular and organismal energetics.* Curr Opin Cell Biol, 2014. 33C: p. 55-66.
3. Polak, P. and M.N. Hall, *mTOR and the control of whole body metabolism.* Curr Opin Cell Biol, 2009. 21(2): p. 209-18.
4. Hara, K., et al., *Raptor, a binding partner of target of rapamycin (TOR), mediates TOR action.* Cell, 2002. 110(2): p. 177-89.
5. Kim, D.H., et al., *mTOR interacts with raptor to form a nutrient-sensitive complex that signals to the cell growth machinery.* Cell, 2002. 110(2): p. 163-75.
6. Pearce, L.R., et al., *Identification of Protor as a novel Rictor-binding component of mTOR complex-2.* Biochem J, 2007. 405(3): p. 513-22.
7. Loewith, R., et al., *Two TOR complexes, only one of which is rapamycin sensitive, have distinct roles in cell growth control.* Mol Cell, 2002. 10(3): p. 457-68.
8. Sancak, Y., et al., *PRAS40 is an insulin-regulated inhibitor of the mTORC1 protein kinase.* Mol Cell, 2007. 25(6): p. 903-15.
9. Wullschleger, S., et al., *Molecular organization of target of rapamycin complex 2.* J Biol Chem, 2005. 280(35): p. 30697-704.

10. Laplante, M. and D.M. Sabatini, *mTOR signaling in growth control and disease.* Cell, 2012. 149(2): p. 274-93.
11. Inoki, K., et al., *TSC2 is phosphorylated and inhibited by Akt and suppresses mTOR signalling.* Nat Cell Biol, 2002. 4(9): p. 648-57.
12. Inoki, K., et al., *Rheb GTPase is a direct target of TSC2 GAP activity and regulates mTOR signaling.* Genes Dev, 2003. 17(15): p. 1829-34.
13. Ma, L., et al., *Phosphorylation and functional inactivation of TSC2 by Erk implications for tuberous sclerosis and cancer pathogenesis.* Cell, 2005. 121(2): p. 179-93.
14. Manning, B.D., et al., *Identification of the tuberous sclerosis complex-2 tumor suppressor gene product tuberin as a target of the phosphoinositide 3-kinase/akt pathway.* Mol Cell, 2002. 10(1): p. 151-62.
15. Thedieck, K., et al., *PRAS40 and PRR5-like protein are new mTOR interactors that regulate apoptosis.* PLoS One, 2007. 2(11): p. e1217.
16. Vander Haar, E., et al., *Insulin signalling to mTOR mediated by the Akt/PKB substrate PRAS40.* Nat Cell Biol, 2007. 9(3): p. 316-23.
17. Lee, D.F., et al., *IKK beta suppression of TSC1 links inflammation and tumor angiogenesis via the mTOR pathway.* Cell, 2007. 130(3): p. 440-55.
18. Inoki, K., et al., *TSC2 integrates Wnt and energy signals via a coordinated phosphorylation by AMPK and GSK3 to regulate cell growth.* Cell, 2006. 126(5): p. 955-68.
19. Gwinn, D.M., et al., *AMPK phosphorylation of raptor mediates a metabolic checkpoint.* Mol Cell, 2008. 30(2): p. 214-26.

20. Feng, Z., et al., *The coordinate regulation of the p53 and mTOR pathways in cells.* Proc Natl Acad Sci U S A, 2005. 102(23): p. 8204-9.

21. Budanov, A.V. and M. Karin, *p53 target genes sestrin1 and sestrin2 connect genotoxic stress and mTOR signaling.* Cell, 2008. 134(3): p. 451-60.

22. Blommaart, E.F., et al., *Phosphorylation of ribosomal protein S6 is inhibitory for autophagy in isolated rat hepatocytes.* J Biol Chem, 1995. 270(5): p. 2320-6.

23. Sancak, Y., et al., *The Rag GTPases bind raptor and mediate amino acid signaling to mTORC1.* Science, 2008. 320(5882): p. 1496-501.

24. Sancak, Y., et al., *Ragulator-Rag complex targets mTORC1 to the lysosomal surface and is necessary for its activation by amino acids.* Cell, 2010. 141(2): p. 290-303.

25. Jewell, J.L., et al., *Metabolism. Differential regulation of mTORC1 by leucine and glutamine.* Science, 2015. 347(6218): p. 194-8.

26. Zoncu, R., et al., *mTORC1 senses lysosomal amino acids through an inside-out mechanism that requires the vacuolar H(+)-ATPase.* Science, 2011. 334(6056): p. 678-83.

27. Pena-Llopis, S., et al., *Regulation of TFEB and V-ATPases by mTORC1.* EMBO J, 2011. 30(16): p. 3242-58.

28. Fang, Y., et al., *Phosphatidic acid-mediated mitogenic activation of mTOR signaling.* Science, 2001. 294(5548): p. 1942-5.

29. Zoncu, R., A. Efeyan, and D.M. Sabatini, *mTOR: from growth signal integration to cancer, diabetes and ageing.* Nat Rev Mol Cell Biol, 2011. 12(1): p. 21-35.

30. Hara, K., et al., *Regulation of eIF-4E BP1 phosphorylation by mTOR.* J Biol Chem, 1997. 272(42): p. 26457-63.

31. Ma, X.M., et al., *SKAR links pre-mRNA splicing to mTOR/S6K1-mediated enhanced translation efficiency of spliced mRNAs.* Cell, 2008. 133(2): p. 303-13.

32. Thoreen, C.C., et al., *A unifying model for mTORC1-mediated regulation of mRNA translation.* Nature, 2012. 485(7396): p. 109-13.

33. Hay, N. and N. Sonenberg, *Upstream and downstream of mTOR.* Genes Dev, 2004. 18(16): p. 1926-45.

34. Gingras, A.C., B. Raught, and N. Sonenberg, *Regulation of translation initiation by FRAP/mTOR.* Genes Dev, 2001. 15(7): p. 807-26.

35. Ma, X.M. and J. Blenis, *Molecular mechanisms of mTOR-mediated translational control.* Nat Rev Mol Cell Biol, 2009. 10(5): p. 307-18.

36. Martin, K.A. and J. Blenis, *Coordinate regulation of translation by the PI 3-kinase and mTOR pathways.* Adv Cancer Res, 2002. 86: p. 1-39.

37. Jastrzebski, K., et al., *Coordinate regulation of ribosome biogenesis and function by the ribosomal protein S6 kinase, a key mediator of mTOR function.* Growth Factors, 2007. 25(4): p. 209-26.

38. Mayer, C., et al., *mTOR-dependent activation of the transcription factor TIF-IA links rRNA synthesis to nutrient availability.* Genes Dev, 2004. 18(4): p. 423-34.

39. Brugarolas, J.B., et al., *TSC2 regulates VEGF through mTOR-dependent and -independent pathways.* Cancer Cell, 2003. 4(2): p. 147-58.

40. Hudson, C.C., et al., *Regulation of hypoxia-inducible factor 1alpha expression and function by the mammalian target of rapamycin.* Mol Cell Biol, 2002. 22(20): p. 7004-14.

41. Ricoult, S.J. and B.D. Manning, *The multifaceted role of mTORC1 in the control of lipid metabolism.* EMBO Rep, 2013. 14(3): p. 242-51.

42. Horton, J.D., J.L. Goldstein, and M.S. Brown, *SREBPs: activators of the complete program of cholesterol and fatty acid synthesis in the liver.* J Clin Invest, 2002. 109(9): p. 1125-31.

43. Horton, J.D., et al., *Combined analysis of oligonucleotide microarray data from transgenic and knockout mice identifies direct SREBP target genes.* Proc Natl Acad Sci U S A, 2003. 100(21): p. 12027-32.

44. Brown, N.F., et al., *The mammalian target of rapamycin regulates lipid metabolism in primary cultures of rat hepatocytes.* Metabolism, 2007. 56(11): p. 1500-7.

45. Peterson, T.R., et al., *mTOR complex 1 regulates lipin 1 localization to control the SREBP pathway.* Cell, 2011. 146(3): p. 408-20.

46. Laplante, M. and D.M. Sabatini, *An emerging role of mTOR in lipid biosynthesis.* Curr Biol, 2009. 19(22): p. R1046-52.

47. Kim, J.E. and J. Chen, *regulation of peroxisome proliferator-activated receptor-gamma activity by mammalian target of rapamycin and amino acids in adipogenesis.* Diabetes, 2004. 53(11): p. 2748-56.

48. Zhang, H.H., et al., *Insulin stimulates adipogenesis through the Akt-TSC2-mTORC1 pathway.* PLoS One, 2009. 4(7): p. e6189.

49. El-Chaar, D., A. Gagnon, and A. Sorisky, *Inhibition of insulin signaling and adipogenesis by rapamycin: effect on phosphorylation of p70 S6 kinase vs eIF4E-BP1.* Int J Obes Relat Metab Disord, 2004. 28(2): p. 191-8.

50. Lamming, D.W. and D.M. Sabatini, *A Central role for mTOR in lipid homeostasis.* Cell Metab, 2013. 18(4): p. 465-9.

51. Um, S.H., et al., *Absence of S6K1 protects against age- and diet-induced obesity while enhancing insulin sensitivity.* Nature, 2004. 431(7005): p. 200-5.

52. Sengupta, S., et al., *mTORC1 controls fasting-induced ketogenesis and its modulation by ageing.* Nature, 2010. 468(7327): p. 1100-4.

53. Yecies, J.L., et al., *Akt stimulates hepatic SREBP1c and lipogenesis through parallel mTORC1-dependent and independent pathways.* Cell Metab, 2011. 14(1): p. 21-32.

54. Umemura, A., et al., *Liver damage, inflammation, and enhanced tumorigenesis after persistent mTORC1 inhibition.* Cell Metab, 2014. 20(1): p. 133-44.

55. Kenerson, H.L., M.M. Yeh, and R.S. Yeung, *Tuberous sclerosis complex-1 deficiency attenuates diet-induced hepatic lipid accumulation.* PLoS One, 2011. 6(3): p. e18075.

56. Cornu, M., et al., *Hepatic mTORC1 controls locomotor activity, body temperature, and lipid metabolism through FGF21.* Proc Natl Acad Sci U S A, 2014. 111(32): p. 11592-9.

57. Csibi, A., et al., *The mTORC1 pathway stimulates glutamine metabolism and cell proliferation by repressing SIRT4.* Cell, 2013. 153(4): p. 840-54.

58. Newsholme, P., et al., *Glutamine and glutamate--their central role in cell metabolism and function.* Cell Biochem Funct, 2003. 21(1): p. 1-9.

59. Li, Z., et al., *Ghrelin promotes hepatic lipogenesis by activation of mTOR-PPARgamma signaling pathway.* Proc Natl Acad Sci U S A, 2014. 111(36): p. 13163-8.

60. Hagiwara, A., et al., *Hepatic mTORC2 activates glycolysis and lipogenesis through Akt, glucokinase, and SREBP1c.* Cell Metab, 2012. 15(5): p. 725-38.

61. Yuan, M., et al., *Identification of Akt-independent regulation of hepatic lipogenesis by mammalian target of rapamycin (mTOR) complex 2.* J Biol Chem, 2012. 287(35): p. 29579-88.

62. Lamming, D.W., et al., *Rapamycin-induced insulin resistance is mediated by mTORC2 loss and uncoupled from longevity.* Science, 2012. 335(6076): p. 1638-43.

63. Carr, C.S. and P.A. Sharp, *A helix-loop-helix protein related to the immunoglobulin E box-binding proteins.* Mol Cell Biol, 1990. 10(8): p. 4384-8.

64. Hodgkinson, C.A., et al., *Mutations at the mouse microphthalmia locus are associated with defects in a gene encoding a novel basic-helix-loop-helix-zipper protein.* Cell, 1993. 74(2): p. 395-404.

65. Hughes, M.J., et al., *A helix-loop-helix transcription factor-like gene is located at the mi locus.* J Biol Chem, 1993. 268(28): p. 20687-90.

66. Martina, J.A., et al., *Novel roles for the MiTF/TFE family of transcription factors in organelle biogenesis, nutrient sensing, and energy homeostasis.* Cell Mol Life Sci, 2014. 71(13): p. 2483-97.

67. Aksan, I. and C.R. Goding, *Targeting the microphthalmia basic helix-loop-helix-leucine zipper transcription factor to a subset of E-box elements in vitro and in vivo.* Mol Cell Biol, 1998. 18(12): p. 6930-8.

68. Beckmann, H., L.K. Su, and T. Kadesch, *TFE3: a helix-loop-helix protein that activates transcription through the immunoglobulin enhancer muE3 motif.* Genes Dev, 1990. 4(2): p. 167-79.

69. Kuiper, R.P., et al., *Regulation of the MiTF/TFE bHLH-LZ transcription factors through restricted spatial expression and alternative splicing of functional domains.* Nucleic Acids Res, 2004. 32(8): p. 2315-22.

70. Settembre, C., et al., *TFEB links autophagy to lysosomal biogenesis.* Science, 2011. 332(6036): p. 1429-33.

71. Martina, J.A., et al., *MTORC1 functions as a transcriptional regulator of autophagy by preventing nuclear transport of TFEB.* Autophagy, 2012. 8(6): p. 903-14.

72. Settembre, C., et al., *A lysosome-to-nucleus signalling mechanism senses and regulates the lysosome via mTOR and TFEB.* EMBO J, 2012. 31(5): p. 1095-108.

73. Roczniak-Ferguson, A., et al., *The transcription factor TFEB links mTORC1 signaling to transcriptional control of lysosome homeostasis.* Sci Signal, 2012. 5(228): p. ra42.

74. Ferron, M., et al., *A RANKL-PKCbeta-TFEB signaling cascade is necessary for lysosomal biogenesis in osteoclasts.* Genes Dev, 2013. 27(8): p. 955-69.

75. Settembre, C., et al., *TFEB controls cellular lipid metabolism through a starvation-induced autoregulatory loop.* Nat Cell Biol, 2013. 15(6): p. 647-58.

76. Sardiello, M., et al., *A gene network regulating lysosomal biogenesis and function.* Science, 2009. 325(5939): p. 473-7.

77. Bellot, G., et al., *Hypoxia-induced autophagy is mediated through hypoxia-inducible factor induction of BNIP3 and BNIP3L via their BH3 domains.* Mol Cell Biol, 2009. 29(10): p. 2570-81.

78. Crighton, D., et al., *DRAM, a p53-induced modulator of autophagy, is critical for apoptosis.* Cell, 2006. 126(1): p. 121-34.

79. Palmieri, M., et al., *Characterization of the CLEAR network reveals an integrated control of cellular clearance pathways.* Hum Mol Genet, 2011. 20(19): p. 3852-66.

80. Deter, R.L. and C. De Duve, *Influence of glucagon, an inducer of cellular autophagy, on some physical properties of rat liver lysosomes.* J Cell Biol, 1967. 33(2): p. 437-49.

81. Shintani, T. and D.J. Klionsky, *Autophagy in health and disease: a double-edged sword.* Science, 2004. 306(5698): p. 990-5.

82. Meijer, A.J. and P. Codogno, *Regulation and role of autophagy in mammalian cells.* Int J Biochem Cell Biol, 2004. 36(12): p. 2445-62.

83. Mijaljica, D., M. Prescott, and R.J. Devenish, *Microautophagy in mammalian cells: revisiting a 40-year-old conundrum.* Autophagy, 2011. 7(7): p. 673-82.

84. Farre, J.C., et al., *Turnover of organelles by autophagy in yeast.* Curr Opin Cell Biol, 2009. 21(4): p. 522-30.

85. Li, W.W., J. Li, and J.K. Bao, *Microautophagy: lesser-known self-eating.* Cell Mol Life Sci, 2012. 69(7): p. 1125-36.

86. Suzuki, K., *Selective autophagy in budding yeast.* Cell Death Differ, 2013. 20(1): p. 43-8.

87. Mijaljica, D., M. Prescott, and R.J. Devenish, *The intricacy of nuclear membrane dynamics during nucleophagy.* Nucleus, 2010. 1(3): p. 213-23.

88. Tolkovsky, A.M., *Mitophagy.* Biochim Biophys Acta, 2009. 1793(9): p. 1508-15.

89. Kaushik, S. and A.M. Cuervo, *Chaperone-mediated autophagy: a unique way to enter the lysosome world.* Trends Cell Biol, 2012. 22(8): p. 407-17.

90. De Duve, C. and R. Wattiaux, *Functions of lysosomes.* Annu Rev Physiol, 1966. 28: p. 435-92.

91. Hamasaki, M., S.T. Shibutani, and T. Yoshimori, *Up-to-date membrane biogenesis in the autophagosome formation.* Curr Opin Cell Biol, 2013. 25(4): p. 455-60.

92. Dunn, W.A., Jr., *Studies on the mechanisms of autophagy: formation of the autophagic vacuole.* J Cell Biol, 1990. 110(6): p. 1923-33.

93. Matsunaga, K., et al., *Autophagy requires endoplasmic reticulum targeting of the PI3-kinase complex via Atg14L.* J Cell Biol, 2010. 190(4): p. 511-21.

94. Ge, L. and R. Schekman, *The ER-Golgi intermediate compartment feeds the phagophore membrane.* Autophagy, 2014. 10(1): p. 170-2.

95. Hailey, D.W., et al., *Mitochondria supply membranes for autophagosome biogenesis during starvation.* Cell, 2010. 141(4): p. 656-67.

96. Moreau, K. and D.C. Rubinsztein, *The plasma membrane as a control center for autophagy.* Autophagy, 2012. 8(5): p. 861-3.

97. Karanasios, E., et al., *Dynamic association of the ULK1 complex with omegasomes during autophagy induction.* J Cell Sci, 2013. 126(Pt 22): p. 5224-38.

98. Hayashi-Nishino, M., et al., *Electron tomography reveals the endoplasmic reticulum as a membrane source for autophagosome formation.* Autophagy, 2010. 6(2): p. 301-3.

99. Eskelinen, E.L., *Fine structure of the autophagosome.* Methods Mol Biol, 2008. 445: p. 11-28.

100. Itakura, E. and N. Mizushima, *Characterization of autophagosome formation site by a hierarchical analysis of mammalian Atg proteins.* Autophagy, 2010. 6(6): p. 764-76.

101. Tan, D., et al., *The EM structure of the TRAPPIII complex leads to the identification of a requirement for COPII vesicles on the macroautophagy pathway.* Proc Natl Acad Sci U S A, 2013. 110(48): p. 19432-7.

102. Mizushima, N., T. Yoshimori, and Y. Ohsumi, *The role of Atg proteins in autophagosome formation.* Annu Rev Cell Dev Biol, 2011. 27: p. 107-32.

103. Hosokawa, N., et al., *Nutrient-dependent mTORC1 association with the ULK1-Atg13-FIP200 complex required for autophagy.* Mol Biol Cell, 2009. 20(7): p. 1981-91.

104. Lamb, C.A., T. Yoshimori, and S.A. Tooze, *The autophagosome: origins unknown, biogenesis complex.* Nat Rev Mol Cell Biol, 2013. 14(12): p. 759-74.

105. Kim, J., et al., *AMPK and mTOR regulate autophagy through direct phosphorylation of Ulk1.* Nat Cell Biol, 2011. 13(2): p. 132-41.

106. Russell, R.C., et al., *ULK1 induces autophagy by phosphorylating Beclin-1 and activating VPS34 lipid kinase.* Nat Cell Biol, 2013. 15(7): p. 741-50.

107. Dove, S.K., et al., *Svp1p defines a family of phosphatidylinositol 3,5-bisphosphate effectors.* EMBO J, 2004. 23(9): p. 1922-33.

108. Stromhaug, P.E., et al., *Atg21 is a phosphoinositide binding protein required for efficient lipidation and localization of Atg8 during uptake of aminopeptidase I by selective autophagy.* Mol Biol Cell, 2004. 15(8): p. 3553-66.

109. Efe, J.A., R.J. Botelho, and S.D. Emr, *Atg18 regulates organelle morphology and Fab1 kinase activity independent of its membrane recruitment by phosphatidylinositol 3,5-bisphosphate.* Mol Biol Cell, 2007. 18(11): p. 4232-44.

110. Obara, K., et al., *The Atg18-Atg2 complex is recruited to autophagic membranes via phosphatidylinositol 3-phosphate and exerts an essential function.* J Biol Chem, 2008. 283(35): p. 23972-80.

111. Polson, H.E., et al., *Mammalian Atg18 (WIPI2) localizes to omegasome-anchored phagophores and positively regulates LC3 lipidation.* Autophagy, 2010. 6(4): p. 506-22.

112. Mauthe, M., et al., *Resveratrol-mediated autophagy requires WIPI-1-regulated LC3 lipidation in the absence of induced phagophore formation.* Autophagy, 2011. 7(12): p. 1448-61.

113. Ohsumi, Y. and N. Mizushima, *Two ubiquitin-like conjugation systems essential for autophagy.* Semin Cell Dev Biol, 2004. 15(2): p. 231-6.

114. Hanada, T., et al., *The Atg12-Atg5 conjugate has a novel E3-like activity for protein lipidation in autophagy.* J Biol Chem, 2007. 282(52): p. 37298-302.

115. Nair, U., et al., *Roles of the lipid-binding motifs of Atg18 and Atg21 in the cytoplasm to vacuole targeting pathway and autophagy.* J Biol Chem, 2010. 285(15): p. 11476-88.

116. Ichimura, Y., et al., *In vivo and in vitro reconstitution of Atg8 conjugation essential for autophagy.* J Biol Chem, 2004. 279(39): p. 40584-92.

117. Fujita, N., et al., *The Atg16L complex specifies the site of LC3 lipidation for membrane biogenesis in autophagy.* Mol Biol Cell, 2008. 19(5): p. 2092-100.

118. Mao, Y., et al., *Hepatitis B virus X protein reduces starvation-induced cell death through activation of autophagy and inhibition of mitochondrial apoptotic pathway.* Biochem Biophys Res Commun, 2011. 415(1): p. 68-74.

119. Reggiori, F., et al., *Atg9 cycles between mitochondria and the pre-autophagosomal structure in yeasts.* Autophagy, 2005. 1(2): p. 101-9.

120. Mari, M., et al., *An Atg9-containing compartment that functions in the early steps of autophagosome biogenesis.* J Cell Biol, 2010. 190(6): p. 1005-22.

121. Young, A.R., et al., *Starvation and ULK1-dependent cycling of mammalian Atg9 between the TGN and endosomes.* J Cell Sci, 2006. 119(Pt 18): p. 3888-900.

122. Webber, J.L. and S.A. Tooze, *Coordinated regulation of autophagy by p38alpha MAPK through mAtg9 and p38IP.* EMBO J, 2010. 29(1): p. 27-40.

123. Itakura, E., C. Kishi-Itakura, and N. Mizushima, *The hairpin-type tail-anchored SNARE syntaxin 17 targets to autophagosomes for fusion with endosomes/lysosomes.* Cell, 2012. 151(6): p. 1256-69.

124. He, C. and D.J. Klionsky, *Regulation mechanisms and signaling pathways of autophagy.* Annu Rev Genet, 2009. 43: p. 67-93.

125. Alers, S., et al., *Role of AMPK-mTOR-Ulk1/2 in the regulation of autophagy: cross talk, shortcuts, and feedbacks.* Mol Cell Biol, 2012. 32(1): p. 2-11.

126. Kim, J., et al., *Differential regulation of distinct Vps34 complexes by AMPK in nutrient stress and autophagy.* Cell, 2013. 152(1-2): p. 290-303.

127. Kimata, Y. and K. Kohno, *Endoplasmic reticulum stress-sensing mechanisms in yeast and mammalian cells.* Curr Opin Cell Biol, 2011. 23(2): p. 135-42.

128. Ogata, M., et al., *Autophagy is activated for cell survival after endoplasmic reticulum stress.* Mol Cell Biol, 2006. 26(24): p. 9220-31.

129. Ding, W.X., et al., *Linking of autophagy to ubiquitin-proteasome system is important for the regulation of endoplasmic reticulum stress and cell viability.* Am J Pathol, 2007. 171(2): p. 513-24.

130. Ding, W.X. and X.M. Yin, *Sorting, recognition and activation of the misfolded protein degradation pathways through macroautophagy and the proteasome.* Autophagy, 2008. 4(2): p. 141-50.

131. Hoyer-Hansen, M. and M. Jaattela, *Connecting endoplasmic reticulum stress to autophagy by unfolded protein response and calcium.* Cell Death Differ, 2007. 14(9): p. 1576-82.

132. Schworer, C.M., K.A. Shiffer, and G.E. Mortimore, *Quantitative relationship between autophagy and proteolysis during graded amino acid deprivation in perfused rat liver.* J Biol Chem, 1981. 256(14): p. 7652-8.

133. Mortimore, G.E., N.J. Hutson, and C.A. Surmacz, *Quantitative correlation between proteolysis and macro- and microautophagy in mouse hepatocytes during starvation and refeeding.* Proc Natl Acad Sci U S A, 1983. 80(8): p. 2179-83.

134. Takamura, A., et al., *Autophagy-deficient mice develop multiple liver tumors.* Genes Dev, 2011. 25(8): p. 795-800.

135. Rusten, T.E. and H. Stenmark, *p62, an autophagy hero or culprit?* Nat Cell Biol, 2010. 12(3): p. 207-9.

136. Xie, Z. and D.J. Klionsky, *Autophagosome formation: core machinery and adaptations.* Nat Cell Biol, 2007. 9(10): p. 1102-9.

137. Komatsu, M., et al., *Homeostatic levels of p62 control cytoplasmic inclusion body formation in autophagy-deficient mice.* Cell, 2007. 131(6): p. 1149-63.

138. Komatsu, M., et al., *The selective autophagy substrate p62 activates the stress responsive transcription factor Nrf2 through inactivation of Keap1.* Nat Cell Biol, 2010. 12(3): p. 213-23.

139. Green, D.R. and B. Levine, *To Be or Not to Be? How Selective Autophagy and Cell Death Govern Cell Fate.* Cell, 2014. 157(1): p. 65-75.

140. Ding, W.X., et al., *Autophagy reduces acute ethanol-induced hepatotoxicity and steatosis in mice.* Gastroenterology, 2010. 139(5): p. 1740-52.

141. Kim, S.J., et al., *Hepatitis B virus disrupts mitochondrial dynamics: induces fission and mitophagy to attenuate apoptosis.* PLoS Pathog, 2013. 9(12): p. e1003722.

142. Pi, H., et al., *Dynamin 1-like-dependent mitochondrial fission initiates overactive mitophagy in the hepatotoxicity of cadmium.* Autophagy, 2013. 9(11): p. 1780-800.

143. Masaki, R., A. Yamamoto, and Y. Tashiro, *Cytochrome P-450 and NADPH-cytochrome P-450 reductase are degraded in the autolysosomes in rat liver.* J Cell Biol, 1987. 104(5): p. 1207-15.

144. Bernales, S., K.L. McDonald, and P. Walter, *Autophagy counterbalances endoplasmic reticulum expansion during the unfolded protein response.* PLoS Biol, 2006. 4(12): p. e423.

145. Thomes, P.G., et al., *Proteasome activity and autophagosome content in liver are reciprocally regulated by ethanol treatment.* Biochem Biophys Res Commun, 2012. 417(1): p. 262-7.

146. Lin, C.W., et al., *Pharmacological promotion of autophagy alleviates steatosis and injury in alcoholic and non-alcoholic fatty liver conditions in mice.* J Hepatol, 2013. 58(5): p. 993-9.

147. Dolganiuc, A., et al., *Autophagy in alcohol-induced liver diseases.* Alcohol Clin Exp Res, 2012. 36(8): p. 1301-8.

148. Donohue, T.M., Jr., R.K. Zetterman, and D.J. Tuma, *Effect of chronic ethanol administration on protein catabolism in rat liver.* Alcohol Clin Exp Res, 1989. 13(1): p. 49-57.

149. Harada, M., et al., *Autophagy activation by rapamycin eliminates mouse Mallory-Denk bodies and blocks their proteasome inhibitor-mediated formation.* Hepatology, 2008. 47(6): p. 2026-35.

150. Tiniakos, D.G., M.B. Vos, and E.M. Brunt, *Nonalcoholic fatty liver disease: pathology and pathogenesis.* Annu Rev Pathol, 2010. 5: p. 145-71.

151. Clark, J.M., F.L. Brancati, and A.M. Diehl, *The prevalence and etiology of elevated aminotransferase levels in the United States.* Am J Gastroenterol, 2003. 98(5): p. 960-7.

152. Ruhl, C.E. and J.E. Everhart, *The association of low serum alanine aminotransferase activity with mortality in the US population.* Am J Epidemiol, 2013. 178(12): p. 1702-11.

153. Singh, R., et al., *Autophagy regulates lipid metabolism.* Nature, 2009. 458(7242): p. 1131-5.

154. Yang, L., et al., *Defective hepatic autophagy in obesity promotes ER stress and causes insulin resistance.* Cell Metab, 2010. 11(6): p. 467-78.

155. Sanyal, A.J., et al., *Nonalcoholic steatohepatitis: association of insulin resistance and mitochondrial abnormalities.* Gastroenterology, 2001. 120(5): p. 1183-92.

156. Liu, H.Y., et al., *Hepatic autophagy is suppressed in the presence of insulin resistance and hyperinsulinemia: inhibition of FoxO1-dependent expression of key autophagy genes by insulin.* J Biol Chem, 2009. 284(45): p. 31484-92.

157. He, Z., et al., *p73 regulates autophagy and hepatocellular lipid metabolism through a transcriptional activation of the ATG5 gene.* Cell Death Differ, 2013. 20(10): p. 1415-24.

158. Sinha, R.A., et al., *Thyroid hormone stimulates hepatic lipid catabolism via activation of autophagy.* J Clin Invest, 2012. 122(7): p. 2428-38.

159. Inami, Y., et al., *Hepatic steatosis inhibits autophagic proteolysis via impairment of autophagosomal acidification and cathepsin expression.* Biochem Biophys Res Commun, 2011. 412(4): p. 618-25.

160. Fukuo, Y., et al., *Abnormality of autophagic function and cathepsin expression in the liver from patients with non-alcoholic fatty liver disease.* Hepatol Res, 2013.

161. Koga, H., S. Kaushik, and A.M. Cuervo, *Altered lipid content inhibits autophagic vesicular fusion.* FASEB J, 2010. 24(8): p. 3052-65.

162. Xiong, X., et al., *The autophagy-related gene 14 (Atg14) is regulated by forkhead box O transcription factors and circadian rhythms and plays a critical role in hepatic autophagy and lipid metabolism.* J Biol Chem, 2012. 287(46): p. 39107-14.

163. Kashima, J., et al., *Immunohistochemical study of the autophagy marker microtubule-associated protein 1 light chain 3 in normal and steatotic human livers.* Hepatol Res, 2013.

164. Serviddio, G., et al., *Targeting mitochondria: a new promising approach for the treatment of liver diseases.* Curr Med Chem, 2010. 17(22): p. 2325-37.

165. Singh, R. and A.M. Cuervo, *Lipophagy: connecting autophagy and lipid metabolism.* Int J Cell Biol, 2012. 2012: p. 282041.

166. Stoka, V., et al., *Lysosomal protease pathways to apoptosis. Cleavage of bid, not pro-caspases, is the most likely route.* J Biol Chem, 2001. 276(5): p. 3149-57.

167. Kleiner, D.E., et al., *Design and validation of a histological scoring system for nonalcoholic fatty liver disease.* Hepatology, 2005. 41(6): p. 1313-21.

168. Martina, J.A. and R. Puertollano, *Rag GTPases mediate amino acid-dependent recruitment of TFEB and MITF to lysosomes.* J Cell Biol, 2013. 200(4): p. 475-91.

169. Yu, L., et al., *Termination of autophagy and reformation of lysosomes regulated by mTOR.* Nature, 2010. 465(7300): p. 942-6.

170. Hoffmann, A., et al., *The IkappaB-NF-kappaB signaling module: temporal control and selective gene activation.* Science, 2002. 298(5596): p. 1241-5.

171. Pallayova, M. and S. Taheri, *Non-alcoholic fatty liver disease in obese adults: clinical aspects and current management strategies.* Clin Obes, 2014. 4(5): p. 243-53.

172. Billen, L.P., A. Shamas-Din, and D.W. Andrews, *Bid: a Bax-like BH3 protein.* Oncogene, 2008. 27 Suppl 1: p. S93-104.

173. Yin, X.M., *Bid, a BH3-only multi-functional molecule, is at the cross road of life and death.* Gene, 2006. 369: p. 7-19.

174. Wang, K., et al., *BID: a novel BH3 domain-only death agonist.* Genes Dev, 1996. 10(22): p. 2859-69.

175. Nunez, G., et al., *Deregulated Bcl-2 gene expression selectively prolongs survival of growth factor-deprived hemopoietic cell lines.* J Immunol, 1990. 144(9): p. 3602-10.

176. Li, H., et al., *Cleavage of BID by caspase 8 mediates the mitochondrial damage in the Fas pathway of apoptosis.* Cell, 1998. 94(4): p. 491-501.

177. Luo, X., et al., *Bid, a Bcl2 interacting protein, mediates cytochrome c release from mitochondria in response to activation of cell surface death receptors.* Cell, 1998. 94(4): p. 481-90.

178. Gross, A., et al., *Caspase cleaved BID targets mitochondria and is required for cytochrome c release, while BCL-XL prevents this release but not tumor necrosis factor-R1/Fas death.* J Biol Chem, 1999. 274(2): p. 1156-63.

179. Footz, T.K., et al., *The gene for death agonist BID maps to the region of human 22q11.2 duplicated in cat eye syndrome chromosomes and to mouse chromosome 6.* Genomics, 1998. 51(3): p. 472-5.

180. Wang, K., et al., *BID, a proapoptotic BCL-2 family member, is localized to mouse chromosome 6 and human chromosome 22q11.* Genomics, 1998. 53(2): p. 235-8.

181. Kvansakul, M., et al., *Vaccinia virus anti-apoptotic F1L is a novel Bcl-2-like domain-swapped dimer that binds a highly selective subset of BH3-containing death ligands.* Cell Death Differ, 2008. 15(10): p. 1564-71.

182. Sax, J.K., et al., *BID regulation by p53 contributes to chemosensitivity.* Nat Cell Biol, 2002. 4(11): p. 842-9.

183. Parrado, A., et al., *The promyelocytic leukemia zinc finger protein down-regulates apoptosis and expression of the proapoptotic BID protein in lymphocytes.* Proc Natl Acad Sci U S A, 2004. 101(7): p. 1898-903.

184. McDonnell, J.M., et al., *Solution structure of the proapoptotic molecule BID: a structural basis for apoptotic agonists and antagonists.* Cell, 1999. 96(5): p. 625-34.

185. Zha, J., et al., *Posttranslational N-myristoylation of BID as a molecular switch for targeting mitochondria and apoptosis.* Science, 2000. 290(5497): p. 1761-5.

186. Lovell, J.F., et al., *Membrane binding by tBid initiates an ordered series of events culminating in membrane permeabilization by Bax.* Cell, 2008. 135(6): p. 1074-84.

187. Slee, E.A., S.A. Keogh, and S.J. Martin, *Cleavage of BID during cytotoxic drug and UV radiation-induced apoptosis occurs downstream of the point of Bcl-2 action and is catalysed by caspase-3: a potential feedback loop for amplification of apoptosis-associated mitochondrial cytochrome c release.* Cell Death Differ, 2000. 7(6): p. 556-65.

188. Degli Esposti, M., et al., *Post-translational modification of Bid has differential effects on its susceptibility to cleavage by caspase 8 or caspase 3.* J Biol Chem, 2003. 278(18): p. 15749-57.

189. Guicciardi, M.E., et al., *Cathepsin B contributes to TNF-alpha-mediated hepatocyte apoptosis by promoting mitochondrial release of cytochrome c.* J Clin Invest, 2000. 106(9): p. 1127-37.

190. Cirman, T., et al., *Selective disruption of lysosomes in HeLa cells triggers apoptosis mediated by cleavage of Bid by multiple papain-like lysosomal cathepsins.* J Biol Chem, 2004. 279(5): p. 3578-87.

191. Desagher, S., et al., *Phosphorylation of bid by casein kinases I and II regulates its cleavage by caspase 8.* Mol Cell, 2001. 8(3): p. 601-11.

192. Zaltsman, Y., et al., *MTCH2/MIMP is a major facilitator of tBID recruitment to mitochondria.* Nat Cell Biol, 2010. 12(6): p. 553-62.

193. Lutter, M., et al., *Cardiolipin provides specificity for targeting of tBid to mitochondria.* Nat Cell Biol, 2000. 2(10): p. 754-61.

194. Kim, T.H., et al., *Bid-cardiolipin interaction at mitochondrial contact site contributes to mitochondrial cristae reorganization and cytochrome C release.* Mol Biol Cell, 2004. 15(7): p. 3061-72.

195. Liu, J., et al., *The cardiolipin-binding domain of Bid affects mitochondrial respiration and enhances cytochrome c release.* Apoptosis, 2004. 9(5): p. 533-41.

196. Lutter, M., G.A. Perkins, and X. Wang, *The pro-apoptotic Bcl-2 family member tBid localizes to mitochondrial contact sites.* BMC Cell Biol, 2001. 2: p. 22.

197. Scaffidi, C., et al., *Two CD95 (APO-1/Fas) signaling pathways.* Embo j, 1998. 17(6): p. 1675-87.

198. Ozoren, N. and W.S. El-Deiry, *Defining characteristics of Types I and II apoptotic cells in response to TRAIL.* Neoplasia, 2002. 4(6): p. 551-7.

199. Yin, X.M., et al., *Bid-deficient mice are resistant to Fas-induced hepatocellular apoptosis.* Nature, 1999. 400(6747): p. 886-91.

200. Deng, Y., Y. Lin, and X. Wu, *TRAIL-induced apoptosis requires Bax-dependent mitochondrial release of Smac/DIABLO.* Genes Dev, 2002. 16(1): p. 33-45.

201. Broaddus, V.C., et al., *Bid mediates apoptotic synergy between tumor necrosis factor-related apoptosis-inducing ligand (TRAIL) and DNA damage.* J Biol Chem, 2005. 280(13): p. 12486-93.

202. Kaufmann, T., et al., *Fatal hepatitis mediated by tumor necrosis factor TNFalpha requires caspase-8 and involves the BH3-only proteins Bid and Bim.* Immunity, 2009. 30(1): p. 56-66.

203. DuBray, B.J., Jr., et al., *BH3-only proteins contribute to steatotic liver ischemia-reperfusion injury.* J Surg Res, 2015. 194(2): p. 653-8.

204. Hsu, S.H., et al., *Hepatic loss of miR-122 predisposes mice to hepatobiliary cyst and hepatocellular carcinoma upon diethylnitrosamine exposure.* Am J Pathol, 2013. 183(6): p. 1719-30.

205. Badmann, A., et al., *TRAIL enhances paracetamol-induced liver sinusoidal endothelial cell death in a Bim- and Bid-dependent manner.* Cell Death Dis, 2012. 3: p. e447.

206. Roychowdhury, S., et al., *Inhibition of apoptosis protects mice from ethanol-mediated acceleration of early markers of CCl4 -induced fibrosis but not steatosis or inflammation.* Alcohol Clin Exp Res, 2012. 36(7): p. 1139-47.

207. Hikita, H., et al., *Mcl-1 and Bcl-xL cooperatively maintain integrity of hepatocytes in developing and adult murine liver.* Hepatology, 2009. 50(4): p. 1217-26.

208. Hikita, H., et al., *BH3-only protein bid participates in the Bcl-2 network in healthy liver cells.* Hepatology, 2009. 50(6): p. 1972-80.

209. Zinkel, S.S., X.M. Yin, and A. Gross, *Rejuvenating Bi(d)ology.* Oncogene, 2013. 32(27): p. 3213-9.

210. Liu, Y., et al., *Proapoptotic Bid mediates the Atr-directed DNA damage response to replicative stress.* Cell Death Differ, 2011. 18(5): p. 841-52.

211. Garrett, W.S., J.I. Gordon, and L.H. Glimcher, *Homeostasis and inflammation in the intestine.* Cell, 2010. 140(6): p. 859-70.

212. Yeretssian, G., et al., *Non-apoptotic role of BID in inflammation and innate immunity.* Nature, 2011. 474(7349): p. 96-9.

213. Zinkel, S.S., et al., *Proapoptotic BID is required for myeloid homeostasis and tumor suppression.* Genes Dev, 2003. 17(2): p. 229-39.

214. Ito, K., et al., *Regulation of oxidative stress by ATM is required for self-renewal of haematopoietic stem cells.* Nature, 2004. 431(7011): p. 997-1002.

215. Kamer, I., et al., *Proapoptotic BID is an ATM effector in the DNA-damage response.* Cell, 2005. 122(4): p. 593-603.

216. Zinkel, S.S., et al., *A role for proapoptotic BID in the DNA-damage response.* Cell, 2005. 122(4): p. 579-91.

217. Maryanovich, M., et al., *The ATM-BID pathway regulates quiescence and survival of haematopoietic stem cells.* Nat Cell Biol, 2012. 14(5): p. 535-41.

218. Ito, K., et al., *Regulation of reactive oxygen species by Atm is essential for proper response to DNA double-strand breaks in lymphocytes.* J Immunol, 2007. 178(1): p. 103-10.

219. Willer, C.J., et al., *Six new loci associated with body mass index highlight a neuronal influence on body weight regulation.* Nat Genet, 2009. 41(1): p. 25-34.

220. Gupte, A.A., H.J. Pownall, and D.J. Hamilton, *Estrogen: An Emerging Regulator of Insulin Action and Mitochondrial Function.* J Diabetes Res, 2015. 2015: p. 916585.

221. Varlamov, O., C.L. Bethea, and C.T. Roberts, Jr., *Sex-specific differences in lipid and glucose metabolism.* Front Endocrinol (Lausanne), 2014. 5: p. 241.

222. Shah, M. and A. Garg, *High-fat and high-carbohydrate diets and energy balance.* Diabetes Care, 1996. 19(10): p. 1142-52.

223. Anstee, Q.M. and R.D. Goldin, *Mouse models in non-alcoholic fatty liver disease and steatohepatitis research.* Int J Exp Pathol, 2006. 87(1): p. 1-16.

224. Sonoda, J., et al., *PGC-1beta controls mitochondrial metabolism to modulate circadian activity, adaptive thermogenesis, and hepatic steatosis.* Proc Natl Acad Sci U S A, 2007. 104(12): p. 5223-8.

225. Liang, H. and W.F. Ward, *PGC-1alpha: a key regulator of energy metabolism.* Adv Physiol Educ, 2006. 30(4): p. 145-51.

226. Giordano, A., et al., *tBid induces alterations of mitochondrial fatty acid oxidation flux by malonyl-CoA-independent inhibition of carnitine palmitoyltransferase-1.* Cell Death Differ, 2005. 12(6): p. 603-13.

227. Bonnefont, J.P., et al., *Carnitine palmitoyltransferases 1 and 2: biochemical, molecular and medical aspects.* Mol Aspects Med, 2004. 25(5-6): p. 495-520.

228. Kuwana, T., et al., *Bid, Bax, and lipids cooperate to form supramolecular openings in the outer mitochondrial membrane.* Cell, 2002. 111(3): p. 331-42.

Curriculum Vitae

Hao Zhang

Education:

Ph.D - Indiana University 2015

M.D. - School of Medicine, Tongji University, China 2009

Publications (journal articles and abstracts):

1. Zhang H* (co-first author), Lin CW*, , Li M, Xiong X, Chen X, Chen X, Charlie Dong X, Yin XM. Pharmacological Promotion of Autophagy Alleviates Steatosis and Injury in Alcoholic and Non-alcoholic Fatty Liver Conditions in Mice. Journal of Hepatology. 2013 Jan 19. pii: S0168-8278(13)00054-8. doi: 10.1016/j.jhep.2013.01.011. Epub 2013 Jan 12.

2. Li M, Khambu B, Zhang H, Kang JH, Chen X, Chen D, Vollmer L, Liu PQ, Vogt A, Yin XM. Suppression of lysosome function induces autophagy via a feedback down-regulation of MTOR complex 1 (MTORC1) activity. Journal of Biological Chemistry. 2013 Dec 13;288(50):35769-80. doi: 10.1074/jbc.M113.511212. Epub 2013 Oct 30.

3. Chen X, Khambu B, Zhang H, Gao WT, Li M, Chen X, Yorshimori T, Yin XM Autophagy induced by calcium phosphate precipitates targets damaged endosomes. Journal of Biological Chemistry. published March 11, 2014 as doi:10.1074/jbc.M113.531855

4. Chen D, Chen X, Li M, Zhang H, Ding WX, Yin XM. CCCP-Induced LC3 Lipidation Depends on Atg9 Whereas FIP200/Atg13 and Beclin 1/Atg14 are Dispensable. Biochemical and Biophysical Research Communications. 2013 Mar 8;432(2):226-30.

5. Hai J, Lin Q, Lu Y, Zhang H, Yi J. Induction of apoptosis in rat C6 glioma cells by panaxydol. Cell Biology International. 2007 Jul;31(7):711-5. Epub 2007 Jan 14.

6. Hai J, Lin Q, Zhang H, Lu Y, Yi J. Cyclic AMP-dependent regulation of differentiation of rat C6 glioma cells by panaxydol. Neurological Research. 2009 Apr;31(3):274-9.

7. Hai J, Lin Q, Lu Y, Yi J, Zhang H. Growth inhibition and induction of differentiation by panaxydol in rat C6 glioma cells. Neurological Research. 2008 Feb;30(1):99-105.

8. Zhang H, Yang CQ. Glycomics as a non-invasive diagnostic method for liver fibrosis. Chinese Journal of Hepatology. 2008 Mar;16(3):239-40

9. Yang CQ, Yang L, Yang WZ, Zhang Z, Zhang H, et al. Mechanism of hepatic satellite cell migration during liver fibrosis. National Medical Journal of China. 2008 Jan 8;88(2):119-22

10. Zhang H, Hai J. The Molecular Mechanisms of Ubiquitin-proteasome system in Cognition. International Journal of Cerebrovascular Disease 2008 (16) 11; 862-5

12. Zhang H, Khambu B, Chen X, Chalasani NP, Liangpungsakul S, Li Y, Yin XM. mTOR-TFEB feedback loop regulates NAFLD development and metabolic syndrome in mice. In preparation.

13. Zhang H, Khambu B, Chen X, Yin XM. Deletion of Bid Protects Against Diet Induced Obesity and Metabolic Syndrome by Upregulation of Fatty Acid Oxidation. In preparation.

14. Zhang H, Chen X, Yin XM. The Dynamics of Liver Autophagy Status during Steatosis Development. Hepatology 54:1440, 2013 AASLD Liver Meeting abstract

15. Yin XM, Zhang H, Lin CW, Chen X, Chen XY. Autophagy regulates steatosis in non-alcoholic fatty liver disease in mouse. Hepatology 54:1157A, 2011 2012 AASLD Liver Meeting abstract

16. Yang Z, Guo N, B Khambu, Zhang H, P Liu, X Yin, M Li Impaired lysosome function can induce autophagy via suppression of mTOR activity. FASEB Journal. 28:738, 2014 Experimental Biology Meeting abstract

17. Zhang H, Khambu B, Chalasani NP, Yin XM. Modulation of Autophagy Affects the Hepatic Pathology in Alcoholic and Non-alcoholic Liver Diseases. FASEB Journal. 27:1221, 2013 Experimental Biology Meeting abstract

Book chapters:

1. Zhang H, Khambu B, Yin XM. Chapter: Autophagy “Signaling pathways in liver disease.” 3rd Edition, Springer, edited by J.F. Dufour and P.-A. Clavien

2. Khambu B, Zhang H, Yin XM. Chapter: Mitophagy in liver “Mitochondria in Liver Disease” Taylor & Francis, edited by Neil Kaplowitz and Derick Han

Fellowships and Awards:

Graduate Student Education Enhancement Award, Indiana University School of Medicine 2012